INCORPORATING ANIMAL MOVEMENT INTO CIRCULAR PLOT AND POINT TRANSECT SURVEYS OF WILDLIFE ABUNDANCE

Rocío Prieto González

A Thesis Submitted for the Degree of PhD
at the
University of St Andrews

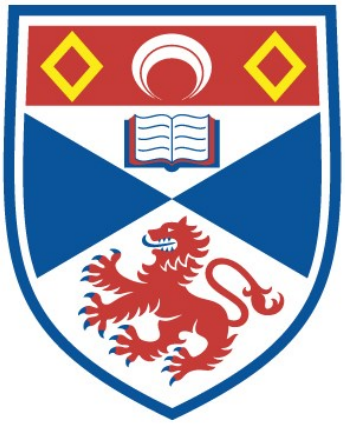

2018

Incorporating Animal Movement into Circular Plot and Point Transect Surveys of Wildlife Abundance

Rocío Prieto González

University of
St Andrews

This thesis is submitted in partial fulfilment for the degree of
Doctor of Philosophy (PhD)
at the University of St Andrews

September 2017

Abstract

Estimating wildlife abundance is fundamental for its effective management and conservation. A range of methods exist: total counts, plot sampling, distance sampling and capture-recapture based approaches. Methods have assumptions and their failure can lead to substantial bias. Current research in the field is focused not on establishing new methods but in extending existing methods to deal with their assumptions' violation. This thesis focus on incorporating animal movement into circular plot sampling (CPS) and point transect sampling (PTS), where a key assumption is that animals do not move while within detection range, i.e., the survey is a snapshot in time. While targeting this goal, we found some unexpected bias in PTS when animals were still and model selection was used to choose among different candidate models for the detection function (the model describing how detectability changes with observer-animal distance). Using a simulation study, we found that, although PTS estimators are asymptotically unbiased, for the recommended sample sizes the bias depended on the form of the true detection function. We then extended the simulation study to include animal movement, and found this led to further bias in CPS and PTS. We present novel methods that incorporate animal movement with constant speed into estimates of abundance. First, in CPS, we present an analytic expression to correct for the bias given linear movement. When movement is defined by a diffusion process, a simulation based approach, modelling the probability of animal presence in the circular plot, results in less than 3% bias in the abundance estimates. For PTS we introduce an estimator composed of two linked submodels: the movement (animals moving linearly) and the detection model. The performance of the proposed method is assessed via simulation. Despite being biased, the new estimator yields improved results compared to ignoring animal movement using conventional PTS.

Declarations

Candidate's declaration

I, Rocío Prieto González, do hereby certify that this thesis, submitted for the degree of PhD, which is approximately 30,000 words in length, has been written by me, and that it is the record of work carried out by me, or principally by myself in collaboration with others as acknowledged, and that it has not been submitted in any previous application for any degree.

I was admitted as a research student at the University of St Andrews in June 2012.

I received funding from an organisation or institution and have acknowledged the funder(s) in the full text of my thesis.

Date: Signature of candidate:

Supervisor's declaration

I hereby certify that the candidate has fulfilled the conditions of the Resolution and Regulations appropriate for the degree of PhD in the University of St Andrews and that the candidate is qualified to submit this thesis in application for that degree.

Date: Signature of supervisor:

Permission for publication

In submitting this thesis to the University of St Andrews we understand that we are giving permission for it to be made available for use in accordance with the regulations of the University Library for the time being in force, subject to any copyright vested in the work not being affected thereby. We also understand, unless exempt by an award of an embargo as requested below, that the title and the abstract will be published, and that a copy of the work may be made and supplied to any bona fide library or research worker, that this thesis will be electronically accessible for personal or research use and that the library has the right to migrate this thesis into new electronic forms as required to ensure continued access to the thesis.

I, Rocío Prieto González, confirm that my thesis does not contain any third-party material that requires copyright clearance.

The following is an agreed request by candidate and supervisor regarding the publication of this thesis:

Printed copy

No embargo on print copy.

Electronic copy

No embargo on electronic copy.

Date: Signature of candidate:

Date: Signature of supervisor:

Underpinning Research Data or Digital Outputs

Candidate's declaration

I, Rocío Prieto González, hereby certify that no requirements to deposit original research data or digital outputs apply to this thesis and that, where appropriate, secondary data used have been referenced in the full text of my thesis.

Date: Signature of candidate:

Acknowledgements

The personal motivation behind this thesis is a combination between my love for cetaceans and my strengths for fighting for what I want, among other important things, a high quality work. During this long process I have to thank many many people in many different ways.

I would first of all like to thank my supervisors, Professor Len Thomas and Dr. Tiago A. Marques. I have no doubt that very few people have been as lucky as I have with respect to their bosses. Thanks for taking me on in the first place! Back in 2012 and despite having a not easy beginning, I had no idea about just how much I would learn and experience throughout this process and I feel very privileged to have been given the opportunity. Thank you both for your way of being, your character, personality and your support all the way. This PhD would be just impossible without you guys. Thank you Len for being a constant inspiration in my life, scientifically of course, but even more importantly, you have been a example to follow as a human being. When I grow up I want to be like you (because you are going to be always older than me, I will have an extra time to catch up...) Thank you Tiago, for all your help since I met you in Portland. For always be open to help everybody, for all the skype times, talking openly (latin blood...) and happiness even in the hard times.

All the CREEMinlas and the great research environment in St Andrews. CREEM is an amazing source of intellectual stimulation, inspiration, teaching abilities, and skills to convey complicated ideas in a simple way. I hope I carry some of that with me... Thanks for the discussions, ideas, endless explanations and useful comments. Thanks for imparting your knowledge and for your advice (from some of the best minds in the field no less). I learnt tonnes with you all. Special thanks to Steve Buckland, Eric Rexstad, Darren Kidney and Ben ("Biiin") Stevenson for their advice and help over this period. I am particularly grateful to Richard Glennie for some in-depth discussions of the animal movement problem, which contributed greatly to my understanding. Moreover, a big

thanks to Monique MacKenzie for taking me along to teach workshops in South Africa, and all the other PhD, students for all the shared moments =).

Many thanks to my friends, both in St Andrews and across the world.
- Hania, you gave me so much in so little time. I am so glad you liked puppies... Thanks for the great time in Zurich and the Sunday's egg tradition!
- My lovely blondies, thank you Jenny and Casey for all our dances, meals, dog walks, excursions, frisbee games, dinners and chats. Thank you for always being there taking care of me, for sharing the best road trip to Spain. Danger! Danger!! Thank you for making me smile when it was not easy and believing in me. Additional thanks for the proofreading of this work.
- Muchas gracias a Aitor, por ser un compañero increible de viaje, por su paciencia, su cariño y amor. Por compartir su familia hasta el punto de parecer casi la mía. Gracias Toñi y Jose Luis por acogerme con los brazos abiertos.
- Our dog friends (human and hairy ones), Silvana, Blue, Stacy, Henry, Shakespeare, Nadya, Jess, Tom, Kim, Glen, Mac, Biiin, Ben, Charlotte, Watson, Jennifer, Rhona, Beauly, Ernest, Tiffany and family, Tobin, Donna, Chloe, Declan, Kirsty, Molly, Merche, Javi, Sara, Alberto and Elvis.
- Elena y Larry, por ser el ejemplo de amigos incondicionales. Gracias Nu, por las llamadas interminables, por estar siempre siempre súper cerca incluso cuando quiero hacerme bola o estamos físicamente lejos. Por todos los paseos perrunos, por unirte a todos los planes y acompañarme en mis locuras. Me haces sentir muy afortunada, friolera mía.
- Buu y Noe. Gracias chicos, a Buu por siempre, y a Noe por abrirme su corazon completamente y sentirla tan cercana. Por recordarme lo que se siente al estar cansado de felicidad. Por cuidarnos tanto (¡a mi y a Doby!) haciendo que parezca fácil.
- A Álvaro y Torete, por ser una super sorpresa en este último período de tesis. Por animarme a ir a la pisci a nadar un montón, los mil y un paseos perrunos y todas las aventuras con zarzas, lluvia, chapuzones y escapadas incluso a Castellón.
- A todos los que me abren la puerta de su casa en mis múltiples viajes, con perro o sin perro. Gracias Rebe, Polo et Iago, por vuestra alegría, por hacerme sentir siempre bienvenida incluso cuando estás de parto, corazón y por todas tus llamadas, eres un cielo. A Mariana por toda tu disposición y ganas. To Jenny's parents for make us feel so welcome and spoiled every time.
- A mis amigos viajantes que me visitan esté donde esté, por alegrarme y quererme. Gracias Vio por ser una incondicional (¿de la insensatez?), pintando mi granja, sufriendo por

mi coche en Gwada, bailando como locas y ¡casi durmiendo en un banco en Edimburgo! Sandra y Gabi Amigo, por seguirme a donde vaya trayendo siempre risas y buenos momentos con ellos. Elena por estar incluso en la distancia cuando no se puede llegar en coche. Mil gracias mi niña. A Merche y Javi, por estar simpre en contacto, la visita a Escocia y cuidar del pinpollo, a mi Tia Tari, por ser una valiente y venir ¡a mi casa con perro incluido!, mi primo Teto y Virginia por vernirnos a ver y por abrirme las puertas de Liencres siempre que he querido. Y por supuestisimo a mis padres.
- To all who are always happy to share amazing trips and give me fuel. Aunty Nadya for showing us New York and making us feel like another member of the family. Thanks for all the good laughs in "the bubble", dinners, salsa classes, vans and studying moments... Shopie (le ti-mouton noir) pour toutes les glaces et randonées à Montpellier, Lyon, et St Andrews, Anne-So pour la superbe semaine de ski dans les Alpes et tout les aventures à Dijon et Beaune. C'est toujours super de partager avec tes parents et profiter de ton énergie.
- Nelly et Laurent, pour leur amitié d'UFF. C'est un vrai plaisir de vous connaître. Vous êtes le joie personnifiée, je vous admire autant que je vous adore. Simplement MERCI!
- Mille mercis a tout le monde de Gwada, pour m'avoir fait découvrir que l'on peut vivre un rêve. Vous avez rendu cette expèrience si magnifique et génial... Vive les cétacés!!

I am grateful to the Centre for Research into Ecological and Environmental Modelling (CREEM) provided funding for my studies.

My cetacean adventure started 8 years ago, and it would be unfair not to thank the scholarship granted by the "La Caixa" Foundation, which allowed me to join the Bioacoustic team at the University of Paris-Sud. There, I applied my theoretical mathematical and statistical knowledge to the theme which inspires me the most: cetaceans. Many thanks to this amazing team who made me feel so welcome.

Lo mejor es siempre para el final...

Mil gracias a mi familia, por estar siempre al otro lado del teléfono, en los buenos y los malos momentos. Especialmente a mis padres, por su amor incondicional, sus mil visitas y sus sacrificios (como aprender a vivir en una casa llena de pelos...), por todo lo que han hecho, hacen y harán durante esta tesis y toda mi vida. A mi Tita, por los tapers de

besos y a mi tia RosaMari por escribirme y estar siempre. Un besazo a mi abuelito Pepe por enseñarme a disfrutar de las cosas importantes de la vida.

A Doby, mi monstruo, mi cachorrillo de 5 años, el pitufín y desastre genético, la bolita de pelos, sin el cual creo que hubiese sido imposible llegar hasta aquí. Por su alegría inconmensurable, sacarme de paseo, y robarme una sonrisa hasta en los días más grises. Por su paciencia, energía y motivación continua. Por hacerme ser mejor persona, disfrutar del momento y aprender a controlar mis gruñidos. Gracias Do, por elegirme, por ser simplemente como eres. ¡Viva el NO espacio personal!

Contents

List of Figures

List of Tables

1

Introduction

1.1 Estimating animal abundance

Animal abundance refers to the absolute number of individuals of a target species in a particular site, which we call the "study region". Animal density is the quotient of the abundance and the area of this site, i.e., the number of individuals per unit area. Both variables are of great ecological importance. For instance, knowing how many individuals there are in an animal population is crucial for wildlife management and conservation (Williams *et al.*, 2002).

A complete census, counting every individual within the study region, is only feasible in very special cases, e.g., the population is small and individuals can be readily identified. The southern resident killer whale population in British Columbia provides an example where this is possible. Killer whales in general are readily amenable to sightings surveys, and this small (< 100 individuals), geographically restricted populations is censused every year by photographing individuals, all of whom are individually identifiable from natural markings (Parsons *et al.*, 2009). While these census methods are the only way of obtaining errorless measurements of abundance and density, unfortunately, for most wildlife populations they would be time consuming, financially prohibitive, and practically or logistically impossible. Therefore, a suite of sampling methods have been developed to address the challenge of estimating the abundance or density of animal populations. They often involve surveying a fraction of the population of the whole study region and rely on the information contained in a sample, in which only a fraction of the population is observed, while accepting that some individuals will be missed. Then, using either design or model based approaches, or a combination of these, one can draw inferences with respect to

the entire population of interest. While these practices decrease fieldwork effort, they introduce uncertainty: one must account for both the number of individuals outwith the sampled area and the number of individuals within the sampled area that were missed. We refer to the sampled area as the covered area. Two common approaches exist: plot sampling (PS) in which all individuals must be detected in the covered area, and methods designed to estimate the probability of detection of individuals missed in the covered region, allowing to account for the missed individuals. Distance sampling (DS) is one among several other possible alternatives, such as mark-recapture studies (MR, Borchers *et al.*, 2002), and one of the most frequently used due to the method's simplicity. Although the methods are also applicable to a variety of objects of interest, including groups of animals, animal cues, plants or fungi, (Buckland *et al.*, 2007, 2015), for simplicity, we will generally refer to objects of interest as animals in the following.

Both methods, PS and DS, assume that animals do not move while the survey takes place, i.e., the survey can be seen as a snapshot in time, during which animals do not move. For mobile animals the violation of this assumption leads to biased abundance estimates. The goal of this thesis is to develop solutions that incorporate information about animal movement in the estimation process, to relax the no movement assumption.

In the remainder of this introductory chapter, I present an overview of distance sampling methods (Section 1.2) followed by some insights into animal movement (Section 1.3), an explanation of my motivation for doing this PhD (Section 1.4), and, lastly, a brief description of the following chapters of this thesis (Section 1.5).

1.2 Conventional Distance Sampling

Distance sampling comprises a suite of methods, namely, line transect sampling (LTS Burnham *et al.*, 1980), point transect sampling (PTS Buckland, 2006), cue counting (Borchers *et al.*, 2009; Marques *et al.*, 2011) and trapping point transects (Buckland *et al.*, 2006; Potts *et al.*, 2012). While this thesis is about incorporating animal movement information in PTS, we focus in this introductory chapter on both PTS and LTS. This is motivated by the fact that, due to the simpler geometry, some of the concepts involved in distance sampling estimators are easier to convey with lines than with points. Moreover, both methodologies, LTS and PTS, were used in the Chapter 2. See Buckland *et al.* (2001, 2015) for a general overview of DS methodology.

A DS survey is carried out by observers who either travel along line transects or are stationed at points. These methods require that samplers (lines or points) are placed within the study region according to some sampling design. Let N be the abundance (i.e., population size) of animals in a study region of size A, and let D be the animal density, $\frac{N}{A}$. The covered area a, is the area which has been sampled. We assume that not all of the animals, but only some n animals will be detected in a by the observers and the proportion of missing animals in a can be estimated by collecting additional information: the detection distances. Thus, when an observer detects an individual (or group, if they occur in clusters) he or she records its distance from either the line or the point. These distances are used to estimate a detection function which models the decay in detection probability with increasing distance from the point or line. The average detection probability, the quantity we require to scale up the number of detected animals to account for those missed, is the expected value of this detection function with respect with all the possible distances.

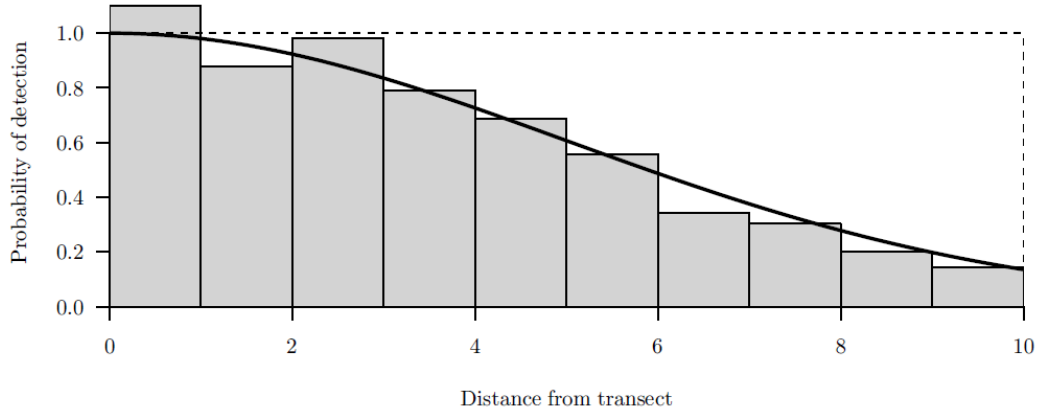

Figure 1.1: A histogram of simulated distances to animals detected by observers walking along a line transect. Truncation distance was set at $w = 10$. The detection function used to simulate these data, $g(y)$, is overlaid (thick solid line). The height of the histogram bars are scaled so that their collective area is equal to $\int_0^w g(y)dy$, the area under the detection function. The average probability of detection P_a, is $E(g) = \int_0^w \pi(y)g(y)dy$ where $\pi(y)$ is the pdf of animal distances (both detected and not detected). For a line transect this pdf is $1/w$, so $E(g) = 1/w \int_0^w g(y)dy$.

N can be estimated as

$$\hat{N} = \frac{n}{\hat{P}_a a} A, \tag{1.1}$$

where n is the number of detected animals in the covered area a, and $\hat{P}_a$ is the estimated average probability of detecting an animal within a. The density estimator is obtained simply by dividing the abundance estimator by A,

$$\hat{D} = \frac{n}{\hat{P}_a a}. \tag{1.2}$$

From a probability density function (pdf) f, fitted to n observed distances, a detection function g (returning the probability of detecting an animal a given distance from the observer, e.g., Figure 1.1) and the average probability of detection for an animal that is in the covered area $P_a = E[g]$ is estimated. Discarding any observations beyond a truncation distance w, the covered area a is $2Lw$ for line transects of total line length L, and $k\pi w^2$ for k point transects. If transects are placed at random, then the underlying distribution of all distances to individuals (detected or otherwise) within distance w is uniform on the interval $[0, w]$ for LTS, or has probability density $\pi(y) \propto y, y \in [0, w]$, for PTS.

Estimated density for LTS is

$$\hat{D} = \frac{n\hat{f}(0)}{2L}, \tag{1.3}$$

where $\hat{f}(0)$ is the value of the pdf of detected distances evaluated at zero distance (Buckland *et al.*, 2001, p. 38-41). Because the area of a strip of incremental width dy at distance y from the line is independent of y, for LTS, $f(y)$ and $g(y)$ have identical shape, only rescaled so that f integrates to unity.

For PTS,

$$\hat{D} = \frac{n\hat{f}'(0)}{2\pi k} \tag{1.4}$$

with $\hat{f}'(0)$ being the derivative of the pdf evaluated at zero. The area of a ring of incremental width dy at distance y from the point is proportional to y, thus $f(y)$ is proportional to $yg(y), y \in [0, w]$. These two estimator expressions make it explicit that the behaviour of the pdf at zero distance is critical for estimating animal density for both PTS and LTS.

1.3 Animal movement

Movement is a fundamental, yet relatively poorly understood population process (Patterson *et al.*, 2008). Understanding how and why animals move and migrate is fundamental

to the effective management and conservation of wild animal populations (Jacoby *et al.*, 2012) and in practice, to create realistic simulation scenarios. Population ecology, which has long focussed on temporal fluctuations in abundance (Turchin, 1998), has more recently considered spatially explicit approaches, leading to a greater appreciation of the importance of movement (Steinberg and Kareiva, 1997). Related species or even populations of the same species may exhibit different scales and patterns of movement. The spatial and temporal structure of movement cycles are based on evolutionarily successful behavioural decisions in response to numerous physical, biological and environmental factors (Liedvogel *et al.*, 2011; Patterson *et al.*, 2008), making it hard to predict them.

A better understanding of the way that wildlife, habitat and humans interact is fundamental due to the rising impacts of human activities on natural resources, with corresponding dramatic losses of biodiversity all over the world. As Jacoby *et al.* (2012) said, "Understanding the cyclical trends involved in movement and the driving forces behind them are vital to the identification and potential mitigation of anthropogenic disruption". Modelling and predicting how animals move, allows us to integrate findings on this behaviour, and hence to be able to provide a more accurate distribution and abundance of animal populations.

There are lots of difficulties associated with observing and recording data for highly mobile and wide-ranging species in their natural habitats. As a consequence, behavioural ecologists are increasingly relying on electronic tags which are attached to animals and track their movements (e.g., Sumner *et al.*, 2009; Langrock *et al.*, 2014). This allows tracking individuals of some species in habitats where direct observation is often impossible (Weng *et al.*, 2005; Block *et al.*, 2002). Tags are designed to store and in some cases transmit data relating to an animal's movement, speed, direction or environment (Rutz and Hays, 2009). Due to the advances in biologging and telemetry techniques, ecologists in recent years rely on such technology to estimate population density, home ranges or identify localised movement patterns. Such advances can provide "24h/day" monitoring of individuals, and it is usual to deal with a big dataset, containing tens of thousands of individual data points (Fancy *et al.*, 1989; Heupel *et al.*, 2010). However, some disadvantages are that these data are a time series of presence-absence for each individual's time and location and it is difficult to account for the interconnectivity of locations as animals move between them.

An example is given by Figure 1.2. It is a track map of a killer whale tagged in the Antarctic in February 2016 and still transmitting in mid June 2016. We can distinguish

between, at least, two different modes of movement: a dynamic directed movement when the whale is migrating, i.e., travelling along the coast of South America, to and from lower latitudes, and a more correlated home range movement within foraging patches near Antarctica. The idea is that animals switch between several movement modes corresponding to different behaviours; travelling, foraging, so on. Developing an understanding of the proximate and ultimate causes for those behaviours not only addresses fundamental ecological questions but has relevance to many other fields, e.g., related to the spread of emerging diseases, the proliferation of invasive species, aeronautical safety as well as the conservation of migrant species.

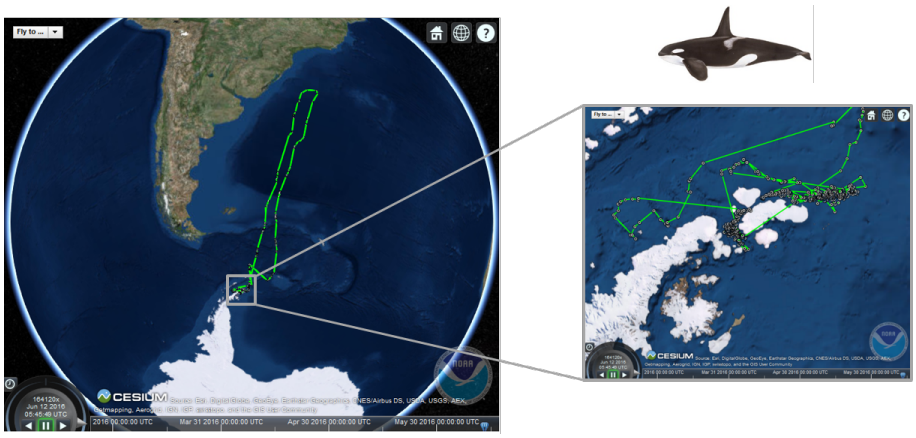

Figure 1.2: Tracking map of a killer whale tagged in the Antarctic. Transmitting from February to June 2016. Figures provided by https://swfsc.noaa.gov/MMTD-KillerWhale-TrackMap.

Migration is central to the life-history adaptations of many animals. For years scientists have been tracking animals and the ways they migrate. Antarctic killer whales, for instance, make rapid, round-trip movements to subtropical waters. These rapid migrations to subtropical waters have been described by Durban and Pitman (2012). Much work has been done in predicting the timing of migrations and how they can be affected by environmental conditions (e.g., Marra *et al.*, 2005). In many respects, however, migration is a special case of the more general prediction problem of when and why animals move between distinct home range centres. In fact, in this thesis we focus on random animal movement independent of any observer present, in particular in two modes of movement: linear movement and animals constrained to a home range area.

1.4 Personal motivation

In a world with increasing environmental concerns, it seems more important than ever to implement effective conservation and monitoring schemes for threatened species. With that purpose in mind, the initial motivation of this work was focused on estimating abundance of cetaceans, using acoustics.

1.4.1 Counting cetaceans using acoustics

Traditionally, animal populations have been monitored visually by researchers, whether on land or at sea. However, there are obvious limits to this approach. Visual surveys cannot take place at night, or in bad weather conditions and they are also expensive in the long term. Furthermore, some species are difficult to survey by sight due to their habitat preferences or behaviour. This is a clear example for cetaceans; many marine mammal species are notoriously challenging to survey, as they spend so little of their time at the sea surface. Sperm whales, for instance, have an average dive of 40 min (Watwood *et al.*, 2006). Another example are beaked whales. During one survey, a beaked whale was tagged in the Bahamas and it spent 85% of the surveyed time submerged below 3 meters (Tyack *et al.*, 2006).

Passive acoustic monitoring provides an alternative method to survey animals. Provided that the species of interest makes a sound that can be used as a cue to indicate that an individual is present, acoustic monitoring can overcome some of the limitations of visual surveys. Acoustic surveys are less sensitive to weather conditions and can be conducted 24 hours-a-day. In addition, acoustic monitoring equipment can be left *in situ* for extended time periods, enabling long term data sets to be collected throughout all seasons. So, based on processed acoustic data, how can we obtain density estimates to monitor their abundance?

Compared to active acoustic monitoring, passive acoustic monitoring (PAM) is unintrusive and is used much more widely. The ability of PAM data to provide insights into cetacean abundance and density has been identified for many years (e.g., McDonald and Fox, 1999; Mellinger *et al.*, 2007). Measures of the minimum number of whales, minimum whale density and relative abundance have appeared in several studies (e.g., McDonald and Fox, 1999; Charif *et al.*, 2001; Gillespie *et al.*, 2005; McDonald, 2006). To generate absolute abundance and density estimates, undetected animals must be accounted for

(both vocalising and non-vocalising, in an acoustics context), and it is often difficult to distinguish and count individual animals from acoustic data. However, large advances in absolute abundance and density estimation using acoustic data have occurred over the last few years (Marques *et al.*, 2013).

Depending on what is counted, cues, groups of cetaceans or individuals, we will face different challenges. In the first two cases we can only estimate the density of cues or groups, unless we have auxiliary data to convert this density into density of animals. These multipliers, cue rate (average number of cues per individual and unit of time) or group size, would have to come from a representative sample taken at the time and place of the main survey. This is easy to say but often hard to do (e.g., Marques *et al.*, 2011). This sometimes leads to an estimation of only whale calls (e.g., Harris *et al.*, 2013; Matias and Harris, 2015). By contrast, distinguishing individuals acoustically results in an abundance estimator. However, using DS methodology, animal movement may become an issue. In particular, cetacean movement is very relevant for long-term fixed acoustic point surveys where individuals call relatively frequently, so that it is feasible to track them, counting them individually several times. Some examples are given in Table 1.1.

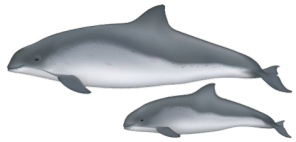	**Harbour porpoises** (*Phocoena phocoena*) When there is a low group size and they call quite frequently.
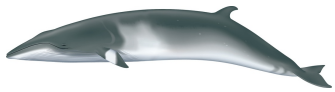	**Minke whales** (*Balaenoptera acutorostrata*) Consecutive calls tend to have the same dominant frequency, and although it changes slowly over time, it may be possible to distinguish individuals.
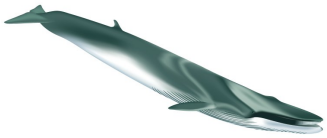	**Fin whales** (*Balaenoptera physalus*) Individuals may be tracked, looking at the detections of calls through time (e.g., Figure 1.3).

Table 1.1: Example of cetaceans that can be distinguished individually by their calls. Illustrations courtesy of The Whale Trail organization (Harbour porpoise and Minke whale) and Uko Gorter (Fin whale) copyright 2003, 2006 all rights reserved.

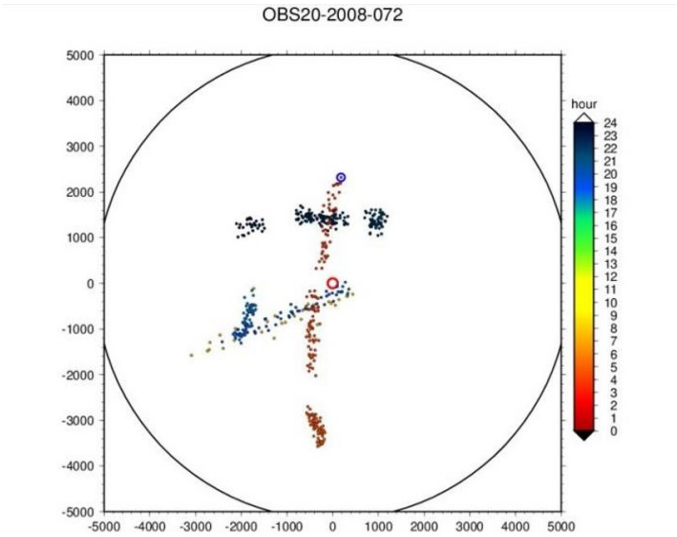

Figure 1.3: Detected fin whale calls by two hydrophones (red and blue circles), deployed at a depth of 2 and 3.5 km respectively of an ocean-bottom seismic station. There is a pattern in the detected calls over 24 hours (indicated by the colours). Plot Courtesy of L. Matias (Cheap DECAF project).

The choice of an appropriate method in a given situation should be a function of the species and habitat characteristics, resources available, desired precision, and objectives of the study. Background knowledge on the environment and the population is therefore invaluable in the choice of the method to use.

1.5 Thesis outline

This thesis outlines a variety of methods aimed at improving animal abundance and density estimation when animal movement occurs.

In the first phase of the thesis work, our goal was to quantify how movement leads to bias. Initial results of our simulation study presented in Chapter 3, showed some unexpected bias in PTS even when animals did not move. This was the reason (and a logical first step) to fully understand the estimation process when assumptions are met, i.e., when animals were stationary. Thus, Chapter 2 investigates the performance of PTS in scenarios involving no animal movement, but with moderate sample size and when the detection function model is selected using standard model selection techniques. Chapter

3 then generalizes these findings to scenarios for both circular plot sampling (CPS) and PTS when animals do move.

The second phase of the thesis work aimed to derive unbiased (or less biased) density estimators for some specific animal movement scenarios. Chapter 4, deals with CPS, which assumed perfect detectability within the sampled circles, while Chapter 5 deals with a more realistic scenario where a probability of detection is estimated using DS methodology and including information on animal movement from an independent source.

This section provides an overview of each chapter.

1.5.1 Chapter 2
Distance sampling under model selection detection functions

Many simulation studies have examined the properties of distance sampling estimators of wildlife population size. When assumptions hold, if distances are generated from a particular detection function model and fitted using the same model, the methods are known to perform well. However, in practice, the true detection function is unknown. Therefore, the standard methods for fitting detection functions to distance sampling data involve selecting among several classes of models. This selection is typically implemented using model comparison tools like Akaike Information Criterion (AIC). In this chapter, we examine the performance of standard distance sampling estimators under model selection. We compare line and point transect estimators given distances simulated from two detection functions, hazard-rate (HR) and exponential power series (EPS), over a range of sample sizes. To mimic the real-world context where the true model may not be part of the candidate set, EPS models were not included as candidates, except for the half-normal parameterization, which is a special case of the EPS distribution.

The findings of this chapter have been published as Prieto Gonzalez *et al.* (2017).

1.5.2 Chapter 3
The effect of animal movement on abundance estimates

As any other method for estimating animal abundance, PS and DS estimators are derived under a number of assumptions that ensure the methods are asymptotically unbiased. One key assumption of both methods is that all animals are detected at their initial

location. In other words, the detection process is assumed to be instantaneous. There are two kinds of animal movement which lead to violations of this assumption: independent of the observer and responsive movement (towards or away from the observer). We focus here on random animal movement independent of the observer. We present the effect of random animal movement using a simulation to quantify bias when detection within the covered area is certain (circular plot sampling, CPS) and when detection falls off with distance from the point (PTS). We also explore the non-linear relationship between bias, detection, and animal movement by varying detectability and movement type. We consider both (1) animals that move in randomly orientated straight lines, which provides an upper bound on bias, and (2) animals that are constrained to a home range of certain radius. Throughout this thesis, we consider only the situation where animal speed is known and constant.

1.5.3 Chapter 4
Including animal movement in circular plot sampling

To estimate abundance, circular plot sampling (CPS) methodology assumes that the animals are immobile and all of those present in the sampled area are detected. If animals were all stationary, then the expected proportion of animals within the circle would give us the density in the covered area, and scaled up for the total region an abundance estimate is obtained. However, when animals are mobile, they can enter into the circular detection region and hence be detected, so as time monitoring increases, more animals would be recorded, resulting in positive bias in abundance estimators. To account for animal movement an extended encounter region is defined: the area within which animals would encounter (i.e., be detected by) the observer, depending on the animal movement and the time interval considered for detection.

Three types of animal movement are considered, all of them with constant speed. Animals that move in randomly orientated straight lines, animals following a random walk (RW) and animals that are constrained to a home range of certain radius with a biased random walk (BRW).

1.5.4 Chapter 5
Including animal movement in point transect sampling

One key assumption of DS methods is that animals do not move while within detection range; in other words, the survey is a snapshot in time. Our interest was to derive a new method relaxing this assumption, so including animal movement in the estimation process. In this chapter we concentrate in PTS, for which the observer is stationary and the problem more serious. Although DS relies upon the idea that wildlife are observed at one instant of time, in practice detections occur over some interval and bias arising for wildlife movement increases with time at the point and animal speed as was shown in Chapter 3.

We propose a novel method based on PTS detectability process for animals moving linearly with constant speed. The conventional detection probability is modelled as a function of distance but as constant over time. To capture this variation over time on the underlying distribution of animals, due to animal movement, we introduce a detection function that takes into account both spatial and temporal variation in detection probability. It is composed of two linked submodels: the movement model and the detection model. The key information considered in the proposed method is the time of the animal's first detection, given that any information on successive detections is not used.

Part I

Before animals move...

2

Distance sampling under model selection detection functions

2.1 Introduction

Distance sampling (DS, Thomas *et al.*, 2002; Buckland *et al.*, 2001, 2015) is used widely for estimating the size and spatial density of wild animal populations. It includes two main methods, line transect sampling (LTS) and point transect sampling (PTS). In both, the observer performs a survey along a randomly located series of lines (LTS) or points (PTS) and measures distances to detected animals. Not all animals in the vicinity of each transect will be detected: typically the proportion of animals detected decreases with increasing distance from the transect. A key concept is the detection function $g(y)$, which models the probability of detecting an animal, given its distance y from the transect. DS analysis uses Horvitz-Thompson-like estimators, since the probability of detection is unknown, and must be estimated (Borchers, 1996; Buckland *et al.*, 2001). (The original Horvitz-Thompson estimator is a method for estimating population size in a stratified sample. Those estimators were introduced to deal with the case where sampling units had different, but known, inclusion probabilities (Horvitz and Thompson, 1952).) This is achieved by fitting a model for the detection function to the observed distances. DS is therefore a composite approach, as it cannot be considered entirely design-based (Fewster and Buckland, 2004; Barabesi and Fattorini, 2013), being dependent on a good model for g. Extrapolation to the wider inference region can then be either design or model based (Buckland *et al.*, 2015).

Other things being equal (without compromising the precision) we prefer an unbiased estimator. DS estimators are asymptotically unbiased when assumptions are met (Buck-

land *et al.*, 2015, p. 117). The method relies on 4 assumptions (Buckland *et al.*, 2001, p. 29-37) :

1. Transects are located at random, ensuring that animals are distributed independently of the transects. This ensures the true distribution of animals with respect to the line or point is known (being uniform or triangular, respectively).
2. The probability of detecting an animal on the transect or point is 1, $g(0) = 1$.
3. Distances are measured without errors.
4. The survey can be seen as a snapshot in time, during which animals do not move.

In simulations where assumptions hold, with data generated from a particular model and fitted using the same model, methods seem to perform well (e.g. Buckland, 2006; Du Fresne *et al.*, 2006; Glennie *et al.*, 2015). However, in real life situations, we face two additional issues not typically accounted for in previous simulation studies. First, the true detection function model is unknown. Therefore, the standard methods for fitting detection functions to distance sampling data, as described by Buckland *et al.* (2001), and which we refer to collectively as "conventional distance sampling", involve selecting among several classes of flexible, semi-parametric models. Buckland *et al.* (2001) recommend that, under most circumstances, this selection is performed using standard model selection techniques such as choosing the model with minimum Akaike Information Criterion (AIC). Second, for a reliable estimate, we need to achieve an adequate number of detections: Buckland *et al.* (2001) recommend at least 60-80 for lines and 75-100 for points. Despite the usual recommendation, reported sample sizes very often do not reach these values (e.g. Buckland, 2006; Williams and Thomas, 2007; Durant *et al.*, 2011).

This study was motivated by finding non-negligible bias in DS estimators, in a simulation scenario involving moderate sample size and model selection, as part of a larger study looking at violation of the no movement assumption. Before animals started moving (thus the assumptions were met) no bias was expected, but was clearly present. Rather than fitting from the true model, we were using model selection, and soon it became apparent that this was the source of the bias. This lead us to question the sample size guidelines, and also the effect of the shape of the true detection function model, in particular under model selection, and hence undertake the study reported here.

Many simulations studies have considered AIC for detection function model selection (e.g. Cassey and Mcardle, 1999; Ekblom, 2010; Borchers *et al.*, 2010) but their main interest was the robustness of DS estimates and its asymptotic properties, so large sample sizes were used. Moreover, the distances came from a particular shape of one detection function. One exception to this is Miller and Thomas (2015), who fit mixture models to a variety of DS detection functions and sample sizes. In some of the more challenging and potentially problematic scenarios considered, they found median biased estimators (an estimate is median-unbiased if it underestimates just as often as it overestimates) of average detection probability (they did not report bias in estimated abundance), even when the sample size was large. On the other hand, if the sample size was low or moderate, median biased estimators were found even in the standard cases, despite not being a comprehensive assessment. However, we have not found any simulation studies that consider the combination of a wide variety of true detection function shapes and range of sample sizes (low, moderate and large) using detection function model selection, hence the novel aspect of this study.

In this chapter, we evaluate by simulation the performance of DS estimators when assumptions $1-4$ hold and the model adopted for fitting the detected distances is selected from a set of candidate models, differentiating two cases: (1) including or (2) excluding the true detection function from the set of candidate models. We also test if the existing sample size recommendations are reliable, and compare LTS and PTS estimators over a range of detection function shapes.

The remaining sections are organized as follows. In Section 2 we describe the simulation scenarios and analysis strategies considered. We then present the main results in Section 3, while many additional results are given in online supplementary materials. Finally, in Section 4, we discuss the implications of our study for both simulation studies and real-world DS surveys.

2.2 Methods

The simulation was conducted using R software (R Core Team, 2014, version 3.2.4). For each simulated dataset, detection function estimation (see Section 2.2.2) was performed using the MCDS engine from the software Distance (Thomas *et al.*, 2010), except for the EPS true model, not available in Distance and hence coded in R. The simulation code is available in Appendix A (hereafter Appx. A).

2.2.1 Data simulation

The focus of our simulation was on the potential relative bias caused by detection function estimation. Hence, we used a very simple study region, animal distribution and spatial sampling scenario. Our results on bias will not be sensitive to these choices, so long as random sampling is used, however, those relating to variance and confidence interval estimation will be (e.g., Prieto Gonzalez *et al.*, 2017). The study region considered for simulation was the covered region: i.e., the area around the observer within which animals may be detected. Because we are focussing on model selection performance for detection function estimation, we ignore inferences beyond the covered area. Hence here surveyed area and covered area are equivalent. For the case of LTS, we arbitrarily assume a line length of $L = 2w$, making the covered area a square of side $2w$ (where w is the truncation distance), while for PTS, the covered area is a circular region of radius w. For both line and point sampling methods, the sample size of observations n was fixed to provide recommendations based on the sample size. This implies that the population size N within the covered region was a random variable, following a negative binomial distribution with expectation $E(N) = \frac{n}{P_a}$ (where P_a is the average probability of detection for the true detection function). Estimators were judged in terms of their ability to estimate this average abundance.

Animal locations were generated randomly from a uniform distribution on the study region. We generated a large enough number $\eta \gg n$ of locations in order to guarantee n detections. We calculated their distances y_i, $(i = 1, \ldots, \eta)$ to the line or point, and according to a given detection function g, a random draw from a Bernoulli with $p = g(y_i)$ determined whether each observation was detected or not, with the first n observations selected for analysis. (We note in passing that direct generation of the distances of detected animals (see, e.g., Buckland *et al.*, 2004, Chapter 11) is more efficient, but that the present study was part of a larger one looking at effects of animal movement, where the direct method is not possible.)

The detections were generated from 8 different parameterizations of 2 detection functions, with 2 parameters each (Figure 2.1): the hazard-rate (HR) and the exponential power series distribution (EPS) (Pollock, 1978).

$$\begin{aligned} &\text{hazard-rate:} && g(y;\sigma,b) &&= 1 - \exp\left(-\left(\frac{y}{\sigma}\right)^{-b}\right) && \sigma > 0;\ \ b > 0 \\ &\text{EPS:} && g(y;\lambda,\nu) &&= \exp\left(-\left(\frac{y}{\lambda}\right)^{\nu}\right) && \lambda > 0;\ \ \nu > 0 \end{aligned} \tag{2.1}$$

When $\nu = 2$ (EPS4), the EPS corresponds to the standard half normal (HN) distribution, frequently used in DS analysis.

In simulations, we fixed the truncation distance to $w = 30$. (While this distance was chosen with a particular application in mind, the results are general as the detection functions can be readily rescaled to any truncation distance.) Parameters of the true detection function were chosen such that $g(w) = 0.1$, in line with the recommendation from Buckland *et al.* (2001) that right truncation occur when $g(w) \approx 0.1$. The parameter values used are shown in Appx. Table A.1. They were chosen so that the resulting

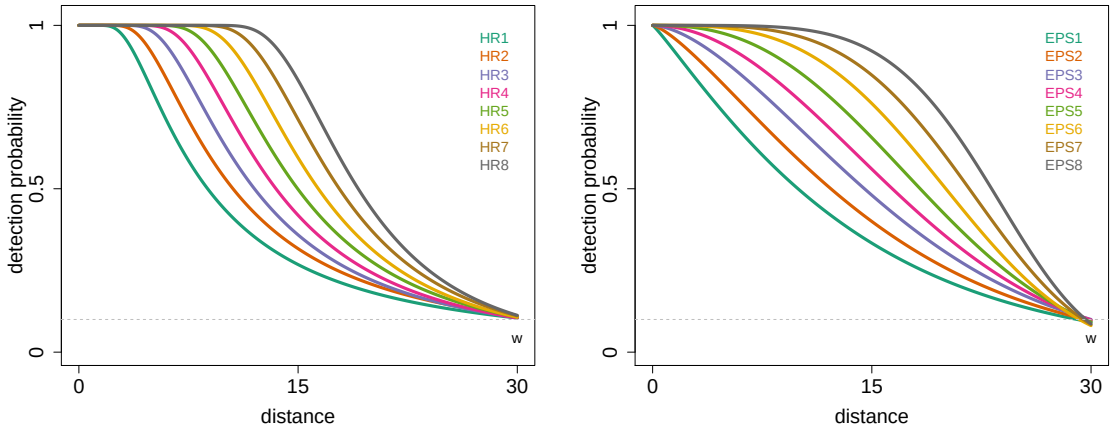

Figure 2.1: Different parametrizations of the true detection function to generate the observed distances. On the left a hazard-rate (HR) and on the right an exponential power series (EPS). The dashed line is $g(w) = 0.1$.

detection functions had a variety of shapes. The shoulder of the detection function is, in mathematical terms, the range of distances from the line or point for which the slope (g') is close to zero and the probability of detecting an animal is close to one. Thus, the shape of the detection functions considered goes from having no shoulder (also known as spiked data) to having a wide flat shoulder (c.f. Figure 2.1).

Sample sizes of $n = \{60, 90, 120, 240, 500, 5000\}$ were used to evaluate the estimator performance. For each sample size we simulated 4000 iterations, to reduce the relative Monte Carlo error associated with the standard error (calculated using Equation (7) in Koehler *et al.*, 2009) to below 1%.

2.2.2 Analysis of simulated data

For each of the simulated datasets, we fitted all the model combinations recommended by Buckland *et al.* (2001). The general form of a detection function is conceptualized in two parts, $g(y) \propto \text{key}(y)[1 + \text{series}(y)]$, a key function and a series expansion. The series expansion is used to provide additional flexibility to fit the data, if required. Each parametric key function was paired with the suggested series adjustment term given by Buckland *et al.* (2001) (Table 2.1).

Table 2.1: Detection function models fitted to the simulated data.

Key function	**Series expansion**
Uniform, $\frac{1}{w}$	Cosine, $\Sigma_{j=1}^{m} a_j cos(\frac{j\pi y}{w})$
Uniform, $\frac{1}{w}$	Simple polynomial, $\Sigma_{j=1}^{m} a_j (\frac{y}{w})^{2j}$
Half-normal, $exp(\frac{-y^2}{2\sigma^2})$	Cosine, $\Sigma_{j=2}^{m} a_j cos(\frac{j\pi y}{w})$
Half-normal, $exp(\frac{-y^2}{2\sigma^2})$	Hermite polynomial, $\Sigma_{j=2}^{m} a_j H_{2j}(y_s)$ where $y_s = \frac{y}{\sigma}$
Hazard-rate, $1 - exp(-(\frac{y}{\sigma})^{-b})$	Cosine, $\Sigma_{j=2}^{m} a_j cos(\frac{j\pi y}{w})$
Hazard-rate, $1 - exp(-(\frac{y}{\sigma})^{-b})$	Simple polynomial, $\Sigma_{j=2}^{m} a_j (\frac{y}{w})^{2j}$

$g(y) \propto \text{key}(y)[1 + \text{series}(y)]$, where y is the distance of the target object, w the truncation distance, and σ and b the scale and shape parameter respectively; m is the maximum number of terms in the series expansion, $a_j \in \mathbb{R} \forall j = 1, \ldots, m$ is the parameter of term j.

As is standard in the Distance software, we selected the number and order of adjustment terms required for the analysis using sequential forward selection, starting with no adjustments and adding one at a time so long as the resulting model had a lower AIC than the previous one. We considered at most 5 parameters for the detection function, the default in the Distance software. When adjustments are selected, the detection function can be non monotonic. The default in Distance, to constrain the fitted functions to be monotonically non-increasing (i.e., either flat or decreasing), was also considered. This is referred to as simulation scenario 1.

A potential source of bias when the true detection function has a wide shoulder is model selection being too conservative or/and the monotonicity constraint. Consequently, we investigated further running five additional simulation scenarios. First (scenario 2.1), we relaxed the monotonicity constraints on the detection function, allowing the curve

to take any possible form, constrained to be non-negative. Second, besides turning off the monotonicity constraint, we also set the number of parameters to be the same in all the candidate models. This should lead to select the model which fit the best when the parameter penalty was the same for all of them. Because the true models both have two parameters, we restrained the number of parameters first to two (scenario 2.2) and then three (scenario 2.3), being the goal of the three parameter model constraint to test whether the 2-parameter detection function was flexible enough. This implies 0 or 1 adjustment terms for HR, 1 or 2 for HN, and 2 or 3 for uniform keys, respectively for Scenarios 2.2 and 2.3. Finally, we constrained the number of parameters to two (scenario 2.4) and three (scenario 2.5) without the monotonicity constraint being lifted (Table 2.2).

Table 2.2: Summary of simulated scenarios

Scenario	**Monotonicity constraint**	**Parameters**
1	Yes	up to 5
2.1	No	up to 5
2.2	No	2
2.3	No	3
2.4	Yes	2
2.5	Yes	3

For all of the simulated scenarios we report results when just the true detection function (HR or EPS) was fitted, and also when model selection, as described above, was performed. In a few cases, an error occurred when fitting the detection function (e.g., due to lack of convergence); in these cases the data were regenerated. Note, when the data were generated from an HR model, the true model was in the candidate set for being selected, whereas the EPS distribution, not being available in Distance, was never included in the candidate set (except for the special case of the half normal parametrization, $\alpha = 2$). As a consequence, we could not use Distance software to fit the EPS under the true model scenarios, and the R function "optim" was used instead. Again, cases where the algorithm did not converge were discarded.

As noted above, we selected a priori parameters such that detection probability at the truncation distance, $g(w)$, was approximately 0.1. Because more truncation tends to reduce the bias when we select the wrong model, we therefore investigated the effect that

truncating the data at the analysis stage has on bias, by using $w = 20$ for a sample size of 240.

2.2.3 Processing of results

The median percentage bias in $\hat{N}$ was estimated for the 4000 replicates of each scenario: for each set of parameters of the HR and EPS true model, in both LTS and PTS scenarios and for each sample size. We calculated both the bias produced by the selected detection function, under model selection (i.e., the function with lowest AIC for each replicate dataset) and by the fitted true detection function. Instead of more commonly used mean percentage bias, we considered median bias to reduce the influence of some very large overestimates of N that occasionally occurred. The mean percentage bias is given in Appx. A. We also show percentage bias in $\hat{P}_a$ in Appx. A, for comparability with Miller and Thomas (2015). For plotting purposes the percentage bias was represented as smooth lines across the eight parametrizations of the true model, to show a pattern with increasing sample size.

Estimator performance was also evaluated by the percentage relative root mean square error (RRMSE), which measures the overall variability, incorporating the variance of the estimator and its bias.

The 95% confidence intervals on average probability of detection were estimated for each iteration. We considered $\hat{N}$ to be log-normally distributed, as described in Buckland *et al.* (2001, Section 3.6.1). We also present in Appx. A coverage probabilities (proportion of intervals containing the true value) for confidence intervals for N.

2.3 Results

As expected, abundance estimators were close to median-unbiased when the true model was fitted, and bias decreased with increasing sample size. By contrast, under model selection, there was a consistent pattern in median bias: bias was negative for data generated from detection functions with a small shoulder and positive for those with a wide shoulder (Fig. 2.2; raw results are given in Appx. Figs. A.1 - A.4). The pattern was stronger for points than lines, and for smaller sample sizes. For the HR model, median bias at $n = 60$ ranged from -3% to $+8\%$ for LTS and -8% to $+15\%$ for PTS. Results were worse for the

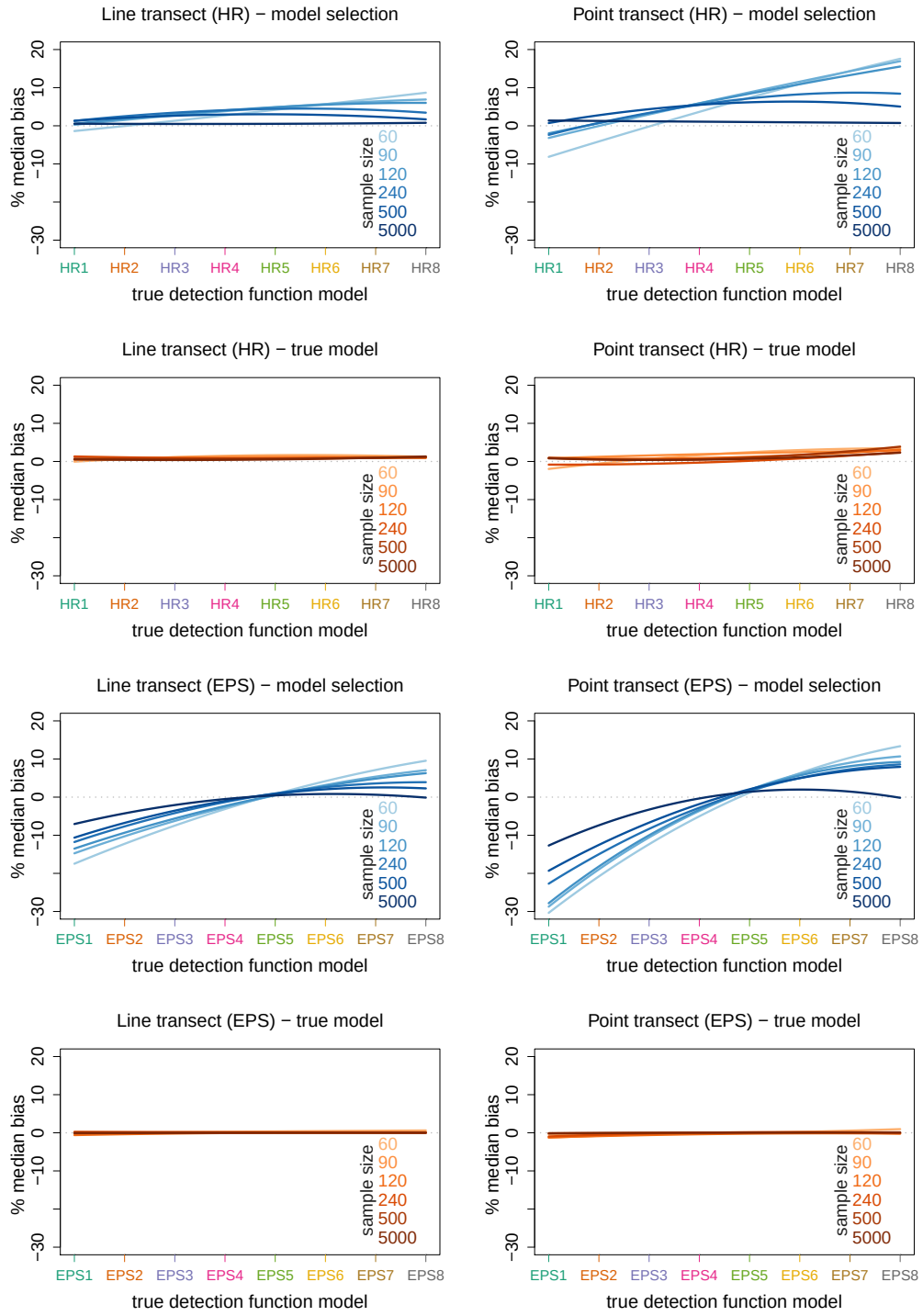

Figure 2.2: Percentage median-bias using detection function model selection (blue lines) and true model (orange lines) as model for inference for 8 sets of parameters of the hazard-rate (HR) and exponential power series (EPS) distributions, over a range of sample sizes, $n \in \{60, 90, 120, 240, 500, 5000\}$. Shown are smoothed lines of the point results. For point results see Appx. Figs. A.1 - A.4.

EPS model, where the true model was not in the candidate set: median bias at $n = 60$ ranged from -15% to $+10\%$ for LTS and -30% to $+10\%$ for PTS. Median bias in P_a was smaller than in N, but followed the same pattern (Appx. Table A.4-A.5). One exception was the EPS model for PTS scenario under model selection, for which spiked data reached 40% bias with $n = 60$. For the recommended minimum sample sizes by Buckland *et al.* (2001), the percentage mean bias in N was generally positive ($< 10\%$ and $< 20\%$ for LTS and PTS respectively) even when the true model was fitted (Appx. Figs. A.5-A.8). The only exception was when using the EPS under model selection where we found negative bias for EPS1-3. The mean bias was generally small when the true model was fitted, and decreased as sample size increased, so that it was effectively zero for n=5000.

To better understand the change in bias with changing detection function shoulder width under model selection, we examined the percentage of times each type of key function + adjustment model was selected, and also the proportion of times a model with k parameters, where $k \in \{0, 1, \ldots, 5\}$, was chosen (Appx. Figs. A.10-A.11). Due to the similar patterns across sample sizes and LTS versus PTS, we focus here on a sample size of 120 observations, which should be adequate for good model selection (Fig. 2.3). More than half of the time (except for HR1-4) a 1-parameter model was selected: either unif+cos (Fourier series), unif+simple polynomial expansion, both with only one adjustment term, or HN with no adjustments. HR was not selected often, even when HR was the true model. In this situation it was selected slightly more when the detection function was spiked or flat. One parameter models took over increasingly as the shoulder of HR detection function widened (e.g., HN takes over HN+cos). When EPS was the true model, unif+simple polynomial expansion seemed to take over from unif+cos with the wider shoulder. When data were generated by an HN (EPS4) function, and hence the true model was included in the set of candidates for model selection, despite the true function not being selected most often, the estimator was nearly median-unbiased. Thus AIC seemed useful for selecting the best model for predicting P_a in the set, which was not always the true model.

Further, to understand how different models being selected influence bias we examined the relationship between the selected model and observed error (i.e., difference between estimate and true value). We focus here on the worst scenario in terms of bias for the selected 120 sample size, i.e., EPS under PTS (Fig. 2.4); results for the other scenarios were similar but less extreme (Appx. Figs. A.12-A.15). For parametrizations with narrow shoulders (EPS1-4) most of the selected models tended to underestimate N. From EPS4

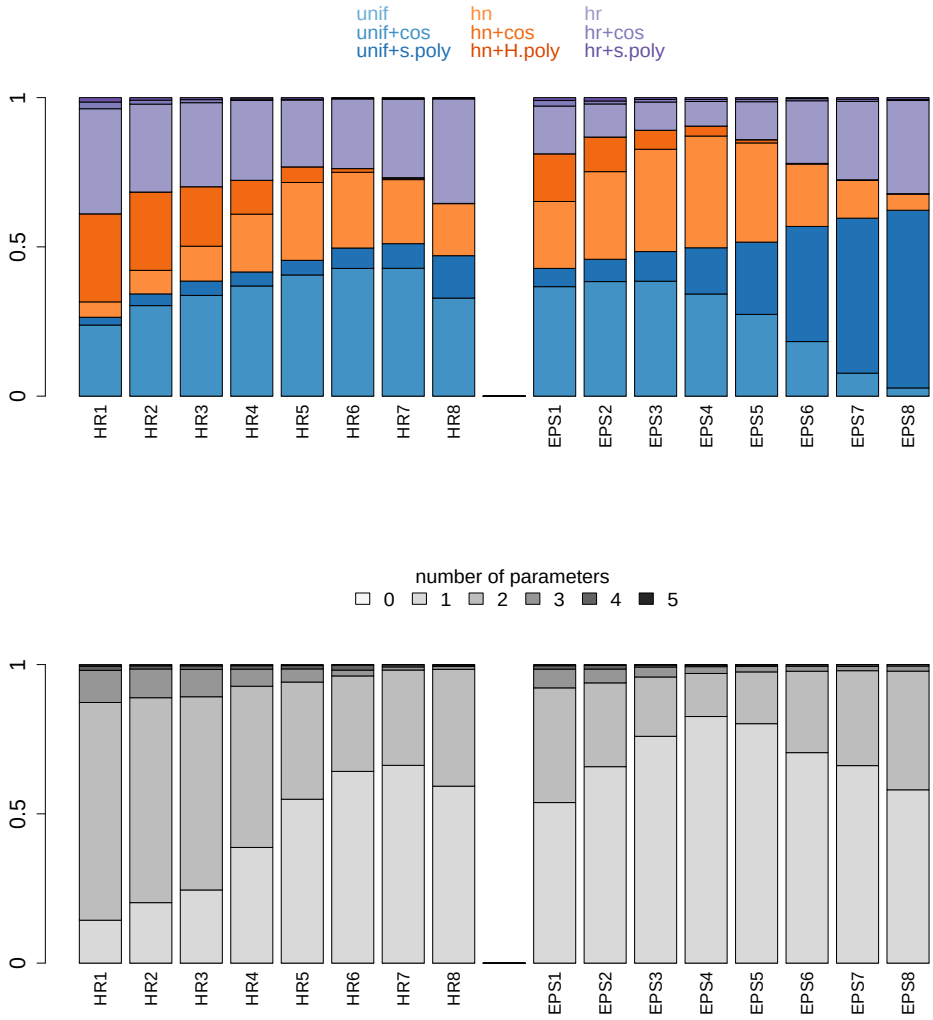

Figure 2.3: Proportion of time each candidate model class (above) and a model with a given number of parameters $k \in \{0, 1, \ldots, 5\}$ (below) is selected in a point transect scenario for the 8 sets of parameters of the hazard-rate (HR) and exponential power series (EPS) distributions, when the number of observations is n=120.

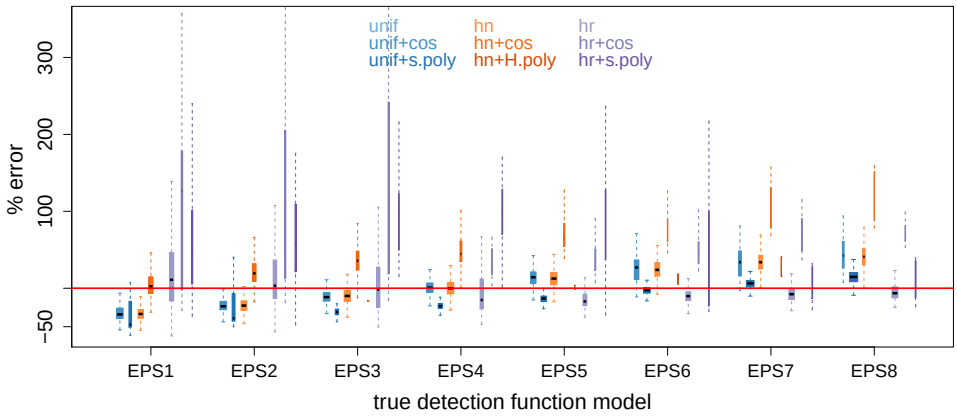

Figure 2.4: Percentage error introduced by each model of the candidate set of model selection detection function, for the 8 sets of parameters of the exponential power series (EPS) distribution under point transect sampling, with a sample sizes $n = 120$. Box plots width is proportional to the number of times each model is selected.

onwards, estimators were unbiased for almost all selected models, until those parametrizations with a flat wide detection function shoulder (EPS7-8) where almost all of the models overestimated N on average. This pattern was consistent for all the selected models except for the HR, which seems to be the only model in the candidate set of model selection with the opposite pattern: from positive to negative error with increasing shoulder width. However even when the HR was the true model, 1 parameter models were more often selected. Outlier sample estimates, with the largest absolute errors, seemed to be associated with the HR + adjustment term models. The number of outliers decreased when sample size increased. When the true model was fitted, the percentage error was smaller (Appx. Figs. A.16-A.19).

Examining the fitted individual detection functions (Fig. 2.5), we see that when the true detection function showed a strong "spike" (i.e., probability of detection declined steeply with increasing distance for small distances, e.g., EPS1), the fitted functions tended on average to be flatter than the true detection function. This resulted in overestimation of P_a and hence underestimation of N. Conversely, when the true detection function had a wide shoulder (e.g., EPS8), the fitted functions tended on average to have a more rounded shoulder and hence underestimated P_a and overestimated N. These pat-

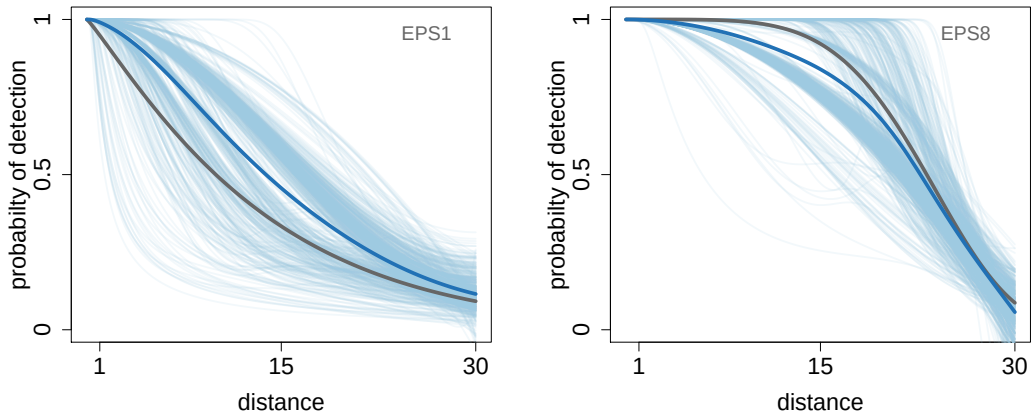

Figure 2.5: Set of detection functions fitted using detection function model selection (in blue lines) with the average detection function represented by the thick blue line, when the data are generated by the EPS1 and EPS8 distribution (grey line) in a point transect sampling with 120 observations scenario.

terns are intuitively sensible once we overlay a representative fitted detection function to the data it is being fitted to. When we had spiked data (e.g., Fig. 2.6), we tended to have models that cut the spike of the observed distance distribution (having a lower intercept), resulting in overestimating $\hat{P}_a$, and therefore underestimating $\hat{N}$. By contrast as the shoulder of the detection function widened, the opposite happens. $\hat{P}_a$ was underestimated since the average detection function had a rounder shoulder leading to a positive error on the density estimate. This did not happen to the same extent when the true model was used (Appx. Figs. A.20-A.21).

The percentage bias when the monotonicity constraint is removed (scenario 2.1) was lower than that of a monotonically decreasing detection function (Appx. Fig. A.22). Moreover, fixing the number of parameters to either two or three respectively (scenarios 2.2 and 2.3), the median bias was even more reduced (Appx. Figs. A.23-A.24). This resulted in nearly median unbiased estimators for a wide shoulder. However, we obtained similar results when the number of parameters was constrained to either two or three while retaining the monotonicity constraint (scenarios 2.4 and 2.5), (Appx. Figs. A.25-A.26).

The results presented above had a Monte Carlo Error $< 1\%$ in the vast majority of cases, with a maximum of 4% (Appx. Fig. A.27).

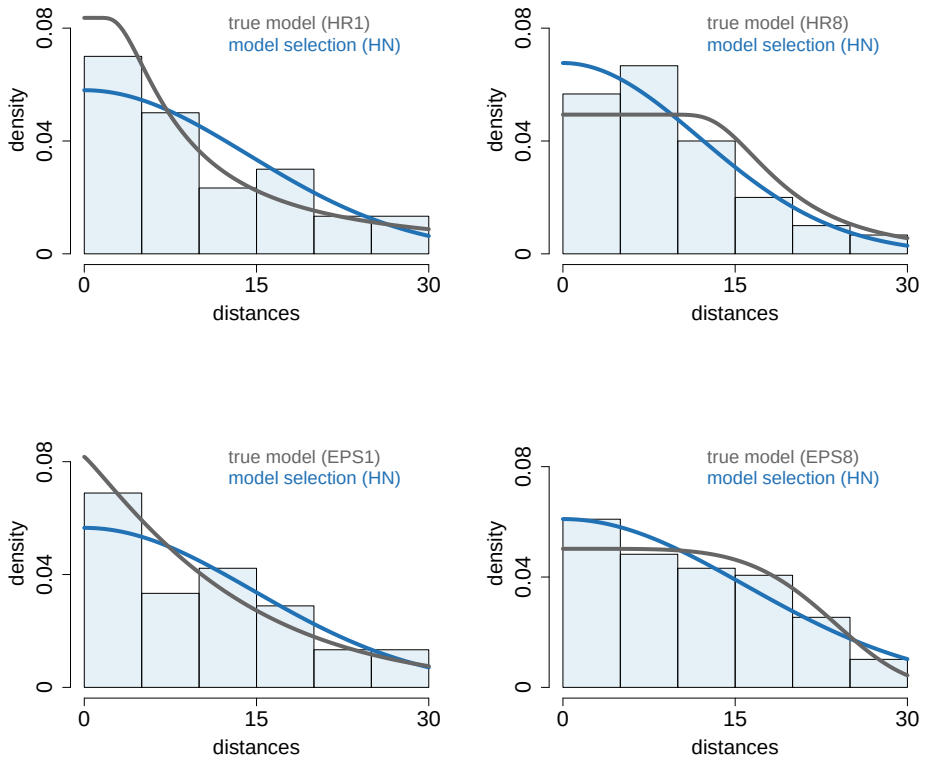

Figure 2.6: Examples of a particular set of observations (with sample size 120) generated by the first and last parametrization of a HR and EPS distribution (grey line) where the model fitted using detection function model selection is an HN (in blue line) for a line transect sampling scenario.

The RRMSE was, as expected, higher for PTS than LTS, and it decreased as the detection function shoulder widened for a given sample size (Appx. Fig. A.28). When the observations came from a HR model the pattern was almost identical under model selection or fitting the true model. However, for smaller sample sizes of the EPS model, the RMSE was higher fitting the true model than under model selection.

Confidence interval coverage was close to the nominal value when the true model was used, and always lower under model selection (Appx. Fig. A.29). Under model selection, for HR there appeared to be no particular pattern with width of the shoulder, and in general (but not always), coverage was closer to the nominal level of 0.95 with a large

sample size. However, for EPS, coverage appeared to be worse for both spiked data and for wide shoulders, and coverage was low even with large sample size (e.g., around 50% for ESP1 and ESP8 with $n = 500$).

Reducing the truncation distance to $w = 20$, did not help with model selection. Simulations showed no significant improvement in the problematic cases (see Appx. Fig. A.30).

2.4 Discussion

The Horvitz-Thompson estimator is unbiased (Horvitz and Thompson, 1952). However, even when assumptions are met, DS Horvitz-Thompson-like estimators are no longer unbiased, but at best asymptotically unbiased. Estimators that are unbiased for P_a will be positively biased for $N = n/P_a$, because symmetric errors about P_a lead to right-skewed errors about $1/P_a$. This is indeed what we found: when the same model is used to generate distance data and analyze those data, the estimates are close to mean-unbiased in $\hat{P}_a$ (see Appx. Tables A.2-A.3) and median unbiased in $\hat{N}$, even for small sample sizes (e.g., $n = 60$); however they were positively mean-biased in $\hat{N}$. Much of the bias was caused by a few (approx 3%) small values of $\hat{P}$ that produced extremely high values of $\hat{N}$ (see also Buckland *et al.*, 2015, p.117). This result applies both to PTS and LTS (although it is much less marked for LTS) over a wide range of detection function shapes and even at moderate sample sizes (e.g., n=240) in some cases. Hence, in the results section, we presented percentage median bias instead of mean bias (results for mean bias are shown in Appx. A).

When standard methods are used to implement selection among a commonly-used suite of candidate models, median bias can occur for some detection function shapes, even at large sample sizes. Under model selection we found median biased in P_a (Appx. Fig. A.9 -in addition to mean positive bias, Appx. Tables A.2 and A.3-) from positive to negative being worse for PTS than LTS. As would be expected, this led to the opposite pattern of median bias in N: negative to positive bias with increasing detection function shoulder width. However, because of the nature of the estimator of $\hat{N}$, estimates were still positively biased even with large sample sizes (e.g., $n = 500$). $\hat{N}$, as expected, remained asymptotically unbiased.

When a realistic (for most studies) sample size (i.e., < 240) is considered, we found the bias under model selection depends on several factors: the shape of the true detection function, the use of monotonicity constraints and the number of parameters of the models in the candidate set used for model selection.

First, the median bias in N varies according to the shape of the detection function. Negative bias is caused when data arising from a spiked detection function, positive when the detection function has a flat wide shoulder, and in between we find unbiased estimators. The reason is that, for a given selected model, in the majority of cases, bias moves from negative to positive with increasing shoulder width (Fig. 2.4, Appx. Figs. A.12-A.15). An exception is the HR and HR+adjustments, which show the opposite trend. However those models need 2 or more parameters to be fitted and, although the true model provides a good fit to these spiked and wide flat shoulder data, it is not always chosen; more often ($> 50\%$) a 1-parameter model is selected instead. Therefore, the average selected detection function has a more rounded shoulder than the true model. This leads to an overestimation of P (underestimation of N) for more spiked detection functions and underestimation of P (overestimation of N) for detection functions with wider shoulders. Note that the spiked EPS1 had twice the percentage bias for PTS than for LTS surveys (Fig. 2.2; Appx. Tables A.3 and A.5): not surprising since the pdf at zero distance is critical and more difficult to estimate in the former than in the latter.

The second factor affecting the bias is the use of the monotonicity constraint in conjunction with the number of parameters of the selected models. The monotonicity constraint is used because we expect a priori that the true detection function is a monotonic non-increasing function of distance from the point or line. However, under some circumstances a simulated dataset is best fit with a non-monotonic function, so the constraint is triggered and the obtained estimates are no longer maximum likelihood estimates but constrained maximum likelihood estimates. This happens when by chance there is a small "bump" (cluster of detections) at some distance away from the line, which unconstrained forward selection of adjustment terms might fit with an extra adjustment. When removing the monotonicity constraint and fixing the number of parameters to be greater or equal than 2, these "bumps" get fitted. This extra flexibility results in a reduction of bias, since P_a is underestimated when using a detection function with narrow shoulder, and overestimated under wide flat shoulder models. The true detection function is naturally expected to be a non-increasing function of distance. Hence the monotonicity constraint is consistent with the process being modelled and therefore, it is sensible. On the other

hand, keeping the monotonicity constraint, while fixing the number of parameters to 2, leads to a similar reduction of bias. For LTS, we obtain median unbiased estimators when the true detection function has a wide shoulder while for PTS median bias is $< 6\%$. As a consequence, if there are no assumption violations and we are still interested in a problematic detection function shape, we suggest keeping using monotonicity constraints and avoid fitting 1-parameter models. Essentially the detection function shape close to zero is critical, so 1-parameter models lack flexibility and there is insufficient information in the few observations close to zero (especially for PTS) for AIC to select a reasonable model.

The same results were found in Prieto Gonzalez *et al.* (2017), where for each simulation iteration, a fixed number, N, of animals were located at random according to a uniform density distribution within the same study region A = 1 km^2. Then, a fixed number of transects were laid at random locations within the area, making the covered area a = 0.30 km^2 in both cases, LTS and PTS.

Bias should not be the only criterion for evaluating estimator performance as we want estimates with a good balance between accuracy and precision. Yet the biased simulation scenarios also result in greater overall variability when narrow shoulder detection functions. We also observe more variability when the true model is fitted and when the sample size is low. The RRMSE for the EPS true model was slightly higher than when model selection is used. This may be due to the optimization routine. When EPS true model is used, fitting occurs in R and we found that the CDS engine in Distance was more robust than optim, the R function we used for optimization. In 17 cases out of 4000 iterations (0.425%) a P_a estimate lower than 0.04 was found, giving high values of N (see Appx. A, Fitting issues section).

Confidence interval coverage was close to the nominal value when the true model was fitted. Due to the bias found when using model selection over spiked data and wide true detection function shoulders, confidence interval coverage declined to almost 50% in these cases. Our results suggest that when a model selection exercise is conducted, accounting for model uncertainty should be considered (Burnham *et al.*, 2011). This should lead to wider intervals and so corresponding improved confidence interval coverage.

Reducing the truncation to $w = 20$, did not reduce bias under model selection scenarios. One might think that the more the data are truncated, the less effect the tail of the detection function has in the estimation of $g(0)$, and hence a more plausible abundance

estimator would be obtained. However, this was not the case here, since no considerable improvement was found in the problematic cases (see Appx. Fig. A.30).

One factor we did not consider is the model selection criterion used to select models. Here, we used AIC (Akaike, 1974) as the selection criterion and automatically chose the model with the lowest AIC (using a forward selection procedure for adjustment terms). AIC was chosen because it is by far the most common option amongst practitioners and it gives the best out-of-sample prediction (Sober, 2002; Burnham and Anderson, 2002). That is to say it is designed to find the "best" model for making predictions (in a RMSE sense) given a new data set. Despite the widespread use of AIC, practice, simulation, and theory indicate that the use of AIC leads to selection of overly complex models when truth is low-dimensional (Taper and Lele, 2010) (Note that the real world tends to be high-dimensional and then AIC does not select overly complex models (Buckland *et al.*, 1997)). On the contrary, in this low-dimensional context, our results suggest that it selects too few parameters on average, leading to overly simple models. Typically, in practice, given a suitable truncation distance, an adequate model for $g(y)$ will include only one or two parameters, sometimes three (Buckland *et al.*, 2001). Here, most of the time ($\gtrapprox 90\%$) less than 3 adjustment terms were required. One of our concerns was that models with fewer parameters would be selected more often. The choice between different model selection approaches, e.g., AIC, AIC with a correction for finite sample sizes (AIC_c), Bayesian information criterion (BIC, Schwarz *et al.* (1978)), likelihood-ratio tests (LRT), reflects the choice of penalty to avoid overfitting and it should depend on the purpose of modelling (Brewer *et al.*, 2016). For instance, BIC tries to find the "true" model if it exists in the candidate set (or a "quasi-true" model otherwise). Shmueli (2010) suggests that AIC is optimal for prediction and BIC for explanatory modelling. However, we did not want to identify the true model as it would never be in the set of candidates in a real analysis (e.g., Buckland *et al.*, 1997). This is in concordance with Aho *et al.* (2014) or Shibata (1981), which show the optimality of AIC, based on the idea that is not possible to have enough data to be able to estimate the true model. AIC_c on the other hand, takes into account sample size by, essentially, increasing the relative penalty for model complexity with small data sets (Hurvich and Tsai, 1989). As sample size gets larger, AIC_c converges to AIC, this is typically the case in distance sampling where sample size is large and the number of parameters is comparatively small, so the two will be little different. The LRT is only applicable when one model is a special case of the other (i.e., the models are nested) and is not designed for model selection for forecasting. We could also have considered

multi-model inference as alternative. This would make an interesting future study, but it would also be important in this case to consider generating models from true detection functions with more than 2 parameters, to better emulate real-world detection functions.

To sum up, among other factors, the degree of bias depends both on sample size and the shape of the detection function data is generated from. A simulation analysis allows us to control both factors, while in real life scenarios we have little control over them. Therefore, we will discuss both situations separately.

2.4.1 Advice on conducting simulation studies

As DS estimators are asymptotically unbiased, with a large enough sample size (e.g., 5000) the bias is negligible. Therefore, when the purpose of the simulation is to evaluate effects of violation of assumptions, without the results being affected by small-sample issues, we recommend using very large sample sizes, so results remain unbiased when all assumptions hold. The disadvantage is that we usually are interested in simulating plausible scenarios and a large sample size is unrealistic in most real life scenarios. For the recommended sample sizes, we advise carefully choosing the shape of the detection function, avoiding functions with no shoulder but also with a wide flat shoulder. We recommend an HN or other model where animals are detected with near certainty until $> 0.1w$ distance and then where detectability declines gradually with distance (i.e., a "round shoulder"). We advise using AIC for conducting model selection, and using the monotonicity constraint when estimating the detection function. Under these circumstances, provided a detection function with the shape recommended above is used, median unbiased estimates of abundance are obtained.

2.4.2 Analysing Real-world Data

Good survey design and field methods are crucial for the performance of DS methods. A critical assessment of assumption violation is fundamental. When all the assumptions are met, our results show that two scenarios lead to large bias: spiked data and wide flat shoulder data. Both are typically avoided using appropriate field procedures. A way to ensure a shoulder (i.e., the shape criteria on the detection function) and hence robust estimation is to ensure adequate search effort at and close to zero distance. This can be checked during a pilot survey, and at early stage of data collection in the main survey,

by examining histograms of the collected distances, and then adapting the field protocol as required (see, e.g., Anderson *et al.*, 2001). Therefore, appropriate field procedures should avoid spiked data and observing spiked data is often indication that an assumption might have been violated. A wide shoulder is also unlikely to be encountered in practice, given the effect of heterogeneity between observations in detection probability caused by differences between animals (size, behaviour, etc.), habitat, observers and sighting conditions. Buckland *et al.* (2004, p.339) demonstrated this via a simulation study; the simulation considered a hazard-rate model with a random scale parameter. The distribution on the scale parameter was meant to reflect heterogeneity in detectability across a range of factors. The resulting true detection function had a more rounded shoulder than any of the individual hazard rates. Hence, the resulting distance data tend to have a rounded shoulder, rather than a wide flat shoulder followed by a steep fall-off, which the HN model would fit much better than an HR. We continue to recommend the use of the monotonicity constraint. "Bumps" in the collected distances are usually spurious due to either randomness or related to poor data collection (e.g., some observer bias, possibly constraints on data collection, or animal movement). In these situations the monotonicity constraint usually helps to estimate P_a.

Modelling a detection function is a skilled process. It is only from the combination of rigorous model selection tools like AIC, goodness of fit tests, and knowledge about the underlying system under study, that the optimal model choice arises. Some a priori knowledge about what detectability might look like and which assumptions are likely to be violated is fundamental to guide the modelling exercise. The ultimate goal is to put in place survey methods leading to data such that results are robust to choices made at the analysis stage. In practice, and perhaps frustrating for practitioners, it is not possible to define a set of cookbook rules for fitting detection functions.

Here we report that bias due to model selection can be considerable. This raises general questions for model selection in real life studies, whenever the true model is unknown. DS is a simple method under which bias from assumption violation is well understood. Our results beg the question of how model selection might affect bias obtained for derived parameters under other techniques, such as capture recapture models.

Part II

When animals refuse to stay still

3

The effect of animal movement on abundance estimates

3.1 Introduction

As any other method for estimating animal abundance, plot sampling (PS) and distance sampling (DS) estimators are derived under a number of assumptions that ensure the methods are asymptotically unbiased. Here we focus on both methods.

Plot sampling assumes that all the individuals within the covered area are detected. This implies that the number of animals in the covered region is fixed, i.e., no animal crosses the boundary during the time the survey take place. Therefore, animal movement across the boundary of the covered area results in violation of this assumption and hence overestimation of abundance due to the arrival of new animals to the encounter region.

In the early development of distance sampling, the original estimators required animals to move, because they were designed for birds that "flush" when observer gets too close. However, as presented in Chapter 2, asymptotically unbiased distance sampling estimators require a set of assumptions to hold (Buckland *et al.*, 2001, pp. 29-37):

1. Transects are located at random, ensuring that animals are distributed independently of the transects. This ensures the true distribution of animals with respect to the lines or points is known (being uniform or triangular, respectively).
2. Animals are detected with certainty at the line or point, $g(0) = 1$.
3. Distances are measured without errors.

4. The survey can be seen as a snapshot in time, during which animals do not move.

If these key assumptions do not hold then estimates of abundance can be substantially biased. Several methodologies have been developed to deal with assumption violations.

The first assumption depends entirely on the researcher(s) conducting the survey. It will hold by design, and usually in practice a regular grid of transects with a random start is preferred to a purely random layout, the latter ensuring an even coverage of the study region and corresponding lower variances when compared to the former (Fewster *et al.*, 2009). A typical violation of this assumption happens when the survey takes place following some paths already existing, along which density might be different from areas away from the paths, and hence extrapolation of the animal density to the wider study region is not possible. Spatially explicit capture-recapture (SECR) or mark recapture distance sampling (MRDS) methods may be used when the second assumption is not met (Borchers *et al.*, 2006; Buckland *et al.*, 2010). Similarly, measurement error models may be applied when the third assumption is violated (e.g., Marques, 2004; Borchers *et al.*, 2010). Finally, Glennie *et al.* (2015) analysed the implications of not meeting the fourth assumption using line transect sampling (LTS). Here, we concentrate on the effect of animal movement on point transect sampling (PTS) abundance estimates.

Wildlife movement has long been recognized as an important problem for DS methodology (Burnham *et al.*, 1980). Conceptually, a DS survey should be a snapshot in time (Buckland, 2006; Buckland *et al.*, 2001, pp. 31), in other words, the survey takes place in an instant of time. The method assumes that movement of animals does not occur while within detection range. Animals are considered to be at a fixed location while the survey takes place, or if they move, that they are detected at their initial location. In LTS this results, conceptually, in probabilistic encounters between a moving observer and immobile animals (Gurarie and Ovaskainen, 2013). Some movement in a LTS context should not be a problem as long as the observer is moving fast relative to the animal's speed (Glennie *et al.*, 2015). Bias from independent animal movement is also reduced by the observer looking ahead a shorter distance and searching further perpendicular to the transect and by ignoring animals that may overtake the observer from behind (Glennie *et al.*, 2015). By contrast we concentrate here in PTS, for which the observer is stationary and the problem of animal movement is therefore more serious - after all, a moving animal is moving infinitely faster than an immobile observer! Although DS relies upon the idea that animals are observed at one instant of time, in practice detections occur over some

time interval. Bias arising from wildlife movement naturally increases with time spent at the point (with the exception of responsive movement away from the observer), thus typically (for songbird surveys) a 5-10 minute interval, as suggested by Bibby (2000) and Buckland *et al.* (2001), is recommended.

We can distinguish two types of animal movement: responsive movement, towards (attraction) or away from (avoidance) an observer, and random movement independent of the observer. Density is overestimated when there is movement towards the observer and underestimated when movement is away from the observer (Bollinger *et al.*, 1988; Buckland *et al.*, 2001, pp. 173). For instance, the size of the bias on PTS estimators (by responsive movement in birds) has been examined using real-world data by Wildman and Ramsey (1985), Bibby and Buckland (1987) and Roeder *et al.* (1987), who considered a range of models for disturbance to account for the "doughnut" effect, in which birds move away from the point as the observer approaches.

In this thesis we focus on independent random animal movement. Encounters defined by animal movement can be modelled, with model parameters representing different behaviours, average animal speed, "disturbance" radius, and so on. However, these are difficult quantities to estimate and hence some models assume that animals behave like particles in an ideal free gas movement model (Hutchinson and Waser, 2007), which is unrealistic in practice. Random movement causes upward bias in estimated abundance for two reasons. First, if animals move, then some will come within detection range during the survey that were not there at the beginning, leading to an inflated encounter rate. Second, animals are more likely to be detected at closer than further distances, and hence for a randomly moving animal the expected detection distance is less than the average animal distance. This under-estimation of the average distance of detected animals leads to an underestimation of detection probability and over-estimation of abundance. This latter effect is worse for PTS than LTS because of the sampler geometry and the effect of the probability of detection at closer distances to the observer.

When movement occurs over an interval of time (responsive or independent of the observer), density in the survey area is no longer representative of the wider area. The aim of this chapter is to evaluate the performance of abundance estimators on both circular plot sampling (CPS) and PTS when animals move during the survey period spent at a circle or point. In Section 3.2 we introduce four models of wildlife movement independent of the observer with constant speed: (1) linear movement independent of the observer

(animals move in straight lines with individual random direction); (2) a simple random walk; (3) a correlated random walk and (4) a biased random walk, with a center of attraction, corresponding, for example, to the situation where we have animals with well defined home ranges. In Section 3.3, a simulation exercise is considered to evaluate the effect of the different animal movement scenarios considered on the performance of both CPS, assuming perfect detectability on the covered circles, and PTS, where animals on the covered circles have imperfect detection. In PTS, when detection falls off with distance from the point, a range of detection functions are used. Standard methods (Buckland et al. 2001) that ignore movement are used to estimate abundance, and we use standard model selection methods to choose among a set of candidate detection functions during the estimation process. The results are presented in Section 3.4. Section 3.5 discusses the obtained results, leading naturally to Chapter 4 and 5, where estimators correcting for the bias found will be considered.

3.2 Animal movement scenarios

For estimating animal abundance when individuals are moving, some animal movement scenarios need to be considered. One way to classify movement models is as either occurring in discrete time or continuous time. Clearly, animal movement occurs in continuous time but we observe it at fixed discrete-time intervals. Thus, continuous time is conceptually and theoretically appealing, although discrete time models are often more tractable and, in practice, more intuitive to interpret (McClintock *et al.*, 2014). The differences and similarities between continuous and discrete versions of mechanistic movement models are explored by McClintock *et al.* (2014), who also indicate under which circumstances one form might be preferred over another.

In this work a discrete time formulation is used. There are two important disadvantages of discrete-time models. (1) The first is related to the necessary discretization of the movement path into a finite number of temporally-regular time steps. Hence, the step length must be specified a priori, but inferences about animal movement from a discrete-time analysis change depending on the time scale used. The specification of the length of the time step is therefore critical and requires very careful consideration (e.g., Codling and Hill, 2005; Hooten *et al.*, 2014), being particularly important that the time step is chosen to match the scale at which behavioural decisions are made. This disadvantage in discrete-time models is an advantage for continuous-time formulation since they

do not depend on a particular time scale, leading to the same results regardless of the temporal resolution of observations (McClintock *et al.*, 2014). (2) Moreover, discrete-time movement models can be more computationally demanding than continuous-time models.

Here, we describe two modes of movement, linear and biased random walk, which are used to examine bias caused by movement in CPS and PTS. Before introducing the biased random walk, we first describe its simpler, unbiased cousin and also the correlated random walk as a contrast with the uncorrelated walk that we deal with in the rest of the Chapter.

While over medium-term and long-term time scales, realistic descriptions of animal movement should account for the fact that animals switch between different behavioural (and so movement) modes. When considering CPS and PTS we note that the time scale within which individual animals can interact with the observers is typically short. Hence, in general, it will be rare that animals switch behavioural mode while within range of the sensor/observer. For this reason, as well as for simplicity, we only consider single modes of movement.

Linear movement and biased random movement were chosen to quantify the effect on abundance estimators because these two modes should bracket the range of bias we expect for a given animal speed. The first represents maximum displacement per unit time for a given speed (given an upper bound on bias), and the latter (since the turning angles will tend to be large) represents minimum displacement.

3.2.1 Linear movement

In this mode, each animal i, is assumed to travel in a straight line with direction being uniform in the circle, $\theta_i \sim U(0, 2\pi)$, at constant speed u. This may be a realistic model to approximate the movement of, for example, migrating animals, or those moving between known foraging patches.

3.2.2 Random walk (Brownian motion)

A random walk (RW), also known as a stochastic, random process or simple isotropic random walk, describes a path that consists of a succession of random steps on some time (Brown, 1828; Pearson, 1905; Spitzer, 2013).

Figure 3.1: Random walks movement scenarios during 5 minute period (300 seconds) with constant speed u =1m/s. All the animal's paths started in the same initial coordinates represented by the grey asterisk.

The movement is uncorrelated (the direction of the movement is independent of the past; there is no "persistence") and unbiased (there is no preferred direction, so direction at each step is random) (Codling *et al.*, 2008). For example, the search path of a foraging animal may, for some animals, be approximated by a random walk. Random walk models are used extensively outside the field of movement modelling, for example the path traced by a molecule as it travels in a liquid or a gas, the price of a fluctuating stock and the financial status of a gambler can all be approximated by random walk models, even though they may not be truly random in reality. The movement process model is therefore a discrete-time, continuous-space, random walk with direction θ in each step uniform in the circle, $\theta_i \sim U(0, 2\pi)$.

3.2.3 Correlated random walk

Correlated random walks (CRWs) involve a movement "persistence" (Codling *et al.*, 2008). This persistence depends on the time step in discrete-time models. The orientation between successive steps is correlated, resulting in a local directional bias. Each step tends to point in the same direction as the previous one, although the influence of the initial direction of motion progressively diminishes over time and in the long term, step orientations are uniformly distributed (Benhamou, 2006). Usually most animals have a tendency to move forwards (termed persistence), hence, CRWs have been frequently used to model animal paths (e.g., Siniff and Jessen, 1969; Skellam, 1973; Kareiva and Shigesada, 1983; Bovet and Benhamou, 1988; Turchin, 1998). Also, over short time scales, highly correlated

random walks can be approximated by straight lines. Thus, the linear movement model is an approximation to this over the time scale of many surveys.

3.2.4 Biased random walk

Paths that contain a consistent bias in a preferred direction or towards a given target are named biased random walks (BRWs), or biased and CRWs (BCRWs) if persistence is also observed (Codling *et al.*, 2008). The bias may be due to various factors influencing the movement: fixed external environmental factors, spatially varying factors, individual or personal choice of direction, or mean-reversion mechanisms such as movement within a home range, among other factors. We focus on the latter, a home-range animal movement.

The home-range concept is central in animal behavior and movement ecology (Turchin, 1998; Blackwell, 1997; Moorcroft and Lewis, 2013). Common approaches for describing home range patterns employ kernel density estimators (where the home range area is described with high density while away from it with low density) (Turchin, 1998). However, numerous mechanistic movement models have been developed to understand home range formation (e.g., Lewis and Murray, 1993; Moorcroft and Lewis, 2013; Van Moorter *et al.*, 2009; Riotte-Lambert *et al.*, 2015; Breed *et al.*, 2017).

Here, we force animals to move exhibiting attraction to a particular point, called the centre of attraction, creating a home range movement (McClintock *et al.*, 2012). The movement process model is therefore a discrete-time, continuous-space, random walk where the direction θ, instead of being held constant as in the linear case, follows a wrapped Cauchy distribution. Other distribution choices (e.g., Von Mises or wrapped normal) could also be used (Codling *et al.*, 2010).

3.3 Methods

The simulation was conducted using (R Core Team, 2016, version 3.2.4). For each simulated dataset, detection function estimation was performed using the MCDS engine from the software Distance 6.2 (Thomas *et al.*, 2010).

3.3.1 Data simulation

For both detectability scenarios (CPS and PTS), the study region was defined as a square with corners at $(0, 0)$, $(\varrho, 0)$, $(0, \varsigma)$, (ϱ, ς), where $\varrho = \varsigma = 1500$ m. The square study region was composed of a grid of circular plots located the central 1km^2, surrounded by a margin of 250m. We supposed observers survey at $k = 256$ systematic point locations, searching to a distance $w = 30$m. Therefore, there are 16x16 points over 1km^2, the grid of circular plots have a 1.25m margin inside the 1km^2 and each circular plot was 2.5m apart from the next circular plot in the north, south, west and east directions (Figure 3.2).

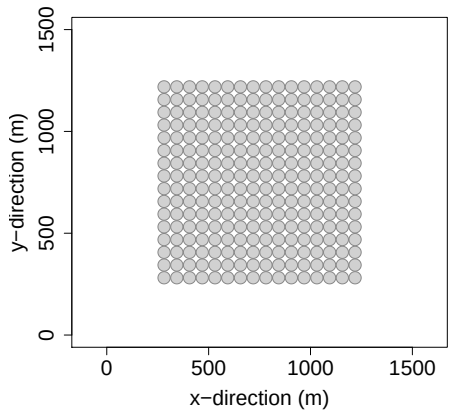

Figure 3.2: Simulated study region and sampling units.

The number of animals within the study region was fixed at 1000. The aim of the margin around the covered region was to avoid edge effects. The buffer was large enough that no animals, restricted to a home range movement, that reach the buffer could get to the circular plots in the time of the survey, and that no animals appearing on the buffer from outside would get to the circular plots. For the particular case of BRW animal movement we assume that when animals exit the study region, they cannot re-enter. (The buffer ensures this restriction has no effect on the number of animals reaching the circular plots.) For animals moving linearly, we adopted a wrap-around model: for each animal that exits across one boundary of the study region, a new animal enters immediately at the same distance along the opposite boundary. This ensures the abundance in the study region remains constant over the simulation period.

3.3.2 Animal movement

The simulation was undertaken in discrete time, with a time step of $\tau = 1$ second. Animals moved consecutively with constant speed $u = \{0, 0.05, 0.1, 0.5, 1\}$ m/s during the surveyed interval of time: a five minute period, corresponding therefore to 300 seconds, i.e., 300 animal steps. Therefore the step length was fixed to $l = u\tau = u$.

Linear movement

Each animal was given an initial random position (i.e., uniform density) in the study region A. The animal direction, θ, was randomly fixed (uniform distribution in the circle) at the beginning.

$$\begin{aligned}(x_1, y_1) &\sim U(A)\\ (x_{j+1}, y_{j+1}) &= (x_j + l\cos(\theta), y_j + l\sin(\theta)) \quad j = \{1, \ldots, 299\}.\end{aligned}$$

Biased random walk

Animals were forced to move exhibiting attraction to a centre of attraction, creating a home range movement (McClintock *et al.*, 2012), where the direction θ, instead of being held constant, followed a wrapped Cauchy distribution. $\theta_{it} \sim$ wrapped Cauchy(μ_{it}, ρ_{it}), for each animal i in a given time t, so the probability density function for turning angle is

$$f_{WC}(\theta; \mu, \rho) = \frac{1}{2\pi}\frac{1-\rho^2}{1+\rho^2-\rho\cos(\theta-\mu)}, \quad 0 \le \theta < 2\pi, \quad 0 \le \mu < 2\pi, \quad 0 \le \rho \le 1. \quad (3.1)$$

The expected turning angle μ, is the angle between the current heading (actual position) of the animal and its centre of attraction and the x-axis from the animal position (considering the animal position as the origin of the coordinate system). The strength of bias to the centre of attraction is defined by $\rho = \tanh(\alpha\delta)$, where $\alpha\delta$ is the scaled distance between the animal location and the centre of attraction. As an animal is located closer to the attraction point, $\rho \to 0$, and the movement direction is uniformly distributed on the unit circle. By contrast, if it is further from it, $\rho \to 1$, and therefore in the limit when far from the home range centre it would walk along the straight line from the current location to the home range centre (see figure 3.3).

The home range radius to the centre of attraction depends on the value of α and the animal speed. The constant α does not have a significant effect in the home range radius over the surveyed interval of time, in this particular case a 5 minute period (see Figure 3.4). On the other hand the animal speed u leads to significant differences. The faster the

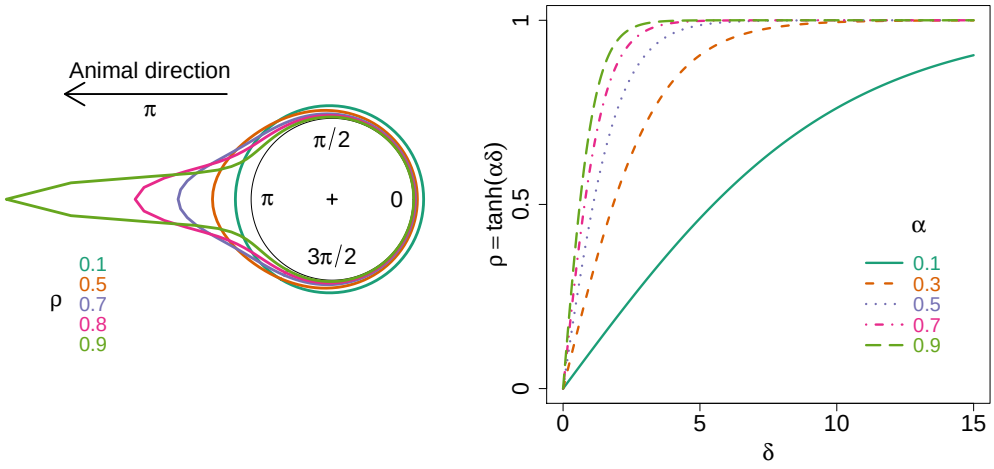

Figure 3.3: On the left, density of a Wrapped Cauchy distribution with $\mu = \pi$ and $\rho = \{0.1, 0.5, 0.7, 0.8, 0.9\}$. On the right dependence of ρ over the distances δ, for different constants $\alpha = \{0.1, 0.3, 0.5, 0.7, 0.9\}$.

animal moves the bigger the home range area becomes. For illustration, an average home range radius as a function of animal speed and strength of bias to the centre of attraction for 1000 biased random walks is shown in Table 3.1 for a range of possible values of both parameters.

Table 3.1: Average radius in meters of the home range area when animal speed $u = \{3, 6, 30, 60\}$m/min, and directional strength constant $\alpha = \{0.1, 0.5, 0.9\}$.

speed (m/min)	α		
	0.1	0.5	0.9
3	1.71	1.44	1.42
6	3.17	2.90	2.74
30	9.62	8.08	7.79
60	18.11	15.31	14.09

In the simulations that follow the constant α was fixed to 0.1, so the home range is more flexible depending on animal speed.

Figure 3.4: Animal biased movement scenarios during 5 minute period (300 seconds) with constant speed u =1m/s and $c = 0.1, 0.5$ and 0.9. All the animals' paths started in the same initial coordinates and have the same centre of attraction represented by the red asterisk.

First, the centre of attraction (p_x, p_y) of each animal is given by the realization of a bivariate uniform random variable in study region A. Then, the initial animal position (x_1, y_1) is chosen using the rejection sampling technique to sample from an approximation of the probability density function of animal positions given its attraction point. Details about how this approximated pdf is derived are given below.

Spatial distribution of the biased random walk

The pdf for the spatial distribution over the total interval of time $[t_1, t_2]$ is as follows (Cheung *et al.*, 2008; Codling *et al.*, 2008).

$$\vartheta_{t_2-t_1}(x,y) = \frac{1}{4\pi\sqrt{D_x D_y}(t_2-t_1)} \exp\left\{-\frac{(x-U(t_2-t_1))^2}{4D_x(t_2-t_1)} - \frac{y^2}{4D_y(t_2-t_1)}\right\}, \tag{3.2}$$

where the direction of each animal step θ_τ follows a wrapped Cauchy(μ, ρ) distribution with pdf given by Equation 3.1, the drift (continuous slow movement from one place to another), U, and diffusion, D_x and D_y in the case of a fixed speed of movement u, are defined as

$$\begin{aligned} U =& \frac{u}{\tau}\rho, \\ D_x =& \frac{u^2}{4\tau}\left(\int_{-\pi}^{\pi}(1+\cos(2\theta))f_{WC}(\theta)d\theta - 2\rho^2\right), \\ D_y =& \frac{u^2}{4\tau}\left(\int_{-\pi}^{\pi}(1-\cos(2\theta))f_{WC}(\theta)d\theta\right). \end{aligned} \tag{3.3}$$

The diffusion coefficients for a wrapped Cauchy angular distribution are:

$$D_x = D_y = \frac{u^2}{4\tau}(1-\rho^2). \tag{3.4}$$

Therefore the long-time steady-state spatial distribution is

$$\vartheta_{t_2-t_1}(x,y) = \frac{1}{\frac{\pi u^2}{\tau}(1-\rho^2)(t_2-t_1)} \exp\left\{-\frac{(x-\frac{u}{\tau}\rho(t_2-t_1))^2+y^2}{\frac{u^2}{\tau}(1-\rho^2)(t_2-t_1)}\right\}. \tag{3.5}$$

This spatial pdf, $\vartheta_{t_2-t_1}$ when $\rho = 0.5$, is shown in Figure 3.5. However, note that in our animal movement case, animals move exhibiting attraction to a particular location, for each unit of time the animal changes the direction depending on the previous position as described in 3.2.4. θ_τ follows a wrapped Cauchy(μ_τ, ρ_τ) distribution where ρ_τ instead of being fixed, is different for each step (as it depends on the distance δ from the home range centre, which itself is changing over time), resulting in an intractable pdf.

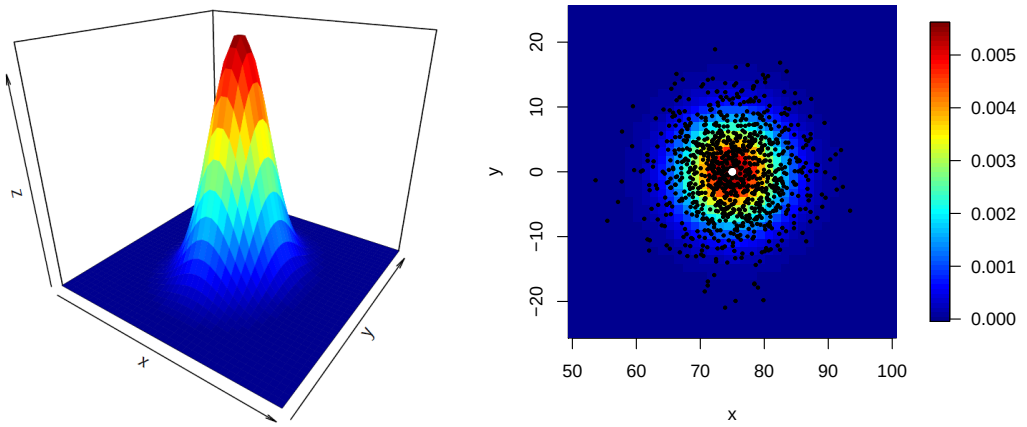

Figure 3.5: Theoretical probability density plots calculated from Equation 3.5 with a wrapped Cauchy angular distribution for a 5 minute interval of time ($t_2 - t_1 = 300$ time steps), with constant speed $u = 0.1$m/s and ρ fixed to 0.5. The end points of 1000 simulated BRWs with start point in (75,0) (in white) are marked as black points.

Figure 3.6 shows the approximated pdf assuming a fixed ρ combined with the end points of 1000 simulated BRWs with the same centre of attraction and animal speed but different constant α. As was stated in Section 3.2.4, $\rho = \tanh(\alpha\delta) \in [0,1]$ depends more

on the animal speed than on the value of α, which does not have a significant effect in the home range radius over the 5 minutes time interval (see Figure 3.4 and Table 3.1, or Figure 3.6 which shows the end point when varying the constant α of 1000 repetitions of the BRWs).

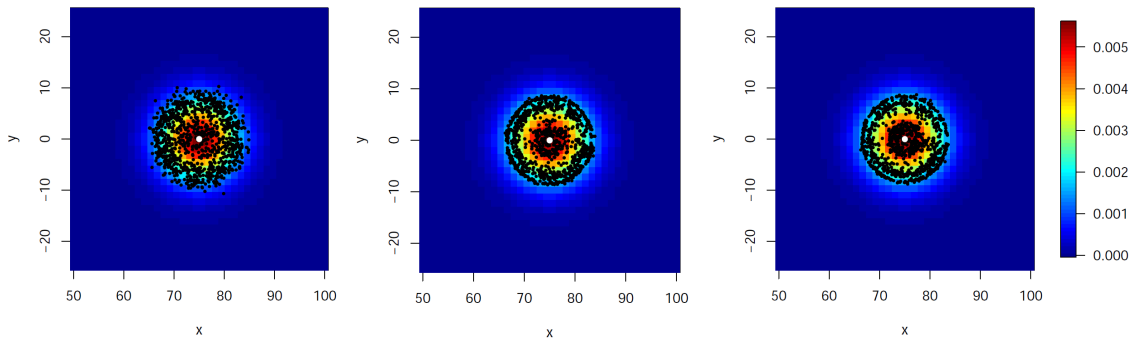

Figure 3.6: Theoretical probability density plots calculated from Equation 3.5 with a wrapped Cauchy angular distribution for a 5 minute interval of time ($t_2 - t_1 = 300$ time steps), with constant speed $u = 0.1$m/s and $\rho = 0.5$. The end points of 1000 simulated BRWs with centre of attraction in (75,0) (the white point), animal speed $u = 0.1$m/s and $\alpha = \{0.1, 0.5, 0.9\}$ where $\rho = \tanh(\alpha\delta)$ are marked as black points.

These theoretical predictions, despite being close to the simulation results, did not match (compare Figure 3.5 with Figure 3.6). We used this approximated pdf with a fixed value for ρ to sample the animal initial position. (Another option to sample the first animal position given its centre of attraction could be to estimate the parameters of a bivariate Normal distribution by simulation, or use a kernel density estimator.) The fixed strength of bias ρ, considered for a given animal speed, was the average strength of bias for the particular home range radius the animal is moving (see Table 3.1) that gives a good approximation to the real pdf. The strength of bias pdf is,

$$f_\rho(\delta|\alpha) = \frac{\alpha\big(1 - \tanh^2(\alpha\delta)\big)}{\tanh(1)}. \tag{3.6}$$

Therefore,

$$
\begin{aligned}
(p_x, p_y) &\sim U(A) \\
(x_1, y_1) &\sim \vartheta_{t_2 - t_1}(p_x, p_y) \quad \text{with } \rho = \{\text{average } \tanh\left(\frac{\delta}{10}\right) \text{ for speed } u\} \\
(x_{j+1}, y_{j+1}) &= (x_j + l\cos(\theta_{j+1}), y_j + l\sin(\theta_{j+1})) \quad j = \{1, \ldots, 299\} \\
\theta_{j+1} &\sim \text{wrapped Cauchy}(\mu_{j+1}, \rho_{j+1}) \\
\mu_{j+1} &= \text{vector}(p_x - x_j, p_y - y_j) \\
\rho_{j+1} &= \tanh\left(\frac{\delta_j}{10}\right) \quad \text{with } \delta_j = \sqrt{(p_x - x_j)^2 + (p_y - y_j)^2}.
\end{aligned}
$$

3.3.3 Detection process

We divide the detection process into two scenarios. First a CPS scenario, where it is assumed that every animal that crossed the circle of radius $w = 30$ was detected. Second, a PTS scenario. The rest of this Section relates to the PTS scenario.

We only used hazard rate (HR) models for the detection function, even though the more pervasive detection function model in the literature is the half normal. We wished to build upon the results of the previous chapter and specify detection functions with low (or known) bias under no movement given estimation that involves model selection, but also to be able to specify detectability at the 1-second time step of this simulation. The HR provided a natural means for this, since it can be derived from a model of instantaneous hazard of detection; this hazard can be integrated over any desired time interval, in particular a one-second period to give a per-second detection function (which is the time step τ, of the simulation) and over 300 seconds to give a per-simulation detection function under no movement. Now we show how the hazard functions we used in the simulation relate to a detection function when animals do not move (assuming that r does not change over time), so as to provide a link with Chapter 2.

The instantaneous hazard is defined as the limit of the number of observed detections per unit time divided by the number of animals at risk, as the time interval tends to 0. In other words, it is the probability of detecting an animal in a instant of time. Thus, the instantaneous hazard is given by,

$$
h(r; c, d) = 1 - \exp\left\{ \int_{t=t_1}^{t_1+dt} k(r)dt \right\} \tag{3.7}
$$

where dt is an instant of time and

$$k(r) = \text{pr}\{\text{an animal is detected at distance } r\} = cr^{-d}, c, d \in \mathbb{R}^+.$$

In the above we use the hazard $k(r)$ recommended by Hayes and Buckland (1983). Then the 1-second probability of detection is

$$h(r; c, d) = 1 - \exp\left\{ \int_{t=t_1}^{t_1+\tau} k(r)dt \right\} = 1 - \exp\{ -\tau cr^{-d} \} = 1 - \exp\{ -cr^{-d} \}. \quad (3.8)$$

It is assumed that the distance r does not change over time, when integrating the hazard over the interval of time. Therefore, if animals move, the 1-second detection function is an approximation. It would be fine for low animal speeds, so there is a small variation in r and hence, the considered speeds ensure that it is a good approximation (since in the maximum speed 60m/min, the displacement of r per second is just a meter).

The hazard rate (HR) process, the usual distance sampling hazard rate detection function, can be obtained from the hazard integrated over the whole surveyed interval of time (if r does not change over time),

$$\begin{aligned} \text{HR}(r; \sigma, b) =& 1 - \exp\left\{ \int_{t=t_1}^{t_2} k(r)dt \right\} = 1 - \exp\left\{ \int_{t=t_1}^{t_2} -cr^{-d}dt \right\} \\ =& 1 - \exp\left\{ -(t_2 - t_1)cr^{-d} \right\} = 1 - \exp\left\{ -\left(\frac{r}{\sigma}\right)^{-b} \right\}. \end{aligned} \quad (3.9)$$

Therefore, both parameterizations are related: $c = \sigma^b/(t_2 - t_1)$ and $d = b$.

Given a particular HR, we check for each second of time the hazard (hr) of the animal being detected. Once an animal is detected, it cannot be re-detected again in the same circular plot. The probability of detection for each animal from each point is based on its distance to the point, using a two-dimensional 1-second hazard rate detection function.

We used five different detectability parametrizations ordered from narrow to wide shoulder ($\{\text{HR}_0, \ldots, \text{HR}_4\}$ and $\{\text{h}_0, \ldots, \text{h}_4\}$; see Figure 3.7 and Table 3.2). In the first three parameterizations (HR_0- HR_2) $\text{HR}(w) \approx 0.1$ as is recommended for PTS. Regarding the detectability process, following the recommendation given in Chapter 2 the 1-second hazard rate detection function should be h_1, so the resulting HR function, over the total interval of time $[t_1, t_2]$, HR_1 has the advised form.

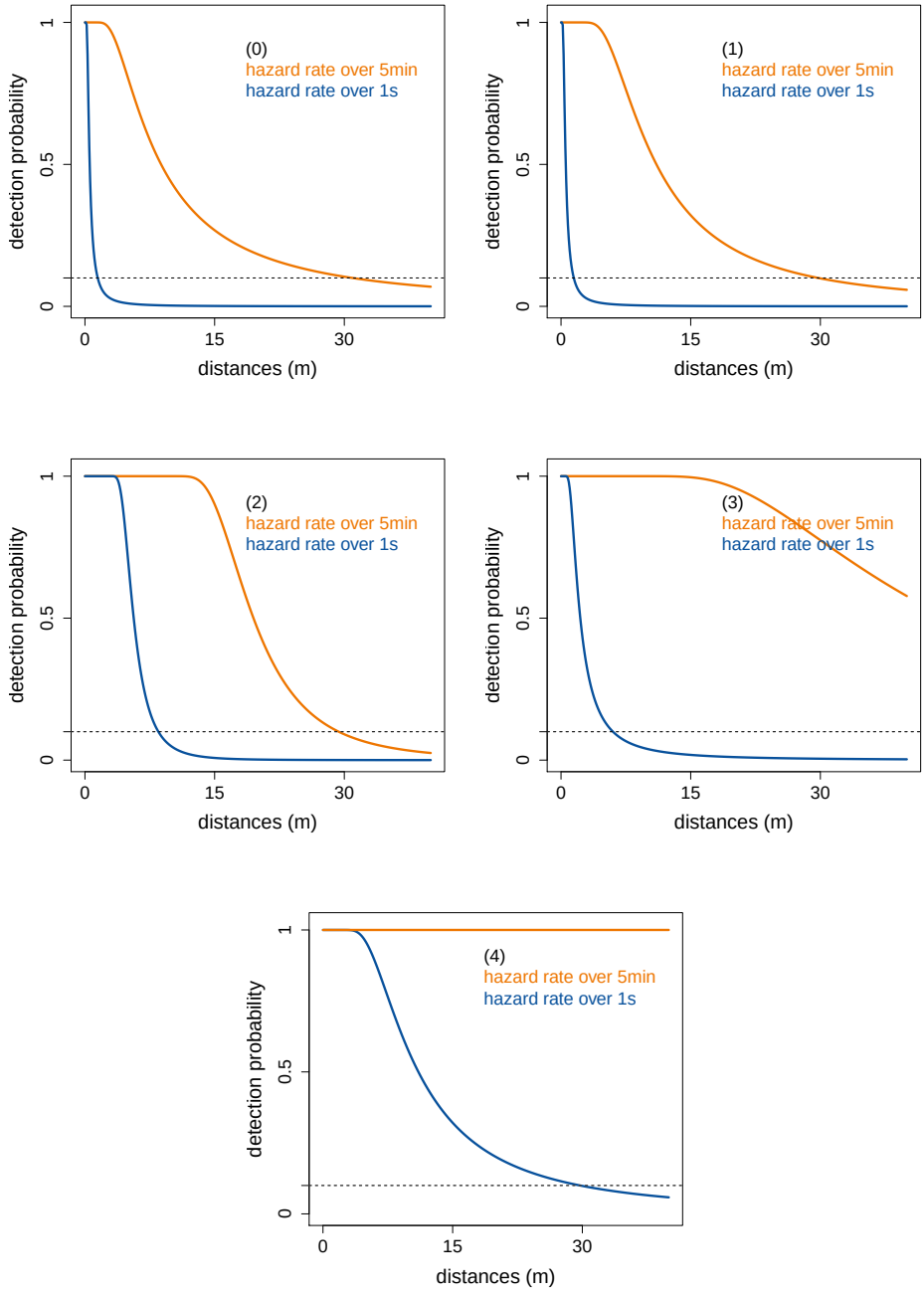

Figure 3.7: Five parametrisations of hazard rate function (orange line) over the whole interval of time $[t_1, t_2]$, versus the hazard rate (blue line) in one time unit τ (considered, in this case, one second). Both functions give the probability of an animal being detected depending on its distance from the point. The dashed line represent 0.1 such as in some cases, $\mathrm{HR}(w) \approx 0.1$.

Table 3.2: Parametrizations of the hazard-rate function integrated over the total interval of time ($t_2 - t_1 = 300$ seconds) and the corresponding hazard rate over 1 second.

Parameterization	hazard rate (HR)		1s–hazard rate (h)	
	σ	b	c	d
0	6.9	1.5	0.06	1.5
1	9.1	1.9	0.22	1.9
2	18	4.6	1982.13	4.6
3	37	1.9	3.18	1.9
4	183.14	1.9	66.40	1.9

From Chapter 2 it is known that when animals do not move, detection functions with smaller shoulder than HR_1 (e.g., HR_0) lead to negative median bias, while there is positive median bias for those with a wider shoulder (e.g., HR_2, HR_3 and HR_4). Therefore, when animals move, the median bias is a combination of the form of the detection function with the effect of the assumption violation.

3.3.4 Analysis of simulated data

In the CPS scenario, we assumed perfect detectability, so the resulting density estimator is given by the quotient between the number of detections and the covered area, and we obtained abundance scaling the density to the whole study region.

In the PTS scenario, we needed to estimate the detection probability to account for the missed animals in the covered area. The density estimate is defined by the number of detections divided by the detection probability and covered area, and in the same way, the abundance estimate is obtained.

We estimated the average probability of detection and the corresponding 95% CI over each minute of time (60, 120, 180, 240, 300 seconds). In other words, $\hat{P}_t$ is the average probability of detection associated with the interval $[t_1, t]$. We used model selection to estimate each detection function. For each of the simulated datasets, we fitted all the model combinations (key function + series adjustment term) recommended by Buckland *et al.* (2001) (see Table 2.1), choosing the model with lowest AIC.

The number and order of adjustment terms required for the analysis was selected using sequential forward selection, starting with no adjustments and adding one at a time so long as the resulting model had a lower AIC than the previous one. We also considered at most 5 parameters for the detection function, as is standard in the Distance software. Following the conclusions given in Chapter 2, we forced the detection function to be monotonic decreasing.

For each scenario we simulated 3000 iterations, to reduce the relative Monte Carlo error associated with the standard error on the abundance estimate (calculated using Equation (7) in Koehler *et al.*, 2009) to below 1%.

For PTS surveys median bias in abundance was presented instead of the mean bias, because the latter was affected by occasional outliers.

3.4 Results

3.4.1 Circular plot sampling

For CPS (animals are certainly detected regardless of their distance to the observer), abundance estimators are unbiased when animals remain static and the bias increased linearly with animal speed and time spent in the observation point for both types of animal movement (Figure 3.8).

When animals move within a home range area, the bias is lower than when they move linearly since their movement is constrained, resulting in fewer animals entering the covered region over time. For instance, animals moving at 6 metres per minute in straight lines versus biased random walks, result in bias of 60% and 10% respectively. The difference in bias between both movements is due to the distance the animal moves. For example, while animals moving linearly at 1m/s will cover an exact distance of 300m, an animal moving as a BRW, may move a maximum distance of 40m during the same interval of time.

All the animals initially in the circular plot (covered area) were detected due to the perfect detectability assumption. The number of detections increased with time spent surveying, since new animals enter into the covered area. Therefore, after the initial second, all detections would occur near the truncation distance w. Note that naturally

how close to w depends on the actual simulation implementations, if the time step τ instead of being a second was infinitely small all distances, except the initial ones, would be virtually w, in this case, 30m (see Figure 3.9).

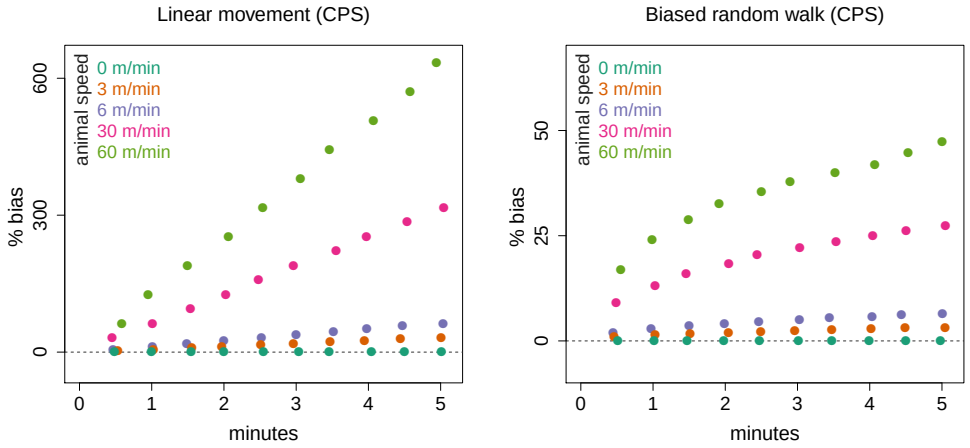

Figure 3.8: Percentage median bias in $\hat{N}$ when animals move linearly (left plot) and in a biased random walk describing a home range (right plot) with different speeds $u = \{0, 3, 6, 30, 60\}$m/min over a 5 minute period, assuming perfect detectability.

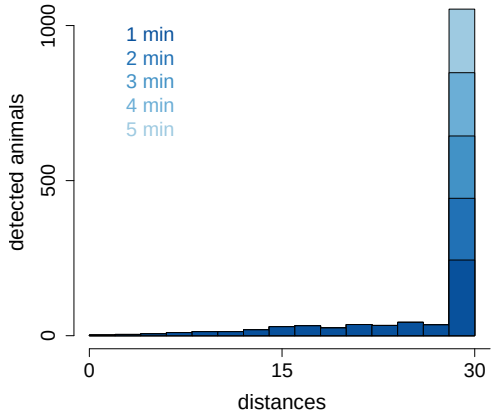

Figure 3.9: Number of detected animals during each minute of the 5 minute period time of surveillance when animals move linearly at constant speed 30m/m.

3.4.2 Point transect sampling

Linear movement

The percentage median bias in abundance estimates for PTS depended on three factors: the time spent surveying at the point, the animal speed and the detection function. For linear animal movement, the first two factors were directly proportional to the median bias. It increased linearly with time spent monitoring, and was worse for higher animal speeds.

Since HR_1 is expected to be unbiased under no movement conditions, while the others may be biased (see Section 3.3.3), we present that scenario first (Figure 3.10). As expected, median bias increases linearly with time monitoring being higher for faster animal speeds. When animals remain still (speed $u = 0$), the effect of the detectability process can be seen easily. In HR_1, the small negative bias for the first minute or two is expected because, effectively, this is a more spiked detection function than the 5 minute one we were targeting, which is unbiased. When animal movement occurs but is ignored, in a 5 minute survey period, median bias ranged from -20% with the lowest speed $u = 3$m/min to 15000% with the fastest speed $u = 60$m/min.

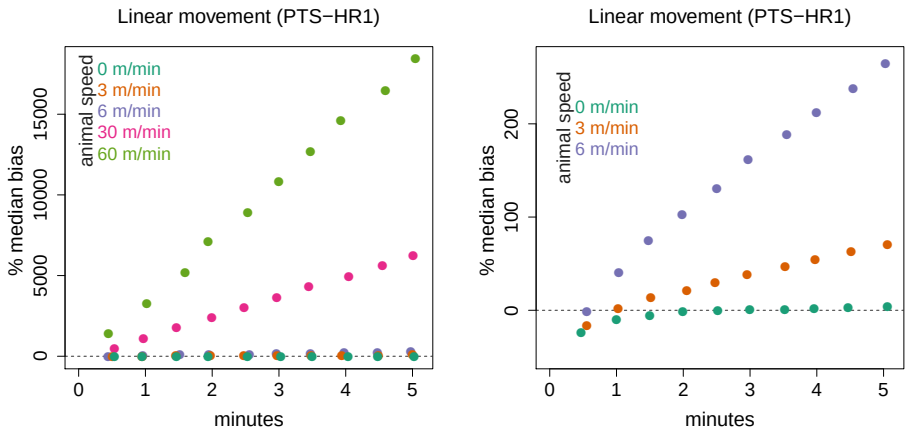

Figure 3.10: Percentage median bias in $\hat{N}$ when animals move linearly with different speeds $u = \{0, 3, 6, 30, 60\}$m/min, over a 5 minute period, assuming the instantaneous hazard of being detected h_1. The right plot shows the 3 slowest moving scenarios, for easier reading.

The effect of detectability can be seen when animals do not move or if they move slowly. This results in positive bias from HR_2 to HR_4, even in the lowest speeds. Waiting the total of the surveyed time (5 minutes), we found unbiased estimates for low speed animals in HR_4, since the detectability is certain (Figure 3.12).

The instantaneous hazard for any given instance is $h_i, i = 0, \ldots, 4$. So the true detection function for an interval of time $(0, t)$ is the complementary of the probability of not being detected during the t instants before: $[1 - (1 - h_i)^t], i = 0, \ldots, 4$.

Figures 3.11 and 3.13 show how the detectability process affects the number of detections produced with increasing observation time. Animals can be detected for two reasons: because they were in the encounter region, thus they have more chances to be detected over time, or because they were outside and they entered the encounter region at some point, and then becoming at risk of being detected. Depending on the detection function, if the detectability is high animals would be detected sooner than if it is low.

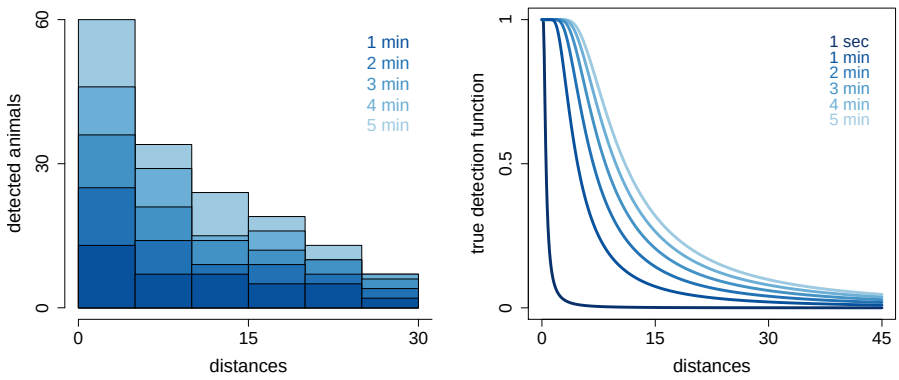

Figure 3.11: Number of detected animals during each minute of the 5 minute period time of surveillance given an h_1 hazard process and that animals move linearly with constant speed $u = 30$m/min (left side). The instantaneous hazard function h_1 and the true detection function for each i-minute interval of time, $i = 1, \ldots, 5$ (right side).

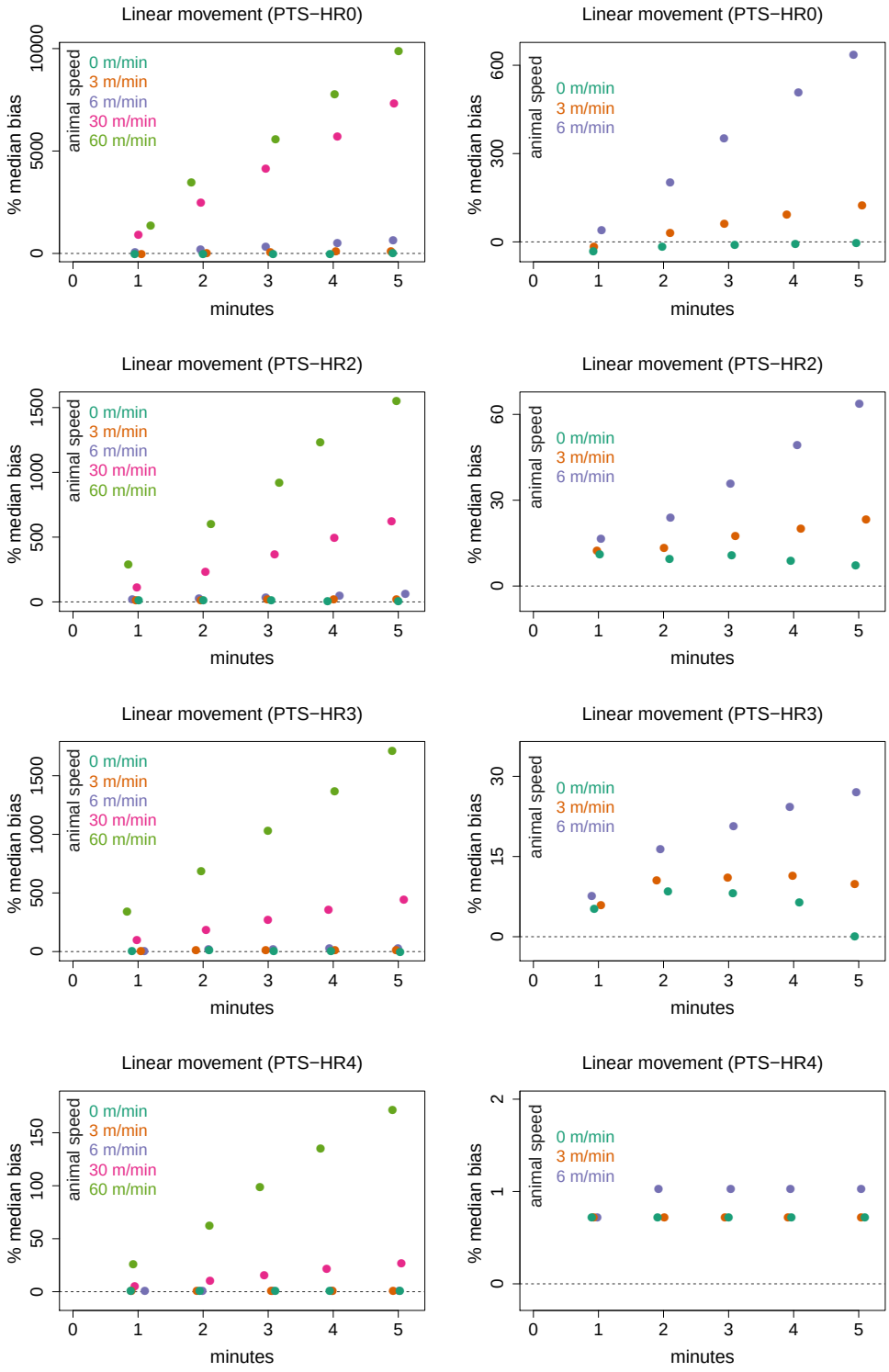

Figure 3.12: Percentage median bias in $\hat{N}$ when animals move linearly with different speeds $u = \{0, 3, 6, 30, 60\}$m/min, over a 5 minute period, assuming the instantaneous hazards of being detected h_0, h_2, h_3 and h_4. The right plot shows the 3 or 4 slowest moving scenarios, for easier reading.

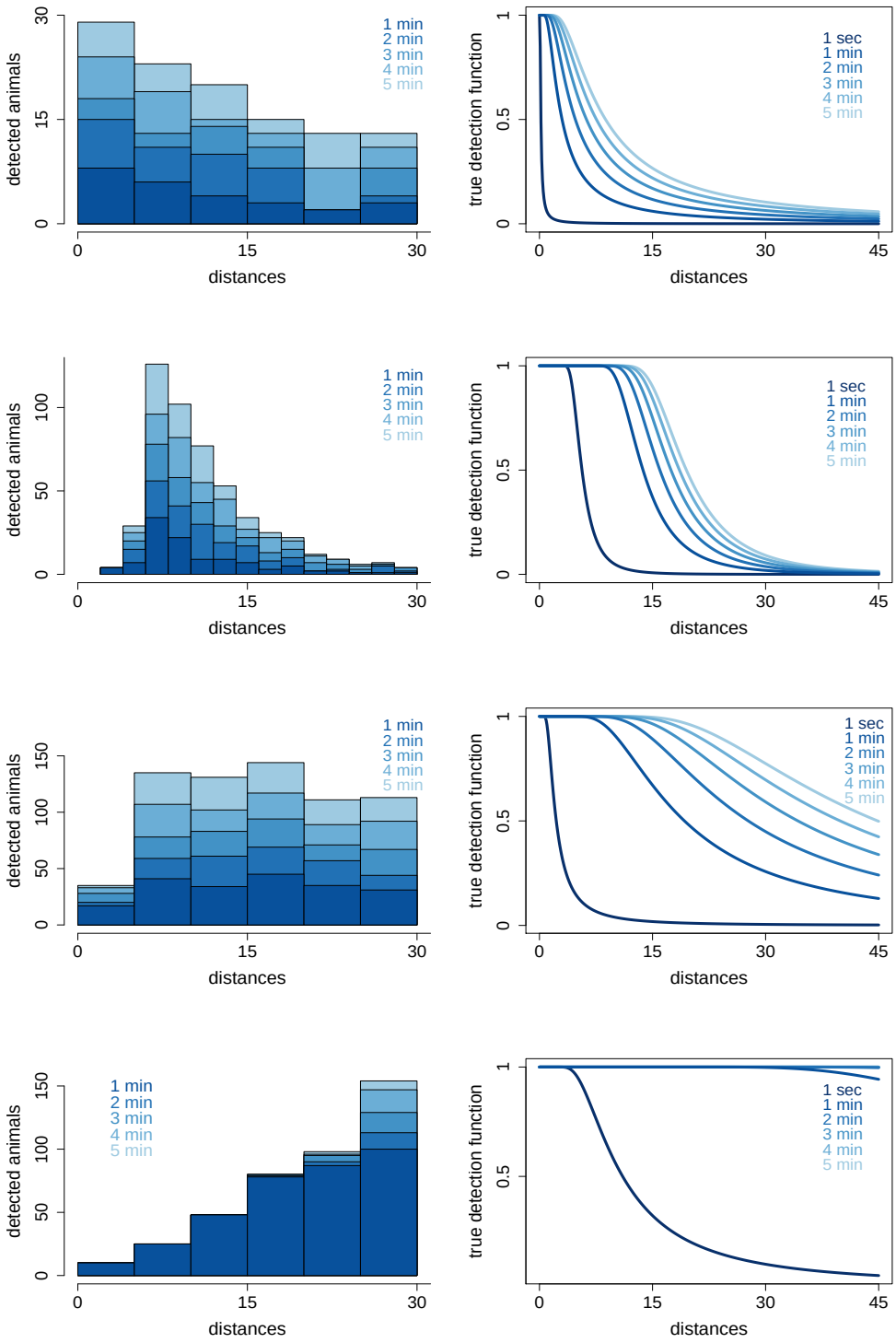

Figure 3.13: Number of detected animals during each minute of the 5 minute period time of surveillance assuming h_0, h_2, h_3 and h_4 the instantaneous hazards of being detected and that animals move linearly with constant speed $u = 30$m/min (left side). The instantaneous hazard function and the true detection function for each i-minute interval of time, $i = 1, \ldots, 5$ (right side).

For example, h_0 and h_1 have a lower detectability than h_2-h_4 and therefore, animals keep being detected over the 5 minute period at close distance to the observation point. On the other hand, due to the wide shoulder of h_2-h_4, almost all the animals closer to the observer were detected during the first minute, so the triangular distribution of animals' distances can be seen. Considering h_3 the histogram of distance to detected animals after the first minute is close to uniform. The reason is the combination of the wide shoulder at closer distance to the observer and the animals entering the detection area that scale up the number of detected animals at larger distances, when the detectability is low. When h_4 is used, detectability is almost uniform after the first minute of time. Hence, the animals detected after the first minute are those far from the centre around the truncation distance and those entering after a while the encounter region.

The average sample size for each detection function parameterization is given in Table 3.3 for each of the minutes surveyed. Note that the parameterizations HR_0 and HR_1 do not reach the minimum recommended sample sizes until the sampled minute 4 and 3 respectively.

Table 3.3: Mean sample size after each minute time (60, 120, 180, 240, 300 seconds), for the five different parameterizations.

Approx. mean sample size	Parameterization				
	0	1	2	3	4
1 minute	25	45	180	230	400
2 minute	50	75	330	420	515
3 minute	70	120	480	625	640
4 minute	100	150	640	830	750
5 minute	125	190	800	1000	875

Biased random walk

Although the general pattern of increasing bias with increasing animal speed was similar to the linear movement scenario, the magnitude of the bias was less for the biased random walk movement (Figures 3.14 - 3.15). There is a certain time when the bias reaches a maximum value and remains similar over time. This is because since the animals are

moving within a home range area, fewer animals enter within detection range because their displacement is constrained over time by the bias towards the home range centre. Moreover once they have been detected in the circular plots nearby this moving area, the animals will no longer be available for detection (as we are assuming we can identify animals), so when animals move linearly new animals keep arriving and hence being detected but not for home range moving animals due to the restriction on movement. Plot sampling in general showed lower bias than PTS, clearly because for animals already on the plot, they tend to be detected when close to the point, so distances are biased down. Then the effect of new animals entering the plot is additional to this, so movement affects the estimation of detection probability in the latter, as well as encounter rate in both.

In general, fewer animals were detected over each successive minute of time. When the detection function has a narrow shoulder (HR_0) abundance is underestimated for animals moving up to 6m/min, during the first 4 minutes of time (see Figure 3.15). For the other detectability cases ($HR_1, \ldots, HR_4$) abundance is overestimated due to a combination of the effect of the animal movement and the detectability process.

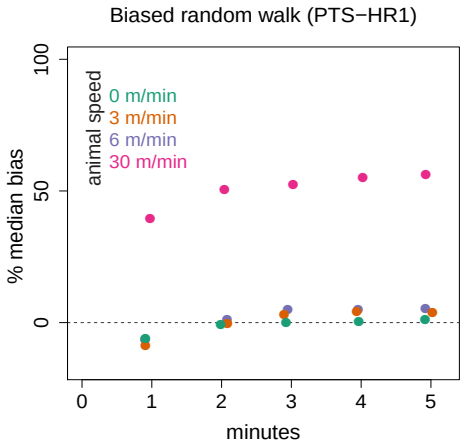

Figure 3.14: Percentage median bias in $\hat{N}$ when animals move within a home range area with different speeds $u = \{0, 3, 6, 30\}$m/min, over a 5 minute period, assuming the instantaneous hazard of being detected h_1.

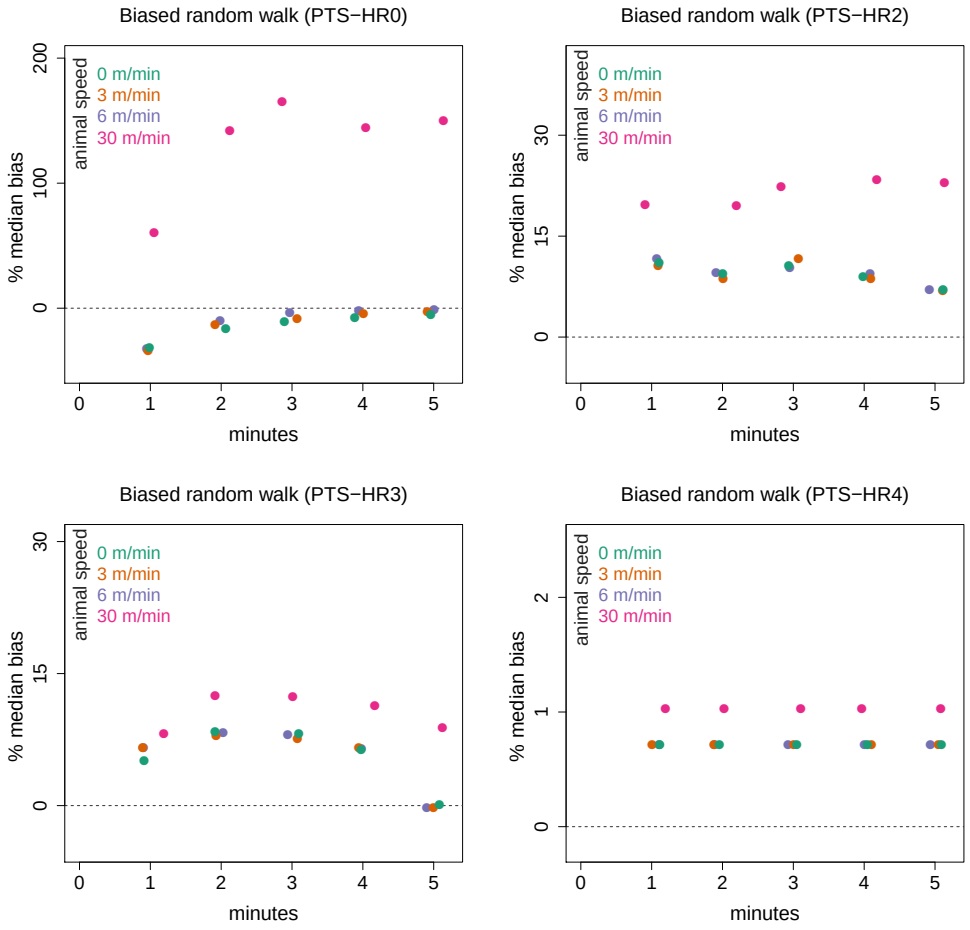

Figure 3.15: Percentage median bias in $\hat{N}$ when animals move within a home range area with different speeds $u = \{0, 3, 6, 30\}$m/min, over a 5 minute period, assuming the instantaneous hazards of being detected h_0, h_2, h_3 and h_4.

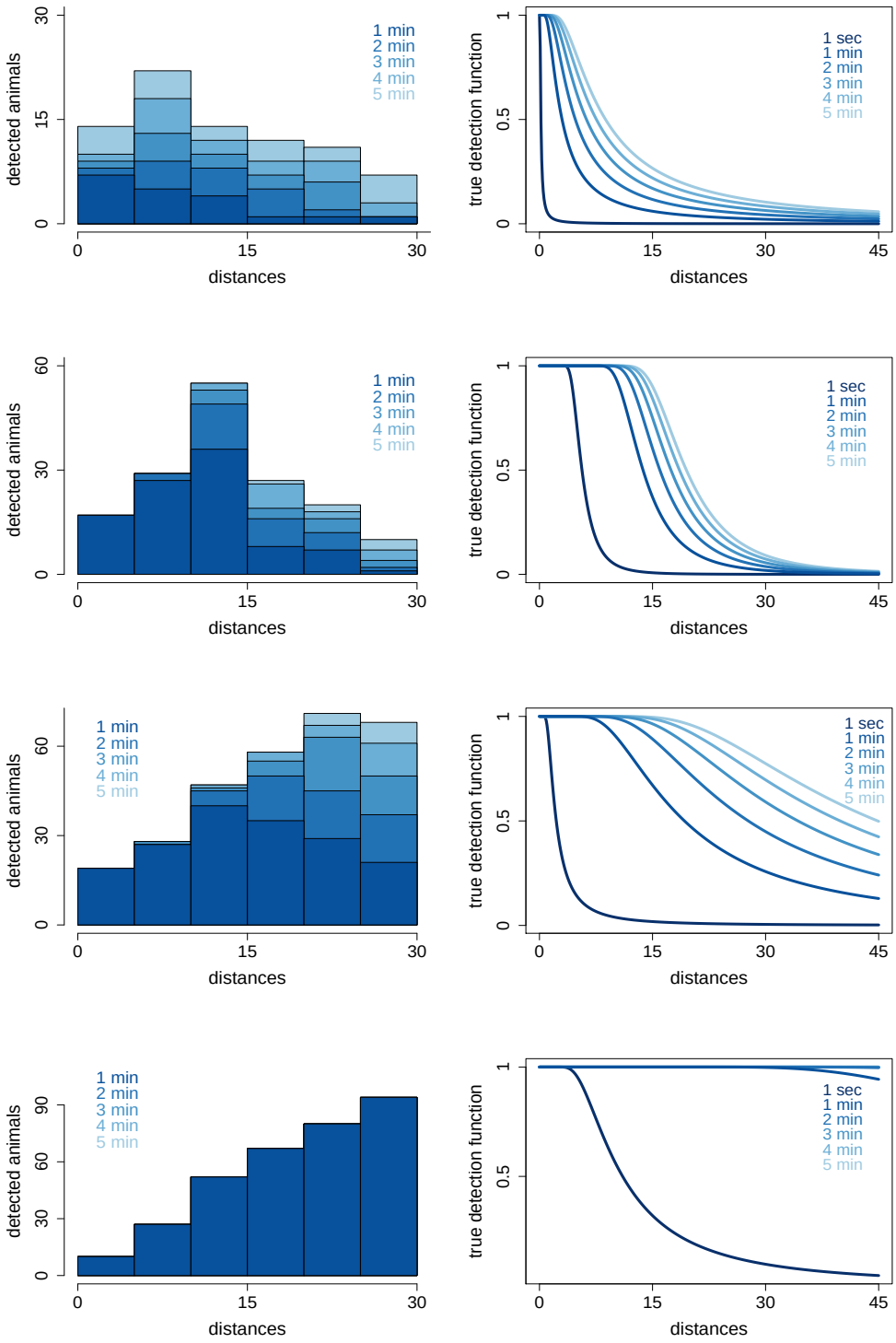

Figure 3.16: Number of detected animals during each minute of the 5 minute period time of surveillance assuming h_0, h_2, h_3 and h_4 the instantaneous hazards of being detected and that animals move within a home range area with constant speed $u = 30\text{m/min}$ (right side). The instantaneous hazard function and the true detection function for each i-minute interval of time, $i = 1, \ldots, 5$ (left side).

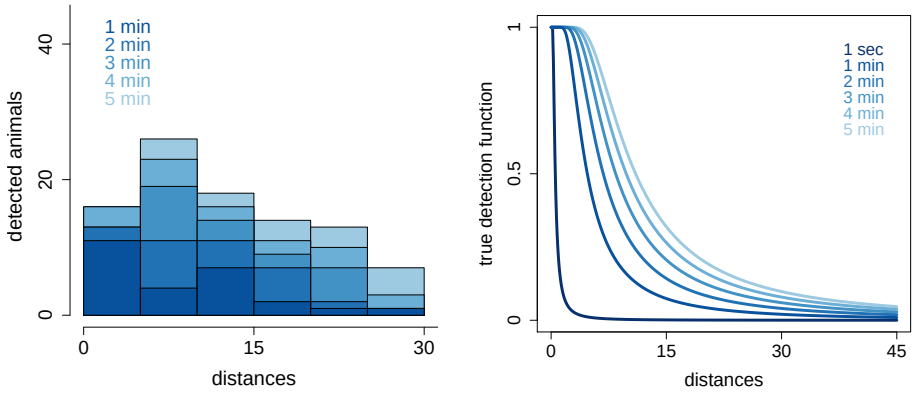

Figure 3.17: Number of detected animals during each minute of the 5 minute period time of surveillance given an h_1 detection process and that animals move within a home range area with constant speed $u = 30$m/min (right side). The instantaneous hazard function h_1 and the true detection function for each i-minute interval of time, $i = 1, \ldots, 5$ (left side).

3.5 Discussion

Wildlife movement when estimating animal abundance is an important practical issue (Howe *et al.*, 2017). In particular, it has long been recognized as a problem for DS surveys (Burnham *et al.*, 1980). In LTS, Glennie *et al.* (2015) found that when mean animal speed is less than observer speed, bias is considerably smaller in LTS than strip transect sampling. By contrast, when mean animal speed exceeds observer speed the bias in LTS becomes comparable with, and may exceed, that of strip transect sampling.

Animal movement is an especially serious problem for point transect studies, in which the observer is stationary (Buckland *et al.*, 2001). Any movement whatsoever is obviously going to be fast in relation to a stationary observer conducting a PTS survey. The longer the observer remains at the survey point, the wider the shoulder of the detection function will be. This advantage is offset by movement of animals into the sampled region and possible double counting of animals, both of which lead to density overestimation.

We found that median bias is considerably smaller in CPS than in PTS, except when using h_4 detectability, possibly because movement affects the estimation of detection prob-

ability in the latter, as well as encounter rate in both. As previously stated, the theoretical aim of PTS (and LTS) is to record the number of subjects and its distance at a single given instant in time. Expressed in other terms, the idea is to capture a "snapshot" in time. Therefore to achieve this while minimising the amount of movement by the subjects during the course of the count, we need a compromise between the time spent at the point and the sample size achieved and the bias. DS requirements need to be met to derive reliable abundance estimates. The balance is therefore to spend enough time at the point to fulfil the DS requirements, such as detecting all animals at and close to zero, while not over-extending the period of surveying. If the time interval is too long then densities are going to be overestimated.

One option to mimic a "snapshot" in time is to use a series of short time windows. An alternative approach descibed by Buckland (2006), consists in more complex field requirements. A reasonable waiting period is desirable, when applying PTS to birds, in which the observer learns about what is happening within the sampled area, (Buckland, 2006). The longer the observer waits, the better the data collection during the surveyed time will be (as long as the observers presence is not disturbing the birds). Then a recommended snapshot (an instant in time survey period) is conducted, where the observer scans the area around and quickly records details. Birds that have been calling from a position before the survey take place, but did not during it, may still be included with the detections if the observer confirms the on-going presence of the same bird, by checking if it is still there after the snapshot is finished. Doing this allows the observer to use all available information in the survey by including known birds which are silent during the snapshot counting period. This approach might be applicable to other species.

There are some aspects that we have not dealt with here. First, note that the survey period can be at a larger scale (of say weeks or even years), but the only assumption is that while at each point animals do not move. Therefore, there is a different related issue due to movement that reflects wider scale movements at the survey level. Theoretical methods can make important contributions to our understanding of animal movement, in particular large scale migrations. In this study we just focus on movements at the survey level. Second, assuming a home range animal movement, we did not consider any particular behaviour, placing the individual centres of attraction at random. However, territorial animals do not overlap centres of attractions, while grouped/familiar animals tend to share them. Third, because of the approximation used in deriving the 1-second hazard rate detection function, we were restricted to use low speeds relative to the fixed

unit of time (in this case, $\tau = 1$s).

3.5.1 Advice for practitioners

According to the literature, responsive movement has been problematic in birds, butterflies or cetacean studies among others (e.g., Ellingson and Lukacs, 2003; Palka and Hammond, 2001; Turnock and Quinn, 1991). When applying PTS to birds, the recommended methodology described in Buckland (2006) and explained above is the best option. The animal movement assumption can be also partially met by not including birds that either fly over the covered area, or enter it during the count (Marsden, 1999; Buckland *et al.*, 1993). Generally, little is lost by the exclusion of these individuals (Buckland *et al.*, 1993). Unfortunately, we cannot apply those techniques to acoustic surveys of cetaceans. Keeping our particular goal in mind, fixed underwater sensors, operating over long periods of time is problematic for PTS surveys (Marques *et al.*, 2013).

One way to sidestep the issue of movement in DS surveys is to utilise stationary objects produced by animals such as nests (Harris and Murray, 1981), burrows (Blihovde, 2006; Stober *et al.*, 2017), or stationary or ephemeral calls (Marques *et al.*, 2011) as the objects of interest. Obviously, violation of the movement assumption is not a problem in such surveys. However to convert the density of this objects (nest, burrows, calls, etc.) into animal density, an additional rate is needed, which should be estimated at the same time and place that the data collection. This raises a new set of questions and problems (Marques *et al.*, 2013).

For cetaceans, cue counts have generally been used. However, the cue rate sometimes is not possible to estimate resulting in cue abundance instead (e.g., Harris *et al.*, 2013). Another alternative used is a series of short time windows to try to mimic a "snapshot" in time, for example a series of 15 second windows was used by Kyhn *et al.* (2012), or 1 second windows by Koblitz *et al.* (2014). This approach was also used for camera-trap distance sampling data by Howe *et al.* (2017).

4

Including animal movement in circular plot sampling

4.1 Introduction

When estimating abundance using circular plot sampling, it is assumed that the animals are immobile and all of those in the covered area are detected. In fact, one needs only assume that no animals cross the boundary of each sampler during the time it is being surveyed, but in general this is only guaranteed if there is no animal movement. An estimator of animal abundance in the covered area is simply the number of detected animals, n, and hence an estimator of total number of animals in the study region is given by

$$\hat{N} = \frac{n}{P_c} \tag{4.1}$$

where P_c is the inclusion probability, i.e., the probability of an animal being included in the sample. One way to deal with animal movement is to undertake a "snapshot" survey. If the covered area consists of a set of circular plots, there is no need to survey them simultaneously, i.e., a snapshot survey will be undertaken for each plot. Then, the inclusion probability is defined as the probability of being in the covered area, in this case if there are k circles and the truncation distance is w, $a = k\pi w^2$, given that it is in the study region A.

$$\hat{P}_c = \frac{a}{A}, \tag{4.2}$$

and therefore,

$$\hat{N} = \frac{n}{a}A. \tag{4.3}$$

Another way to define the covered area a is

$$a = k \int_0^\infty 2\pi r q(r) dr, \tag{4.4}$$

where, $q : \mathbb{R}^+ \longrightarrow [0, 1]$, $q(r)$ is the probability of animal presence in a circular plot at the snapshot instant given its distance r to the centre of the circle, so $q(r) = 1 \; \forall r \in [0, w]$ and $q(r) = 0$ otherwise. This, therefore, leads to

$$a = k \int_0^w 2\pi r dr = k\pi w^2. \tag{4.5}$$

Snapshot surveys are hard to implement in practice; also some survey methods (such as fixed passive acoustic surveys) naturally lend themselves to surveying over large time periods. In this case, if animals were stationary, then the expected proportion of animals within the circle would be the inclusion probability P_c. However, when animals are mobile, even if the animals happen to be outside the plot when the survey starts, they can enter into the covered circular region and hence be detected. Therefore, we expect to record more animals with increasing time spent monitoring, leading to positive bias in abundance estimators that naively use the above formulation, i.e., that ignore animal movement. The idea behind accounting for animal movement consists in defining an *effective extended encounter region*: the area where animals that originated at locations within this area would encounter (i.e., be detected by) the observer, depending on the animal movement and the time interval. In other words, it is analogous to the effective detection area in conventional distance sampling (CDS), i.e., an area such that as many animals within it are not detected as are detected outside it.

4.1.1 Effective extended encounter region

When the survey is not a snapshot in time for a single point (i.e., when it occurs over an interval of time $[t_1, t_2]$) and animals do move, animals that start outside the covered area may end up inside the point and hence be detected. Animals could finish inside or outside, as long as they have been through the covered area, and hence detected. The covered region is the union of k circular plots. For ease of explanation, we assume only one plot; results are readily generalized to multiple plots since the k different points do not need to be covered in a single time interval, the only requirement is that each can be considered to be independent. The probability of presence in a circular plot is lower with increasing distance from the circle. Imagine an animal located very close to the circumference of the

circular plot, e.g., at distance $w + \epsilon$ for some small $\epsilon \in \mathbb{R}^+$. If that animal moves, the probability of moving towards the circle is almost one half, and this probability declines with increasing distances ($\epsilon \to \infty$). Hence, the inclusion probability over an interval of time $[t_1, t_2]$ is defined by

$$\hat{P}_{c_{t_2-t_1}} = \frac{a_{t_2-t_1}}{A}, \tag{4.6}$$

where $a_{t_2-t_1}$ is the effective extended encounter region during the time interval $[t_1, t_2]$,

$$a_{t_2-t_1} = \int_0^\infty 2\pi r \, q_{t_2-t_1}(r, u) \, dr \tag{4.7}$$

where $q_{t_2-t_1}(r, u)$ is the probability of animal presence in a circular plot, during an interval $[t_1, t_2]$, given its distance r_{t_1} to the centre of each circle at time t_1 and speed u. In particular, if animals move at constant speed in a straight line with random bearing during this time, the inclusion probability is higher because animals cover a longer distance than with any other type of movement, leading to a larger probability of presence in a circular plot and so effective extended encounter region.

4.1.2 Abundance estimator including animal movement

If $n_{t_2-t_1}$ is the number of detected animals during the interval of time $[t_1, t_2]$ on the circular plot, dividing the detections by the effective extended encounter region would provide an unbiased density estimator, leading therefore to an abundance estimator, given that animals move with a knowm movement mode and constant speed.

$$\hat{N} = \frac{n_{t_2-t_1}}{a_{t_2-t_1}} A. \tag{4.8}$$

In the remainder of this Chapter we consider three types of animal movement, all of them with constant speed. Animals that move in randomly orientated straight lines (Section 4.2), and those for which movement can be described by a diffusion process (Section 4.3), which we further subdivide into animals following a random walk (RW; Section 4.4) and animals that have a home range, defined via a biased random walk with bias towards the home range centre, which acts as a centre of attraction (BRW; Section 4.5). An analytic expression for the bias for the linear movement is presented, which allows us to correct for the bias under this scenario. For the diffusion movement processes, two methods are proposed. (1) Using the mean dispersal distance (MDD, expected absolute distance from the origin to the end of the path) for the RW and BRW a

correction is applied leading to a reduction on bias, but still biased abundance estimators. When animals move within a home range area, exhibiting attraction to a particular centre of attraction, the MDD is estimated by simulation. (2) A simulation based approach, modelling the probability of animal presence in the encounter region, which results in a 3% or less bias in abundance estimators. A possible alternative, involving estimating the first passage time, is a current research problem and is discussed in Section 4.6.

4.2 Linear animal movement

For moving animals in a straight line, each animal is assumed to travel at constant speed u with direction being uniform in the circle, $\theta \sim U(0, 2\pi)$. Therefore, in an interval of time (t_1, t_2): $t_1, t_2 \in \mathbb{R}^+, t_1 < t_2$; an animal in an initial position (x_{t_1}, y_{t_1}) would end in $(x_{t_1} + u(t_2 - t_1)\sin(\theta), y_{t_1} + u(t_2 - t_1)\cos(\theta))$. Thus, the probability that the animal is in a circular plot of radius w at some time within an interval (t_1, t_2) conditional on the direction θ (see Figure 4.1) is the size of the effective extended encounter region, divided by the total study region,

$$\frac{\pi w^2 + 2w(t_2 - t_1)u}{A}. \tag{4.9}$$

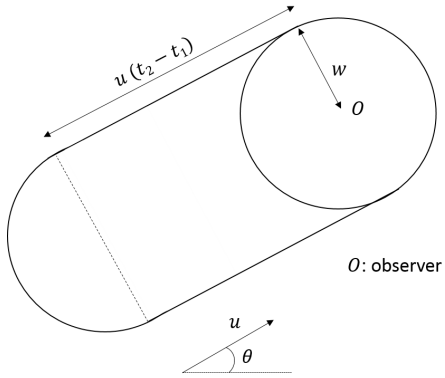

Figure 4.1: Extended encounter region, i.e., the area within which an animal present within it at time t_1 will be detected by the observer within the time interval $[t_1, t_2]$ given it moves in a straight line at constant speed u and direction θ.

If $\hat{N}$ is obtained by Equation 4.3, ignoring animal movement, then we overestimate abundance, having a positive bias of

$$\frac{2(t_2 - t_1)u}{\pi w} \times 100\%, \tag{4.10}$$

and a corrected abundance estimate is

$$\frac{\hat{N}}{1+\frac{2(t_2-t_1)u}{\pi w}}. \tag{4.11}$$

Note that the correction given by Equation 4.11 assumes that $\hat{N}$ is estimated using conventional circular plot sampling analysis (CPS, i.e., assuming that animals are static), so ignoring that animals move when actually they do linearly with constant speed. Our goal, however is to incorporate the knowledge of how animals move into CPS analysis leading to unbiased estimators.

We now derive an expression for the probability of presence in a circular plot $q_{t_2-t_1}(r,u)$. Since we are assuming perfect detectability, all animals within a distance w of the centre will be detected. Thus, $q_{t_2-t_1}(r,u)=1\ \forall r \leq w$.

The main advantage of animals moving in straight lines (as opposed to stochastic movement modes) is that we know the distance they travel during a time interval (t_1,t_2). We denote this distance $\xi = u(t_2-t_1)$. Therefore animals that are further than $w+\xi$ from the circular plot centre will be never present in the circle, regardless of the direction θ they move. When animals are outside but able to reach the circular plot ($w < r \leq w+\xi$), we distinguish two different cases, depending on how far away the animal is at time t_1 from the edge of the circle. In both, the probability of an animal being at some time within the encounter region (i.e., entering), given that it is equally likely to move in any direction $\theta \sim U(0,2\pi)$, is given by:

$$q_{t_2-t_1}(r,u) = \frac{\gamma}{2\pi}, \quad \gamma \in [0,2\pi),$$

where γ is the angle defined by animals entering in the circular plot. Note that γ sometimes is the angle between both tangents from the animal's position to the edge of the circular plot, but not always. In some cases, ξ, the length the animal moves, it is shorter than the distance of the tangent and therefore, γ is the angle defined by the intersection of the circular plot with the circumference centred in the animal position and radius ξ. Both cases are discussed below.

First, when the animal's distance from the circle is small, such that the tangent of the animal initial position to the circular plot is less than or equal to the distance moved, i.e., $\eta \leq \xi$ (see Figure 4.2),

$$\eta \leq \xi \iff \sqrt{r^2-w^2} \leq \xi \iff r \leq \sqrt{w^2+\xi^2}$$

$$\sin\left(\frac{\gamma}{2}\right) = \frac{w}{r}$$

$$\Longrightarrow \quad q_{t_2-t_1}(r,u) = \frac{\gamma}{2\pi} = \frac{1}{\pi}\arcsin\left(\frac{w}{r}\right).$$

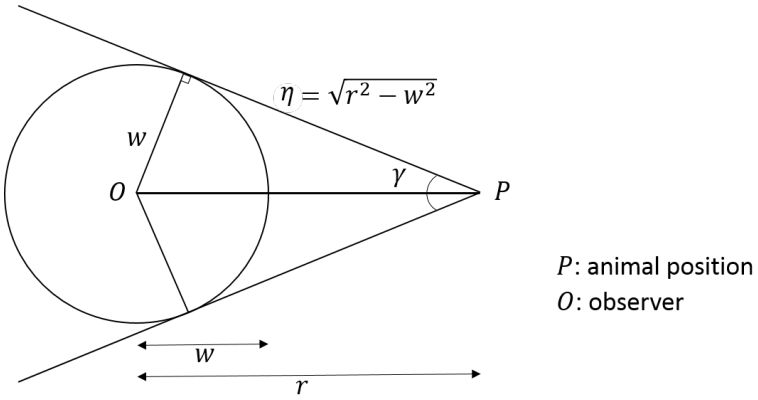

Figure 4.2: Geometry when animal starts at distance r ($w < r \leq \sqrt{w^2+\xi^2}$) outside the circular plot (a circle of radius w). Angle γ of an animal moving into a circular plot, so it would be detected. Shown here is the particular case when the animal moving distance ξ is greater than the tangent η of the animal initial position to the encounter region.

Second, if $\eta > \xi$ (see Figure 4.3), then $\sqrt{w^2+\xi^2} < r \leq w + \xi$

$$\cos\left(\frac{\gamma}{2}\right) = \frac{r-x}{\xi},$$

where x is the distance $\overrightarrow{OX}$, X being the middle point of the $\overline{QR}$ segment. Therefore, x is the $x-$coordinate of Q and R. Q, R are the intersection of

$$\begin{cases} x^2 - y^2 = w^2 \\ (r-x)^2 - y^2 = \xi^2. \end{cases}$$

So, $y^2 = x^2 - w^2 = x^2 + r^2 - 2xr - \xi^2$ and $x = \frac{w^2}{2r} - \frac{\xi^2}{2r} + \frac{r}{2}$.

$$\text{Then, } \cos\left(\frac{\gamma}{2}\right) = \frac{r - \frac{w^2}{2r} + \frac{\xi^2}{2r} - \frac{r}{2}}{\xi}$$

$$\Longrightarrow \quad q_{[t_1,t_2]}(r,u) = \frac{\gamma}{2\pi} = \frac{1}{\pi}\arccos\left(\frac{r^2 - w^2 + \xi^2}{2\xi r}\right).$$

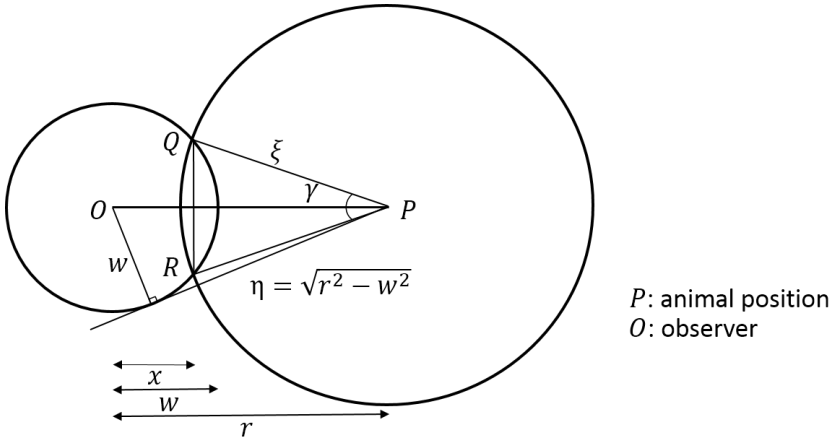

Figure 4.3: Geometry when animal starts at distance r ($\sqrt{w^2+\xi^2} < r \leq w+\xi$) outside the circular plot (a circle of radius w). Angle γ of an animal moving into a circular plot, so it would be detected. Here is shown the particular case when the animal moving distance ξ is less than the tangent η of the animal initial position to the encounter region.

In summary, the encounter region presence function $q(r)$ is defined by the following piecewise function:

$$q_{t_2-t_1}(r,u) = \begin{cases} 1 & \text{if} \quad r \leq w \\ \frac{1}{\pi}\arcsin\left(\frac{w}{r}\right) & \text{if} \quad w < r \leq \sqrt{w^2+\xi^2} \\ \frac{1}{\pi}\arccos\left(\frac{r^2-w^2+\xi^2}{2\xi r}\right) & \text{if} \quad \sqrt{w^2+\xi^2} < r \leq w+\xi \\ 0 & \text{if} \quad r > w+\xi \end{cases} \tag{4.12}$$

ξ being the distance animals travel during this time, so when animals move linearly $\xi_{\text{LM}} = u(t_2 - t_1)$.

As in the example before, an animal located very close to the circumference of the circular plot, at distance $w+\epsilon$ for some small $\epsilon \in \mathbb{R}^+$, has a probability of moving towards the circle of almost one half:

$$\frac{1}{\pi}\arcsin\left(\frac{w}{w+\epsilon}\right) \xrightarrow[\varepsilon\to 0]{} \frac{1}{\pi}\frac{\pi}{2} = \frac{1}{2}.$$

When animals are immobile, the probability of presence in a circular plot is 1 if they are inside the circle or 0 otherwise, resulting in a encounter region $a_{[t_1,t_2]}$ of k times the area of each circular plot, i.e., the exact same area as if a snapshot survey was being considered. However, when animals are mobile, the probability of presence in the encounter region

$q_{t_2-t_1}(r,u)$ depends on the length of the survey (t_2-t_1) and on the animal speed u (Figure 4.4). Given the probability of presence in a circular plot, we can estimate the area where the animals must originate to have a chance of being detected. The longer the observer surveys or the faster the animals move, the larger the area from where detected animals could have started moving from.

Effective extended encounter region

$$a_{t_2-t_1} = \int_0^{\infty} 2\pi r\, q_{t_2-t_1}(r,u)\, dr.$$

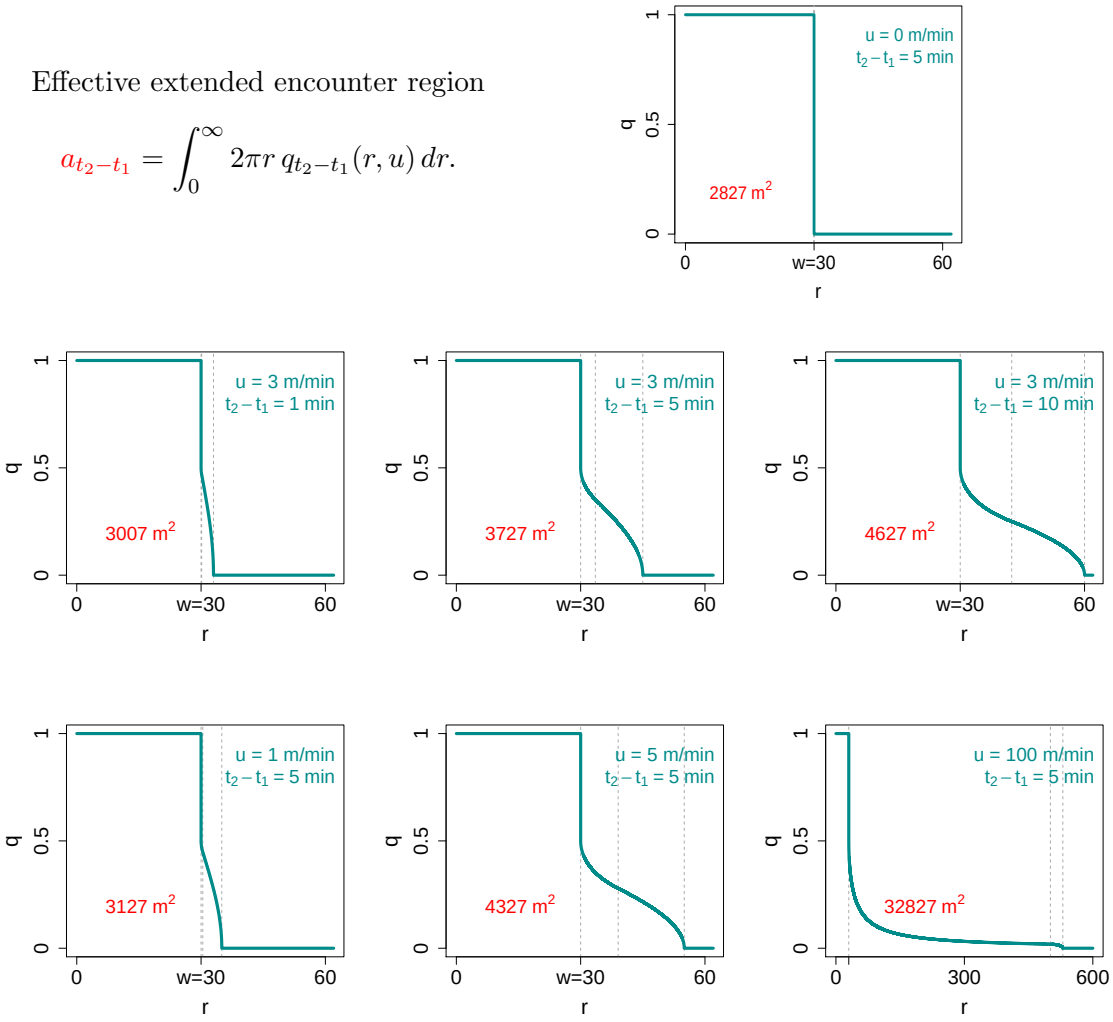

Figure 4.4: Probability of presence in a circular plot given the animal distance to the observer when (1) animals move at speed 3m/minute, during 1, 5 and 10 minute period survey time and (2) when animals move at speed $u = 1, 5, 100$m/minute, during the 5 minute period survey time. The dashed lines correspond to the 4 branches of the function. The area of the effective extended encounter region is shown in red.

Given the above expression for the probability of an animal presence in a circular plot, we now derive an analytic expression for the effective extended encounter region $a_{t_2-t_1}$:

$$a_{t_2-t_1} = k \underbrace{\int_0^\infty 2\pi r\, q(r)\, dr}_{I}.$$

$$I = \underbrace{\int_0^w 2\pi r dr}_{(1)} + \underbrace{\int_w^{\sqrt{w^2+\xi^2}} 2\pi r \frac{1}{\pi} \arcsin\left(\frac{w}{r}\right) dr}_{(2)} + \underbrace{\int_{\sqrt{w^2+\xi^2}}^{w+\xi} 2\pi r \frac{1}{\pi} \arccos\left(\frac{r^2+\xi^2-w^2}{2\xi r}\right) dr}_{(3)}.$$

$$(1) = \int_0^w 2\pi r dr = \pi w^2.$$

$$(2) = \int_w^{\sqrt{w^2+\xi^2}} 2r \arcsin\left(\frac{w}{r}\right) dr = r^2 \arcsin\left(\frac{w}{r}\right) + w\sqrt{r^2-w^2}\Bigg]_w^{\sqrt{w^2+\xi^2}}$$

$$\uparrow$$

$$\text{by parts} \quad u = \arcsin\left(\frac{w}{r}\right) \qquad dv = 2r dr$$

$$du = \frac{-w}{r\sqrt{r^2-w^2}} dr \qquad v = r^2$$

$$= (w^2+\xi^2) \arcsin\left(\frac{w}{\sqrt{w^2+\xi^2}}\right) + w\xi - \frac{\pi}{2} w^2.$$

$$(3) = \int_{\sqrt{w^2+\xi^2}}^{w+\xi} 2r \arccos\left(\frac{r^2+\xi^2-w^2}{2\xi r}\right) dr$$

$$= r^2 \arccos\left(\frac{\xi^2+r^2-w^2}{2\xi r}\right) - \frac{1}{2}\sqrt{-\xi^4+2\xi^2(r^2+w^2)-(r^2-w^2)^2}$$

$$- w^2 \arctan\left(\frac{\xi^2-r^2+w^2}{\sqrt{-\xi^4+2\xi^2(r^2+w^2)-(r^2-w^2)^2}}\right)\Bigg]_{\sqrt{w^2+\xi^2}}^{w+\xi}$$

$$= -(w^2+\xi^2) \arccos\left(\frac{\xi}{\sqrt{w^2+\xi^2}}\right) + \frac{1}{2}\sqrt{-2\xi^4+2\xi^2(2w^2+\xi^2)} + \frac{\pi}{2} w^2.$$

Hence, we have an analytical expression for the effective extended encounter region that can be used in Equation 4.8 to correct for the bias produced by animal moving in

straight lines at constant speed.

$$a_{t_2-t_1} = k\left[\pi w^2 + (w^2+\xi^2)\arcsin\left(\frac{w}{\sqrt{w^2+\xi^2}}\right) + w\xi - (w^2+\xi^2)\arccos\left(\frac{\xi}{\sqrt{w^2+\xi^2}}\right) + \frac{1}{2}\sqrt{-2\xi^4+2\xi^2(2w^2+\xi^2)}\right].$$

4.2.1 Simulation study

All simulations were conducted using (R Core Team, 2016, version 3.2.4) as described in Chapter 3, for 1000 iterations. Applying the abundance estimator of equation 4.8, which corrects for animal movement, we obtained unbiased estimates regardless of the animal speed or the time spent monitoring at each point (Figure 4.5).

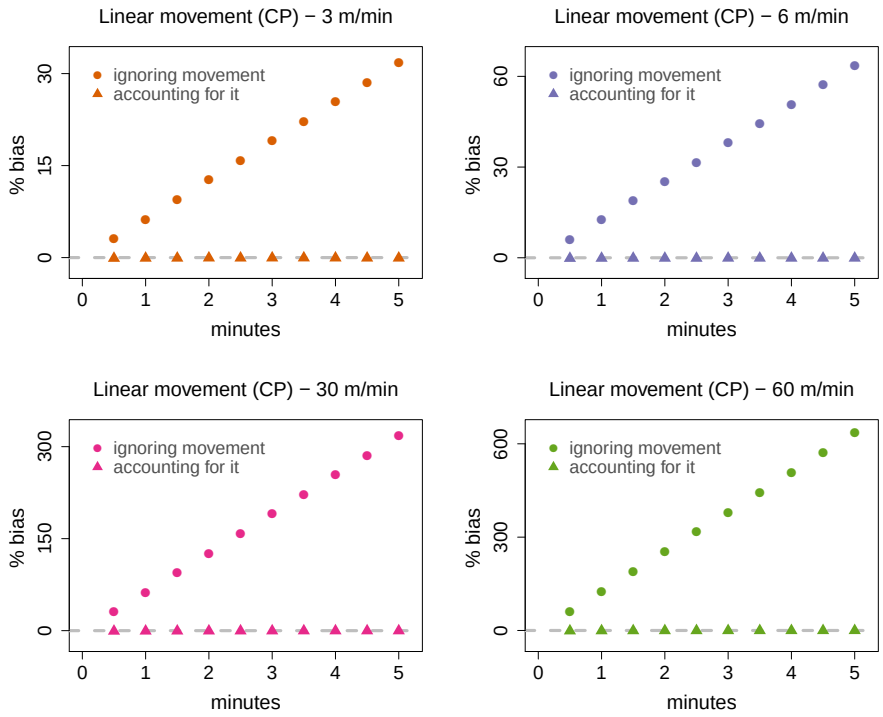

Figure 4.5: Percentage bias in abundance for circular plot sampling when animals move linearly, ignoring animal movement and correcting for it, using abundance estimator of equation 4.8.

The results obtained with this simulation could be obtained analitically using equations

4.10 and 4.11. Equivalent results (unbiased abundance estimators) were obtained by using the correction of Equation 4.11 when applying CPS analysis.

4.3 Diffusion process movement

Traditionally diffusion describes how a group of individual particles spread out from a point source due to the irregular motion of each particle. When applied to animals, diffusion may be viewed alternatively as a description of the distribution of some animal population or the expected location of an individual animal in space and time (McKenzie *et al.*, 2009). Hence, for many ecological systems, diffusion models are appropriate for describing the distribution of animals in time and space (Turchin, 1991; Holmes *et al.*, 1994). However, despite the interest in the pdf of animal locations, we are focussed here on the path of individual animals, since the first time an animal crosses the circle boundary is our parameter of interest.

Working in discrete time, animal movement defined by diffusion processes can be described as a correlated random walk (CRW) dependent on three parameters: number of steps τ, step length (animal displacement l), and the distribution of turning angles $f(\phi)$ (Byers, 2001). Note the important difference between the direction of movement θ_j, and the turning angle $\phi_j = \theta_{j+1} - \theta_j$. The pathways of individuals can be described using quantities such as the mean squared displacement (Kareiva and Shigesada, 1983), the fractal dimension or tortuosity (With, 1994; With *et al.*, 1999), and the mean first passage time (Johnson *et al.*, 1992b).

To account for animal movement in this case, the idea is the same as before. The difference is that instead of knowing the exact distance that an animal moves during the surveyed time period, now we will deal with a pdf of spatial distances. Two approaches are described:

1. Approximation based on mean dispersal distance

The first considers an approximation to derive a simple correction. We estimate the mean dispersal distance (i.e., mean distance moved after ν steps) and use this in the formulation developed in the previous section for linear movement (evaluating the effective extended encounter region using the probability of presence in a circular plot function and using Equation 4.8, we have a correction of bias). Therefore, basically, the generalization of the method is based on the estimation of the average distance travelled by an animal

during the survey period. This will underestimate the probability of presence, and so the estimator of N will still be positively biased. Nevertheless, it is straightforward to apply and should be less biased than no correction.

2. Simulation-based approach to estimate the probability of presence in a circular plot.
The second approach is based on simulation, where multiple random paths are generated over a range of distances from the sampler, and the form of the probability presence function is estimated empirically (depending on the animal's initial distance to the observer). This approach should yield an unbiased estimator of N, but is computer-intensive.

The above methods are applied in two situations: random walk (Section 4.4) and biased random walk (Section 4.5).

4.4 Random walk

The simple random walk (SRW, also known as Brownian motion, ideal gas or Isotropic Random Walk) is the basis of most of the theory of diffusive processes. The animal is equally likely to move in each possible direction, independent of the direction at all previous times. Therefore, the direction of each animal step θ_τ follows a uniform distribution in the circle with pdf, $f(\theta) = \dfrac{1}{2\pi}$, $\theta \in [0, 2\pi]$.

The RW with constant speed u produces the standard diffusion (or heat) equation (Codling *et al.*, 2008, see Figure 4.6)

$$\vartheta_{t_2-t_1}(x, y) = \frac{1}{\frac{\pi u^2}{\tau}(t_2 - t_1)} \exp\left\{-\frac{x^2 + y^2}{\frac{u^2}{\tau}(t_2 - t_1)}\right\}. \tag{4.13}$$

4.4.1 Approximation based on mean dispersal distance

An animal trajectory in an interval of time $[t_1, t_2]$ is defined by ν successive steps of constant length (since we are considering a second the time unit τ, the displacement $l = 1u$ the animal speed). Assuming that an animal in an initial position (x_{t_1}, y_{t_1}) travels

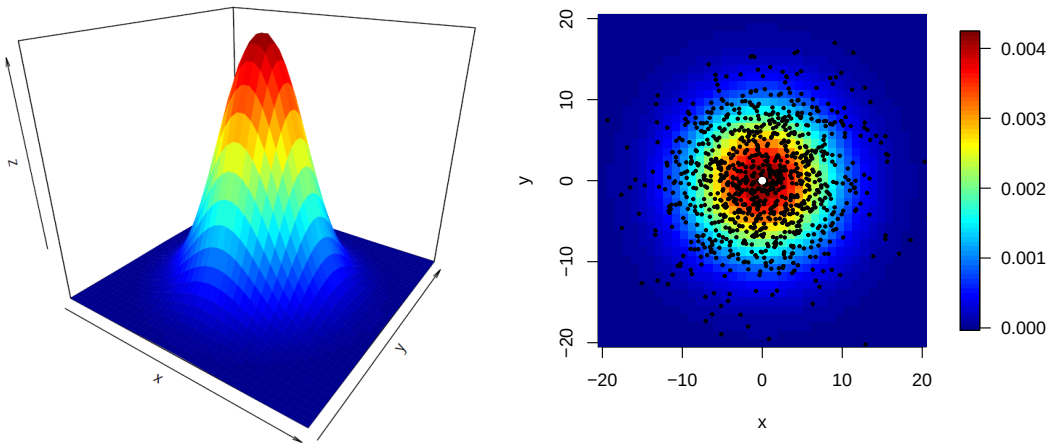

Figure 4.6: Theoretical probability density plots calculated from Equation 4.13 with a uniform in the circle angular distribution for a 5 minute interval of time ($t_2 - t_1 = 300$ time steps), with constant speed $u = 0.1$m/s. The end points of 1000 simulated RWs with initial position in (0,0) (in white) are marked as black points.

with constant speed and a variable step direction θ_j $(j = 1, \ldots, \nu)$ during this interval, its final position is

$$(x_{t_2}, y_{t_2}) = \left(x_{t_1} + l\left(\sum_{j=1}^{\nu} \sin(\theta_{t_j}) \right), y_{t_1} + l\left(\sum_{j=1}^{\nu} \cos(\theta_{t_j}) \right) \right). \tag{4.14}$$

The mean dispersal distance (MDD), is the expected absolute distance from the origin after ν steps. Despite being an intuitive statistic, it is difficult to state it explicitly. Supposing a 2-dimensional space, and $\vartheta_{t_2-t_1}(x, y)$ the pdf for the spatial distribution in the long-time limit over the total interval of time $[t_1, t_2]$, the mean of the absolute dispersal distance is defined by

$$E(R_{t_2-t_1}) = \int_{\mathbb{R}^2} \sqrt{x^2 + y^2} \vartheta_{t_2-t_1}(x, y) dx dy. \tag{4.15}$$

The MDD can be writen in terms of the mean square displacement (MSD; Codling *et al.*, 2008). The MSD is the expected value of the square of the absolute distance from the origin, and it gives a measure of the spatial spread of the population with time (Codling *et al.*, 2008). The MSD is

$$E(R^2_{t_2-t_1}) = \int_{\mathbb{R}^2} (x^2 + y^2) \vartheta_{t_2-t_1}(x, y) dx dy. \tag{4.16}$$

Equations of Kareiva and Shigesada (Kareiva and Shigesada, 1983) use the CRW parameters (move lengths, turning angles, and total moves) to predict the MSD, but this is less meaningful than the MDD about which the population would be distributed and our parameter of interest. If $\vartheta_{t_2-t_1}(x,y)$ is known , it is straightforward to calculate the MSD. Calculating the MDD however, it is mathematically very difficult (McCulloch and Cain, 1989; Wu *et al.*, 2000; Byers, 2001) in most cases. Kareiva and Shigesada (1983) derived a general formula for the MSD in a CRW and Codling *et al.* (2008) reduces it to a much simpler form in particular cases. Some of these cases are RWs and BRWs. Therefore an estimation of MSD, and hence MDD, since they are both related, is derived.

The "root mean square" distance from the starting point is $\sqrt{\nu}$ where ν is the number of steps taken in $[t_1, t_2]$; since the unit time is considered to be 1 second, $\nu = t_2 - t_1$.

$$E(R^2_{t_2-t_1}) = (t_2 - t_1)u^2 \qquad \sqrt{E(R^2_{t_2-t_1})} = \sqrt{t_2 - t_1}u. \tag{4.17}$$

Bovet and Benhamou (1988) derive the following approximate relationship between MDD and MSD, based on the idea of the location coordinates X and Y of a CRW with a symmetrical distribution $g(\phi)$ for the turning angle at each step (in other words, animals exhibit equal probability of turning clockwise or anticlockwise), follows a normal distribution with equal variance.

$$E(R_{t_2-t_1}) = \frac{\sqrt{\pi E\big(R^2_{t_2-t_1}\big)}}{2}. \tag{4.18}$$

It can be generalized to d dimensions, the expected total distance travelled from the origin is asymptotically ($t_2 \to \infty$)

$$E(R_{t_2-t_1}) \longrightarrow \sqrt{\frac{2\tau}{d}}\frac{\Gamma(\frac{d+1}{2})}{\Gamma(\frac{d}{2})}u, \tag{4.19}$$

where Γ is the Gamma function. So, in our 2-dimensional case,

$$\begin{aligned} E(R_{t_2-t_1}) &\approx \sqrt{t_2 - t_1}\frac{\Gamma(\frac{3}{2})}{\Gamma(1)}u = \Gamma\Big(\frac{3}{2}\Big)\sqrt{t_2 - t_1}u \\ &= \frac{\sqrt{\pi}}{2}u\sqrt{t_2 - t_1}. \end{aligned} \tag{4.20}$$

The probability of presence in a circular plot $q_{t_2-t_1}$ is defined as Equation 4.12, if animals move linearly $\xi_{\mathrm{LM}} = u(t_2 - t_1)$, while when animals move following a random walk, the average distance animals travel during the time interval is $\xi_{\mathrm{RW}} = \frac{\sqrt{\pi}}{2}u\sqrt{t_2 - t_1}$. Then,

the effective extended encounter region $a_{t_2-t_1}$ (Equation 4.7) is used to correct for RW moving animals and hence derive an abundance estimator using Equation 4.8.

Figure 4.7 shows that when we ignore animals moving as a RW, abundance can be overestimated, with bias increasing with animal speed. The above method for correcting bias, as expected, give us biased estimators since it is an approximation. However, as discussed later in Section 4.6 truncating by the recommended time (i.e., truncating the duration of the survey period) results in unbiased estimators.

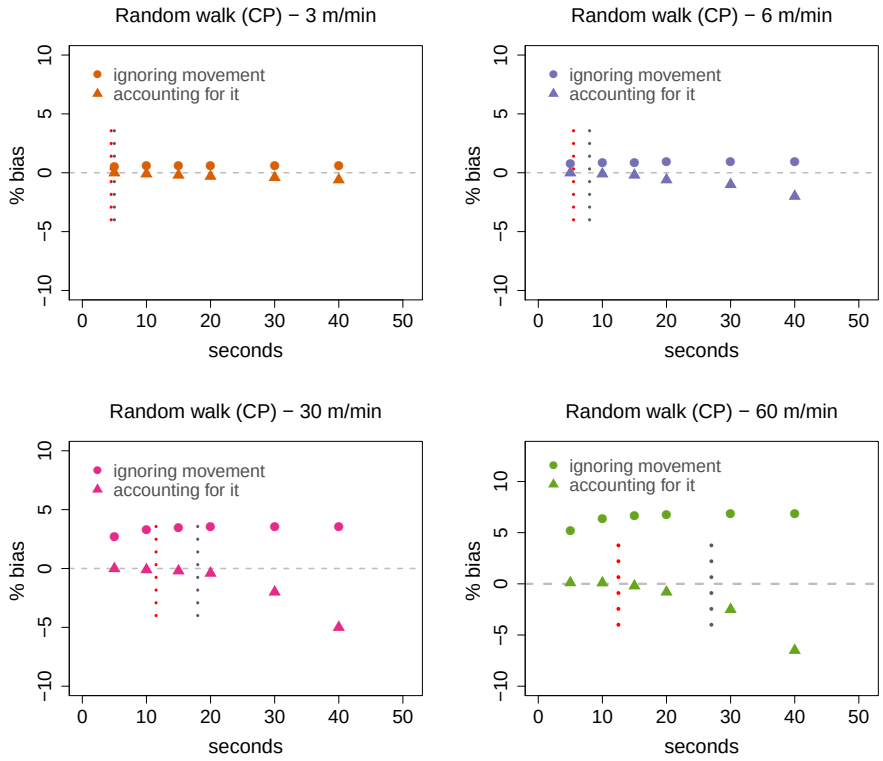

Figure 4.7: Percentage bias on abundance for circular sampling when animals follow a random walk, ignoring animal movement and correcting for it, using abundance estimator of equation 4.8 with the MDD. The grey dotted line represents the last time an animal was detected across all simulations, while the red dotted line is the mean (across simulations) time an animal was last detected (see Section 4.6).

4.4.2 Simulation-based approach to estimate probability of presence in a circular plot

The idea is to use simulation to estimate the probability of presence in a circular plot $q_{t_2-t_1}$ and then apply this to estimate the effective extended encounter region (Equation 4.7). We then use this $a_{t_2-t_1}$ to estimate the abundance using Equation 4.8.

To model the probability of entering the encounter region, given an animal's initial distance to the centre of the circle, the function is split in three different cases. All animals starting inside the circle will be present. All animals further away from the point transect centre than $w+u(t_2-t_1)$ will not enter the covered area. We use simulation to evaluate the proportion of present animals when they start their path between w and $w+u(t_2-t_1)$. The distance interval $[w, w+u(t_2-t_1)]$ was divided in 20 non-equidistant points and 21 bins, being at closer distances near the truncation distance w and more separated after some fixed threshold. The reason was that $q_{t_2-t_1}$ the probability of presence in the encounter region decreases very sharply near w, being near 0 or 0 at larger distances from w and we are interested in its decay, so the partition is the finest near w. At each of the distances along the interval, i.e., over a range of different distances, 1000 walks were simulated and used to estimate the proportion of detected animals. We use a Generalized Additive Model (GAM; Wood, 2012) to estimate the curve , so $q_{t_2-t_1} \in [0,1]$ is

$$q_{t_2-t_1}(r,u) = \begin{cases} 1 & \text{if} \quad r \leq w \\ \hat{\beta} + s(r,u) & \text{if} \quad w < r \leq w + u(t_2-t_1) \\ 0 & \text{if} \quad r > w + u(t_2-t_1), \end{cases} \tag{4.21}$$

with $\beta \in \mathbb{R}$ the intercept and s is the smooth function. An example is given in Figure 4.8, where we compare the probability of presence in the encounter region for animals moving linearly versus a Brownian motion movement at the same speed, $u = 3$m/min, during a 5 minute period. The main difference between both probabilities is at closer distance to the boundary $w = 30$, the probability when an animal moves in a straight line to enter into the circle is half, but animals moving randomly have a probability of presence of almost 1. In the first step the probability would be the same for both, however as time and steps increase an animal moving randomly is almost certain of being detected after 5 minutes. On the other hand, the probability of presence in the encounter region decreases more quickly with random walkers than with animals moving linearly.

This method, as expected, leads to unbiased estimators (see Figure 4.9).

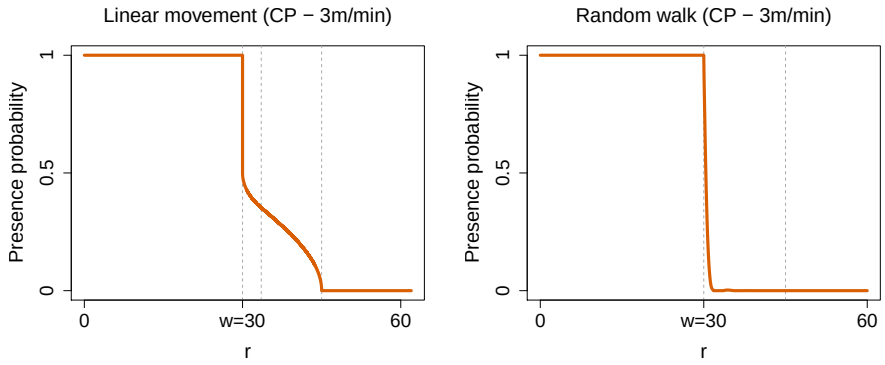

Figure 4.8: Probability of presence in the encounter region for animals moving linearly and following a SRW at constant speed $u = 3$m/min over a 5 minute interval.

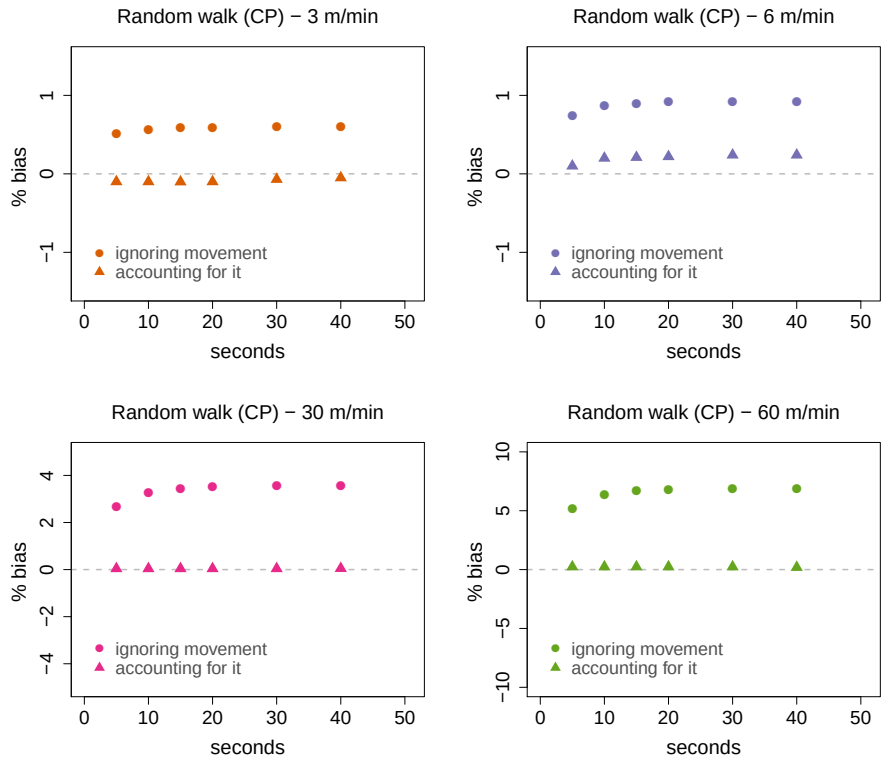

Figure 4.9: Percentage bias on abundance for circular sampling when animals follow a random walk, ignoring animal movement and correcting for it, using abundance estimator of equation 4.8, modelling the probability of presence by simulation.

4.5 Biased Random Walk

In Biased Random Walk (BRW) is also possible to quantify the direction, functional form and magnitude of the movement bias (Codling *et al.*, 2010). We use the same model as described in Chapter 3.2.4: animals exhibit attraction to a particular point (the "centre of attraction"), creating a trajectory that tends to stay within a "home range" (McClintock *et al.*, 2012). The direction of each animal step θ_τ follows a wrapped Cauchy(μ_t, ρ_t) distribution where the expected movement direction μ is the direction between the actual position of the animal and its centre of attraction. The strength of bias to the centre of attraction is defined by $\rho = \tanh(c\delta)$, where $c\delta$ is the scaled distance between the location and the centre of attraction and varies in each time step τ.

4.5.1 Approximation based on mean dispersal distance

A first approximation to use the MSD distance to find the MDD is to take the square root of the MSD, but this may overestimate by up to 12.4% the actual MDD (Byers, 2001). A correction factor that multiplies the square root of the MSD to obtain the MDD may be obtained by simulation (Byers, 2001). Another option is to estimate directly by simulation the MDD value. To do so, we simulate 1000 BRW's with a common centre of attraction, sampling the initial animal position from the pdf and estimating the dispersion distance at the end of the path (Figure 4.10).

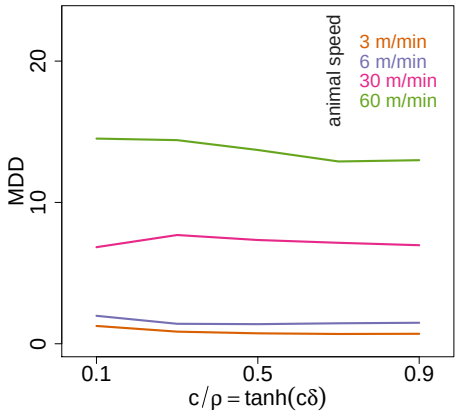

Figure 4.10: Mean dispersal distance (MDD) for 1000 BRWs at 5 minute period $[t_1, t_2]$, with different values of strength constant $c = \{0.1, 0.3, 0.5, 0.7, 0.9\}$ and animal's speed.

The MDD used for different speeds to estimate the effective extended encounter region when $c = 0.1$ are given in Table 4.1.

Table 4.1: Mean dispersal distance (MDD) of the home range area of 1000 BRWs over 5 minute period $[t_1, t_2]$, for different animal's speed $u = \{3, 6, 30, 60, 180, 300\}$m/min, when the strength constant $c = 0.1$.

speed (m/min)	3	6	30	60	180	300
$\text{MDD}_{[t_1,t_2]}$	1.3	2.0	6.8	14.5	39.7	60.2

One option is to assume a linear relationship between the MDD and time, however to be more precise we can model the MDD, using GAMs, over the observation interval of time for $c = 0.1$ (Figure 4.11).

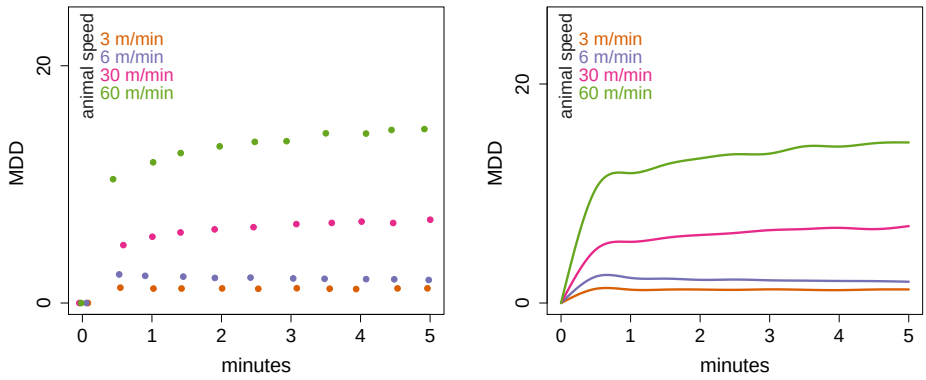

Figure 4.11: MDD for 1000 BRWs over 5 minute period $[t_1, t_2]$, with strength constant $c = 0.1$ and different animal's speed $u = \{3, 6, 30, 60, 180, 300\}$m/min. In the right side, shown are smoothed lines of raw results (left side).

The effective extended encounter region is estimated using the probability of presence in a circular plot (Equation 4.12 based on a straight line movement) with $\xi_{\text{BRW}} = \text{MDD}_{[t_1,t_2]}(u)$, the average distance animals travel during the surveyed interval of time. Then, with Equation 4.8 an abundance estimator is obtained (Figure 4.12).

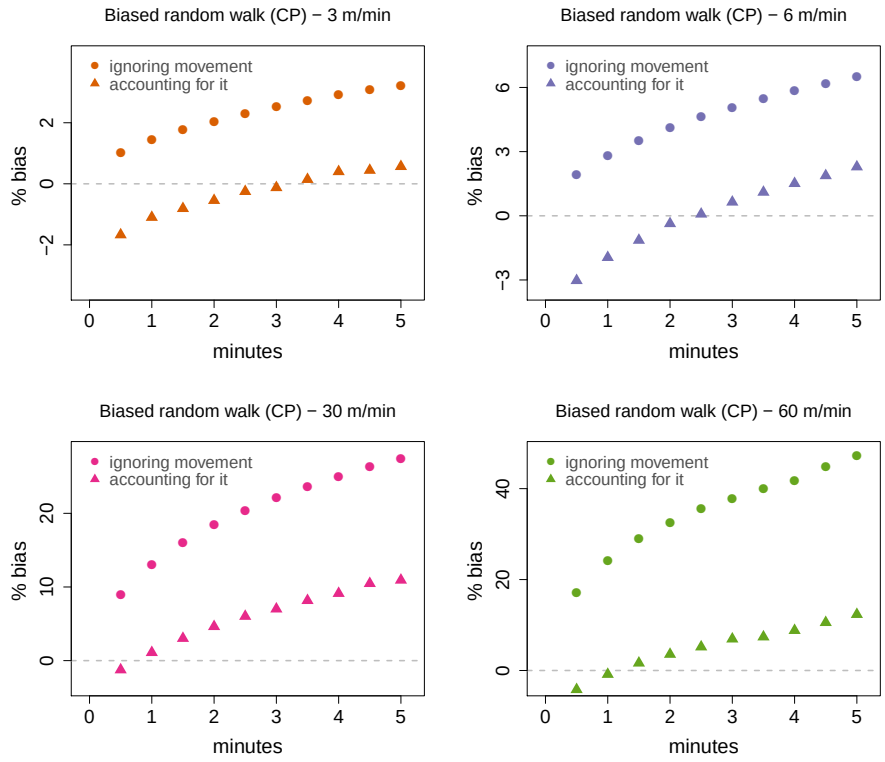

Figure 4.12: Percentage bias on abundance for circular sampling when animals follow a biased random walk, ignoring animal movement and correcting for it, using abundance estimator of equation 4.8.

When we ignore animal movement abundance is overestimated and the bias increases with animal speed. The correction using the MDD, is less biased than ignoring animal movement but still biased.

4.5.2 Simulation-based approach to estimate probability of presence in a circular plot

The probability of presence in a circular plot (Equation 4.21) is estimated by simulation, in the same way that we did for the SRW (see Section 4.4.2). When ignoring animal movement, abundance is overestimated and the bias increases with animal speed. However when estimating by simulation the probability of presence in the encounter region, we obtained unbiased estimators (Figure 4.13).

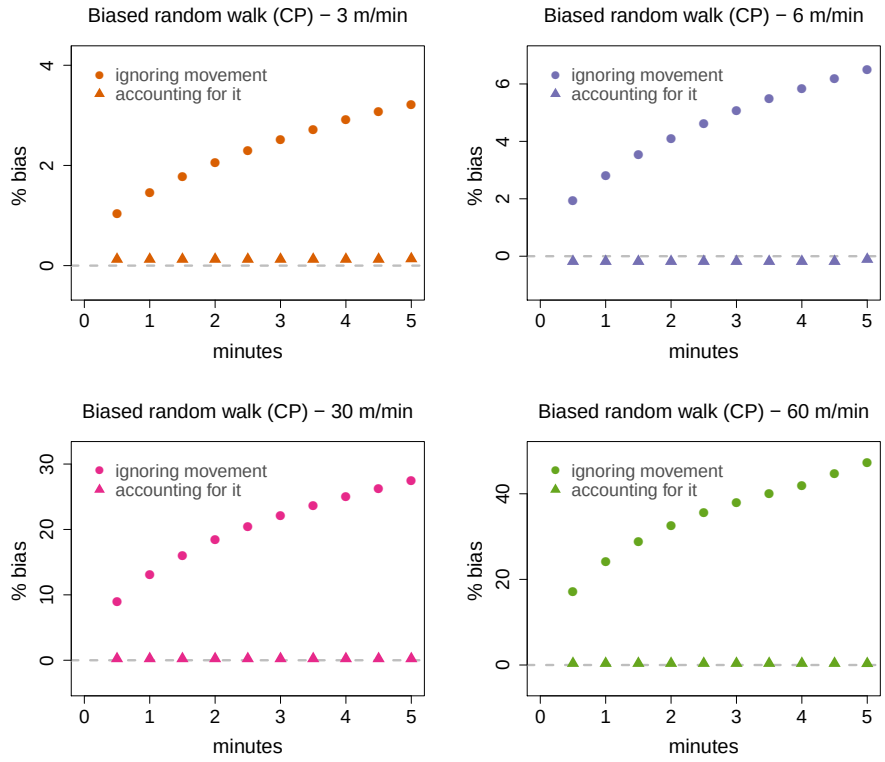

Figure 4.13: Percentage bias on abundance for circular sampling when animals follow a biased random walk, ignoring animal movement and correcting for it, using abundance estimator of equation 4.8, modelling the probability of presence by simulation.

4.6 Discussion

For animals moving linearly with constant (known) speed, applying the analytic correction results in unbiased abundance estimators. The distance an individual travels, regardless of the type of movement, is fixed. The advantage of the linear movement is that the distance between the start and the end point is known, and so the probability of presence in the covered region gives us an analytic correction of bias. This is not the case with the other animal movement scenarios defined as a diffusion process. Despite deriving an approximation using the average distance an animal moves, when applying the probability of presence in a circular plot we are assuming a straight distance between the start point and the end of the walk. In a linear movement the MDD has to be the same path the

animal travels, however, with a random (biased or not) walk, for a given MDD there are an infinite number of paths that the animal might have traveled. An example is given in Figure 4.14, where for the same MDD (in black) three different random walks (in grey) are proposed. Hence, when applying the probability of presence in a circular plot we are

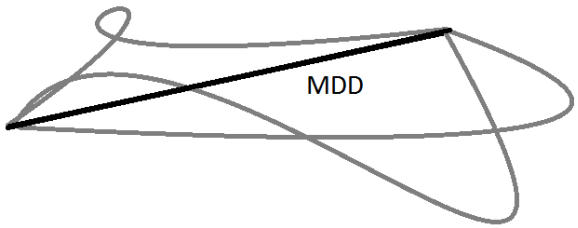

Figure 4.14: Possible random walks paths an animal could move (in grey) given a fix mean dispersal distance (in black) between the start and end point of its path.

ignoring this randomness of movement, in which some animals may be detected even if the MDD would not have been large enough for it to be detected given its original location, assuming a straight line movement.

Conditional of the considered hazard for detection , when animals follow a random walk with constant speed, no animals are detected after the first minute (see Figure 4.7)), not even those travelling at the fastest speed (60m/min), despite the fact that the survey period was 5 minutes. Almost all the animals are detected during the first seconds of time and very few (one or two per iteration) enter the circular plot within the initial surveyed minute and only the animals with the highest speed (in this case animal moving at 60m/min). The reason is that animals have reached their average radius of spatial movement over this time. The time between the first and the last detection is directly proportional to animal speed (shorter time for slow animals versus faster ones). The extended encounter region depends on the length of surveyed time and the movement pattern. However, in this setting, as we are using the correction for linear animal movement applied to a home range animal movement, it only depends on the length of the surveyed time interval, ignoring the actual movement of the animals. Therefore, if we correct for the full 5 minute period but animals are only detected during the first minute, abundance is underestimated at the end of the time period. For this particular situation, a possible workaround is reducing the survey time, such that the ratio of number of detected animals divided by the encounter area accounting for movement is more realistic.

This shorter time can be chosen in a variety of ways, but hopefully the results will be not dependent on its choice. In the simulation framework we have chosen this shorter time as the average time of the last detection across the iterations of a given scenario, and we obtain unbiased abundance estimators.

For animals moving showing attraction to a point via a biased random walk, to derive a direct equation for the MDD is more complicated and remains an open problem (Codling *et al.*, 2008). We found that the abundance estimator of equation 4.8, as expected, does not lead to unbiased estimators when animals do not move in straight lines.

A better approach is an analytical method based on the first passage time to estimate the probability that a sample path crosses the boundary of the circular plot at least once in the surveyed interval of time and hence the animal is sampled. This approach, despite providing an analytical correction for the bias, is complex even for the simplest cases we consider. Instead of focusing on dispersal distances, in this approach we focus on the proportion of animal paths crossing the observation circular plot. The distance travelled will be different, depending on which part of the circle we are talking about. For example, there is the nearest point on the circle to the animal's position at t_1, but it may not cross the circle there, it may instead go right around and come in the circle from the back.

An intuitive approach to find a measure for search effort is to ask how much time the animal uses along the path before entering the encounter region. The time used will depend on the size of the area and on the speed and tortuosity of the walk within the area (Fauchald and Tveraa, 2003). Therefore, for modeling search time as a function of animal movement, theory from the physical and mathematical literature on first passage time is used. The first passage time (FPT) is defined as the time required for a random variable, such as an animal's location in space, to go from a given starting point to a predefined endpoint (Redner, 2001). In this case would be the time required for an animal to cross a circle with a given radius (e.g., Johnson *et al.*, 1992a), and is a reasonable measure for the search effort along a pathway.

Though much of the FPT theory has been previously developed (Ovaskainen, 2008; Redner, 2001; Kou and Zhong, 2016), and discussed in the physical literature it has not been widely placed in the context of animal movement (McKenzie *et al.* (2009) do so synthesizing the FPT theory using examples from animal movement and deriving a general equation for FPT from a random walk in a heterogeneous environment.) This is perhaps because of its highly theoretical treatment to date. Berg (1993) was the first to

discuss FPT in an ecological context. FPT was also proposed as an alternative to mean squared displacement to characterize diffusion behaviour (Johnson *et al.*, 1992a) and used to identify optimal search strategies (Bénichou *et al.*, 2005). Moreover, as Kou and Zhong (2016) say "Despite various attempts since the 1960s, there are few analytical solutions available".

The problem we first consider is of a random walker performing a simple, unbiased random walk (equal probability of going in all directions) with an absorbing boundary (if the animal crosses the boundary it will stay inside the bounded area) in two dimensions. We are more interested in the probability ($Z_{t_2-t_1}$) that a sample path crosses the boundary at least once during the surveyed interval than in the first passage density at some particular point (Durbin and Williams, 1992).

$$Z_{t_2-t_1} = \int_{t_1}^{t_2} z(t)dt,$$

where $z(t)$ FPT density function. Therefore an abundance estimator is,

$$\hat{N} = \frac{n_{t_2-t_1}}{Z_{t_2-t_1} a_{t_2-t_1}} A.$$

Estimate the FPT for RW and BRW diffusion movement is very complicated and we were not able to do it, despite being the best approach for arriving to an analytic correction of bias.

Therefore the only unbiased method for correcting for animal movement we offer is to model by simulation the probability of animal presence in a circular plot. The main downsides of the simulation approach are that it is computer-intensive and requires some computing skills to implement. For any analytic approach one might derive we would need to know how the animals move nearby the observation point to estimate this proportion without bias. In other words, responsive movement needs to be considered, since animals may exhibit different behaviours depending on the area where we are collecting the data. Assuming that the animal movement is known (accounting for both the observer presence and the encounter area) a simulation is then the best way to account for animal movement into CP abundance estimators.

The approach could readily be generalized to uncertain movement parameters u by in each simulation sampling from a distribution of such parameters, or by superimposing samples of animal paths taken from, e.g., tag data.

5

Including animal movement in point transect sampling

5.1 Introduction

Conventional DS (CDS) estimators require that the underlying distribution of animals with respect to the samplers is known. When DS assumptions hold, CDS is based on the three functions shown in Figure 5.1: the true distribution of animals, the detection function and the distribution of observed distances. If transects are placed at random (or more commonly following a systematic grid), then the underlying distribution of all distances to individuals (detected or not) within distance w is on average uniform on the interval $[0, w]$ for LTS, or has probability density $f(r) \propto r, r \in [0, w]$, for PTS (top of Figure 5.1). Obtaining a DS estimator of animal density involves the estimation of the proportion P_a, of all individuals within the truncation distance that were detected, using their detection distances. This probability of detection is given by the quotient of the areas beneath the distribution of observed distances and the hypothetical detection function that arises from perfect detection (the dashed line in the bottom of Figure 5.1).

DS methods are based on the idea of a snapshot, where the underlying assumption about the distribution of animals needs to be satisfied. However, PTS surveys take place during an interval of time (t_1, t_2), during which animals may move. When animals move, the animal distribution is the same at the initial time t_1 but depending on the animal movement, the distribution of animals that remains to be detected at different distances would change over time. If animals move randomly, at any instant of time, in other words taking a "snapshot" in time, with a random placement of transects on average the usual

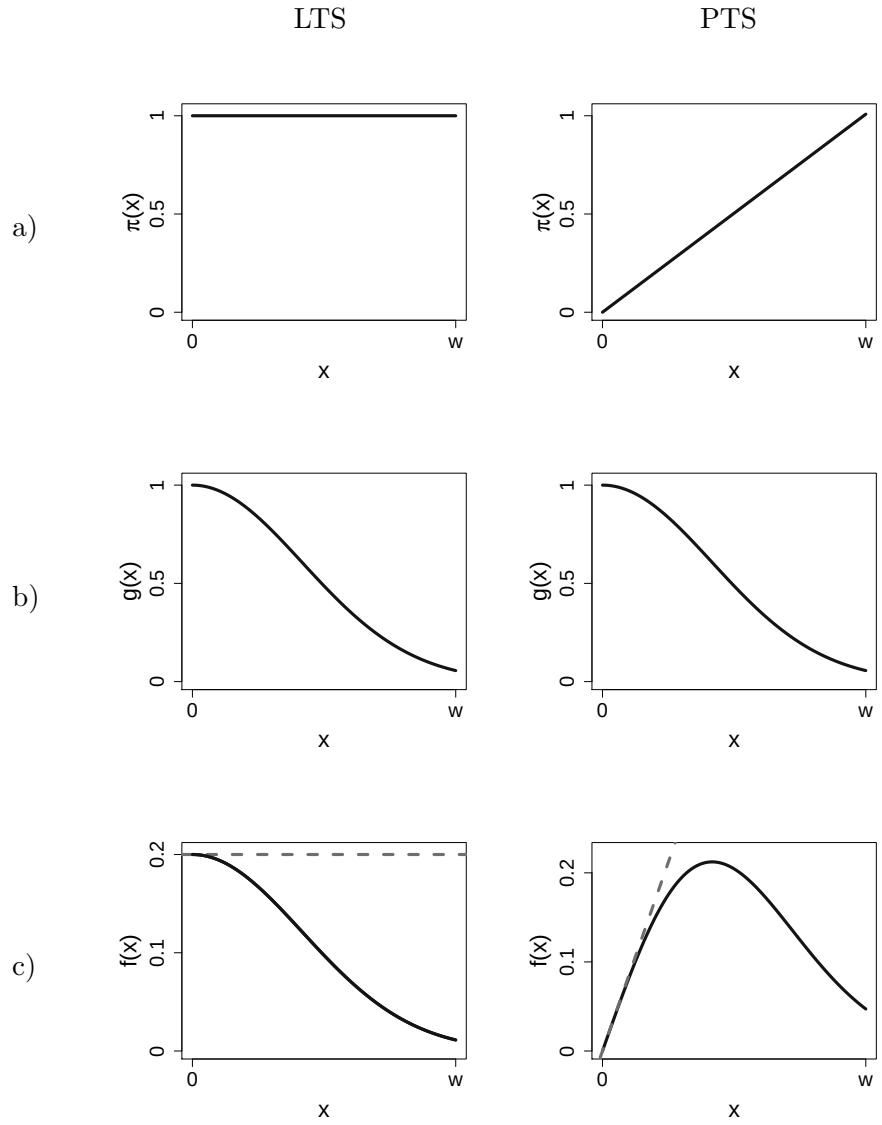

Figure 5.1: a) True distribution of animals, b) detection function and c) distribution of observed distances. w represents a truncation distance, the distance beyond which no detections are considered.

CDS animal distribution $\pi(x)$ is obtained (Figure 5.1a). However, in the presence of undetected responsive movement, we can think of it as a change in the $\pi(x)$. Turnock and Quinn (1991) use the change in $\pi(x)$ as the key idea to correct the abundance in LTS estimators when responsive movement occurs.

In this chapter, we consider animals moving linearly with constant speed u and random direction θ in the circle. To build unbiased PTS estimates of abundance, our main interest is to define the distribution of animals that remain to be detected during the survey, knowing how the animals move. Under random movement, there are two processes occurring simultaneously: (1) encounter rate increases (as animals that would be too far off to be detected by a snapshot come into the vicinity of a point) and (2) estimated detectability decreases, as randomly-moving animals are more likely to be detected at smaller rather than large distances, so their average distance of detection is smaller than their average position over the time of the survey, leading to underestimation of distances. Both of these lead to an overestimation of density if movement is ignored, the former (mostly) through the encounter rate and the latter (mostly) through bias in the detection function.

The conventional detection probability is modelled as a function of distances but as constant over time. To capture this variation over time in the underlying distribution of animals, we introduce a detection function that takes into account both spatial and temporal variation in detection probability. It is composed of two linked submodels: the movement model and the detection model. Hence, to estimate this probability of detection over time we concentrate our attention on a kind of removal process. We can think of it as a removal process in the sense that animals are at risk of being detected, and when detected are removed from the population that is at risk. At each instant the risk will be dependent on the distance from animal to the point, and hence will change over time due to the movement process.

The remaining sections are organized as follows. In Section 2 we describe the detection process including animal movement. We define a probability density function of distances and times at which first detection of an animal occurs. Based on this, we then derive two abundance estimators. Implementation of these estimators was unsuccessful in time available. In Section 3, therefore, we discuss possible implementation strategies based around a simulation study.

5.2 Detection process including animal movement

As described in Chapter 4 in a circular plot sampling scenario, when animals are mobile, even if the animals happen to be outside the plot when the survey starts, they can enter into the covered circular region and hence be detected. However, here we are assuming imperfect detectability, as in most applications we are likely to miss some animals in the covered area. There are two possibilities for an animal detection over a survey time interval to occur at a given instant of time: (1) the animal could have been available for detection to begin with (i.e., being inside the covered area when the survey begins), and been detected while inside, or (2) the animal could be unavailable for detection when the survey period begins (i.e., outside the covered area) and after entering the covered area, while the recording period is ongoing, it was detected. CDS methods consider all detections to be of the first kind. Therefore, as in the presence of animal movement we expect to record more animals with increasing time spent monitoring, we need to combine animal movement and the detection process, so we must include how the animals might have moved to account for the second kind of detections.

In the following section we describe a likelihood which, given a model assumed for the animal movement, will take as data the first time each animal is detected and its distance to the centre of the circular plot when the detection occurs. This likelihood will allow estimation of density in the presence of animal movement.

5.2.1 Likelihood

Consider a survey occurring over a time period $[t_1, t_2]$. Define $f(R,T) : \mathbb{R}^+ \times \mathbb{R}^+ \longrightarrow \mathbb{R}^+$ as the probability density function (pdf) of detecting an animal for the first time in the time interval $(T, T + dT)$ and the distance interval $(R, R + dR)$ from the centre of the circular plot, conditional on the survey time period $[t_1, t_2]$. Usually it is simpler to assume that the survey time period starts at 0 ($t_1 = 0$ and $t_2 > 0$) but for generality, we keep both limits explicit. We assume that animals move in a straight line with constant and known speed u and random direction θ uniformly distributed on the circle; for brevity, we omit this from the definitions of quantities in the formulation below.

$$
\begin{aligned}
f(R,T) = & \text{ pr}\{\text{an animal being within the distance interval } (R, R+dR) \text{ and time interval} \\
& (T, T+dT) \mid \text{animal is detected}\} \\
= & \frac{\text{pr}\{\text{an animal being detected within the distance interval } (R, R+dR) \text{ and time } (T, T+dT)\}}{\text{pr}\{\text{an animal is detected}\}} \\
= & \frac{\widetilde{f}(R,T)}{P_{t_2-t_1}},
\end{aligned}
\tag{5.1}
$$

Details about the numerator $\widetilde{f}(R,T)$ and denominator $P_{t_2-t_1}$ involved in this pdf are presented next.

For the numerator, define $\widetilde{f}(R,T) : \mathbb{R}^+ \times \mathbb{R}^+ \longrightarrow \mathbb{R}^+$ as the pdf of detecting for the first time an animal at distance R to the centre of the circular plot and at time $T \in [t_1, \infty)$. Note that $f(R,T)$ and $\widetilde{f}(R,T)$ are both pdfs, but they have different support since the detections on $f(R,T)$ are conditioned on the interval of time of the survey, i.e., $f(R,T) : \mathbb{R}^+ \times [t_1, t_2] \longrightarrow \mathbb{R}^+$ and $\widetilde{f}(R,T) : \mathbb{R}^+ \times [t_1, \infty) \longrightarrow \mathbb{R}^+$.

$$
\begin{aligned}
\widetilde{f}(R,T) = & \text{ hazard of detection within the distance interval } (R, R+dR) \text{ and time interval} \\
& (T, T+dT) \ \times \ \text{pr}\{\text{the animal is not detected during the interval } (t_1, T)\}.
\end{aligned}
\tag{5.2}
$$

In the second part of the above expression we need to include information on how the animal has moved prior to the detection. We assume that the initial animal position follows a uniform distribution in 2-dimensional space. Then, given detection at distance R, the distribution of animal's possible initial positions at time t_1 forms a circle of known radius (since both speed and the elapsed time are known) centred at the position of detection. Conditional on an animal initial position (at time t_1) and a particular θ direction, the travelled path is known. Hence:

$$
\begin{aligned}
\widetilde{f}(R,T) = & \text{ hazard of detection within the distance interval } (R, R+dR) \text{ and time interval} \\
& (T, T+dT) \ \times \ \text{pr}\{\text{the animal is not detected over all possible paths during} \\
& \text{the time interval } (t_1, T)\} \\
= & \, k(R,T) \times \\
& \text{pr}\{\text{the animal is not detected over all possible paths during the interval } (t_1, T)\}.
\end{aligned}
\tag{5.3}
$$

Because we do not know the travelled direction, we must integrate over all possible directions. This leads to

$$\widetilde{f}(R,T) = k(R,T)\int_{\theta=0}^{2\pi}\frac{1}{2\pi}\,\mathrm{pr}\{\text{the animal is not detected during the interval } (t_1,T) \mid \text{moving linearly with constant speed } u \text{ and direction } \theta\}\,d\theta. \tag{5.4}$$

For each fixed direction θ, the probability of not detecting an animal is the density of initial animal position times the density of not detecting the animal over the path, where the path is known, so

$$\begin{aligned}\widetilde{f}(R,T) &= k(R,T)\int_{\theta=0}^{2\pi}\frac{1}{2\pi}\left[1-\left(1-\exp\left\{-\int_{t=t_1}^{T}k\big(x(t\mid R,T,u,\theta),t\big)dt\right\}\right)\right]\Pi\big(R_{t_1}(\theta)\big)d\theta \\ &= k(R,T)\int_{\theta=0}^{2\pi}\frac{1}{2\pi}\exp\Bigg\{-\underbrace{\int_{t=t_1}^{T}k\big(\underbrace{x(t\mid R,T,u,\theta)}_{(2)},t\big)\,dt}_{(1)}\Bigg\}\,\underbrace{\Pi\big(R_{t_1}(\theta)\big)}_{(3)}\,d\theta.\end{aligned} \tag{5.5}$$

We explain in turn below the different components (1), (2) and (3), with details about the notation used.

► **(1)**

Define the hazard function of being detected at distance x and time t

$$k(x,t)dt = \mathrm{pr}\{\text{an animal at distance } x \text{ is detected during } (t+dt) \mid \text{not detected up to time } t\}. \tag{5.6}$$

The "hazard" that an animal would be detected by the observer, if the observer is assumed to search with constant effort during the surveyed interval of time $[t_1,t_2]$, is independent of time; hence $k(x,t) = k(x)\forall t \in [t_1,t_2]$. We refer to $k(x,t)$ as the instantaneous hazard, which follows the analogous terminology in the survival analysis literature, where hazard functions are routinely used to describe the risk of an event occurring (in the survival literature that event is typically death, here is the detection). We use the hazard $k(x) = cx^{-d}, c,d \in \mathbb{R}^+$ given by Hayes and Buckland (1983), and so

$$\widetilde{f}(R,T) = k(R)\int_{\theta=0}^{2\pi}\frac{1}{2\pi}\exp\left\{-\int_{t=t_1}^{T}k\big(x(t\mid R,T,u,\theta)\big)dt\right\}\Pi\big(x_{t_1}(\theta)\big)\,d\theta. \tag{5.7}$$

► **(2)**

$x(t \mid R, T, u, \theta)$ denotes the distance of the animal from the observer at time $t \in [t_1, T]$ conditional on the animal being detected at distance R at time T and that it was moving linearly with constant speed $u \geq 0$, and direction $\theta \in [0, 2\pi)$. For simplicity and without loss of generality, we define an animal at distance R from the observer to be in the position $(r, 0)$ and the observer at $(0, 0)$ (see Fig. 5.2). Therefore, fixing the direction θ, we define

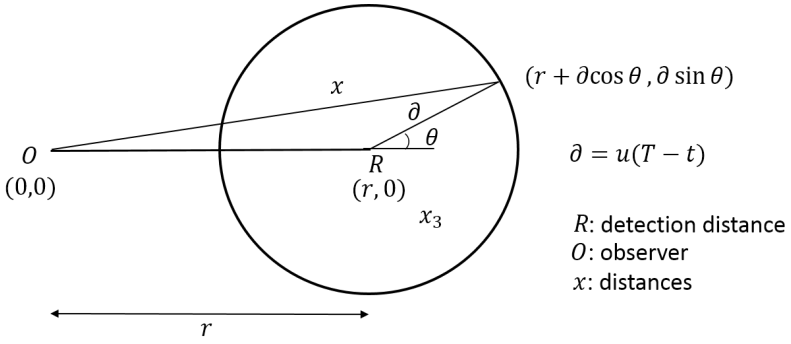

Figure 5.2: Radial distance x between the observer O at $(0, 0)$ and the animal possible location at time $t \in [t_1, T]$, given that the animal was seen at time T and distance R, and it was travelling linearly at constant speed u. For example, given a particular animal direction of movement θ, the animal position at time t is known.

the distances for each $t \in [t_1, T]$ as follows:

$$\begin{aligned} x(t \mid R, T, u, \theta) =& \sqrt{(R + u(T-t)\cos\theta)^2 + (u(T-t)\sin\theta)^2} \\ =& \sqrt{R^2 + (u(T-t))^2 + 2Ru(T-t)\cos\theta}\,, \qquad t \in [t_1, T],\ u > 0,\ \theta \in [0, \pi]. \end{aligned} \tag{5.8}$$

► **(3)**

Define $\Pi(x_t(\theta \mid R, T, u))$ as the probability density function of an animal being within distance interval $(x, x + dx)$ in the time interval $(t, t + dt)$ conditional on the animal being detected at distance R at time T and that it was moving linearly with constant speed $u \geq 0$ and θ direction, $\theta \in [0, 2\pi)$. In particular $\Pi(x_{t_1}(\theta \mid R, T, u))$ is the pdf of initial distances (at $t = t_1$) given that the animal has been detected at distance R at time T and that it was moving linearly with constant speed $u \geq 0$ and direction θ. The true (unconditional) distribution of animal distances with respect to the point at $t = t_1$ is triangular for PTS (the same as in conventional DS when animals do not move), hence $\Pi(x) \propto x$. Knowing the animal speed u and direction θ, the initial animal distance to the

observer is known (see Figure 5.2 with $t = t_1$). Hence,

$$\Pi(x_{t_1}(\theta \mid R, T, u)) \propto \sqrt{R^2 + (u(T - t_1))^2 + 2Ru(T - t_1)\cos\theta}\,.$$

The cumulative distribution function (cdf) of distances from a point to an animal, given that the animal is within the covered area including animal movement (in other words, the circle or radius $w + u(t_2 - t_1)$ centred on the observer), and irrespective of whether they are detected, is

$$\text{pr}\{R \le r\} = \frac{\pi r^2}{\pi\big(w + u(t_2 - t_1)\big)^2}. \tag{5.9}$$

Thus, the pdf of radial distances is obtained by differentiation

$$\Pi(r) = \frac{2r}{\big(w + u(t_2 - t_1)\big)^2}, \tag{5.10}$$

and

$$\Pi(x_{t_1}(\theta \mid R, T, u)) = \frac{2\sqrt{R^2 + (u(T - t_1))^2 + 2Ru(T - t_1)\cos\theta}}{\big(w + u(t_2 - t_1)\big)^2}. \tag{5.11}$$

We now turn to the denominator of equation 5.1. This denominator $P_{t_2-t_1}$, is defined as the probability of detecting an animal during the survey time.

$$\begin{aligned} P_{t_2-t_1} =& 1 - \text{ pr}\{\text{an animal is not detected during the survey period}\} \\ =& 1 - \int_{x_{t_1}} \int_{\theta=0}^{2\pi} \frac{1}{2\pi} \underbrace{S_{t_2-t_1}\big(x_{t_1}(\theta)\big)}_{\downarrow} \underbrace{\Pi\big(x_{t_1}\big)}_{\downarrow}\, d\theta\, dx_{t_1}. \\ & \qquad\qquad (4) \qquad\quad (5) \end{aligned} \tag{5.12}$$

We describe each component (4) and (5) separately.

► **(4)**

$S_{t_2-t_1}\big(x_{t_1}(\theta)\big)$ is the "survival" function (i.e., probability of remaining undetected) of the animal starting at initial distance x_{t_1}, following the direction θ, during the sampled time interval $[t_1, t_2]$,

$$x(t \mid x_{t_1}, u, \theta) = \sqrt{x_{t_1}^2 + (u(t - t_1))^2 + 2x_{t_1}u(t - t_1)\cos\theta} \qquad t \in [t_1, t_2],\ \ u > 0. \tag{5.13}$$

$$
\begin{aligned}
S_{t_2-t_1}\big(x_{t_1}(\theta)\big) &= \exp\Big\{ -\int_{t=t_1}^{t_2} k\big(x(t \mid x_{t_1}, u, \theta)\big)dt \Big\} \\
&= \exp\Big\{ -\int_{t=t_1}^{t_2} c\Big(\sqrt{x_{t_1}^2 + (u(t-t_1))^2 + 2x_{t_1}u(t-t_1)\cos\theta}\Big)^{-d} dt \Big\}.
\end{aligned}
\tag{5.14}
$$

► **(5)**

$\Pi\big(x_{t_1}\big)$ is the pdf of animal distances to the observer, when the animal is at initial distance x_{t_1} (at $t = t_1$),

$$
\Pi(x_{t_1}) = \frac{2x_{t_1}}{\big(w + u(t_2 - t_1)\big)^2}. \tag{5.15}
$$

x_{t_1} is the radial initial distance for an animal that has a non-zero probability of being detected during the time interval $[t_1, t_2]$, so goes from 0 to $w + u(t_2 - t_1)$.

$$
\begin{aligned}
P_{t_2-t_1} =& 1 - \int_{x_{t_1}=0}^{w+u(t_2-t_1)} \int_{\theta=0}^{2\pi} \frac{1}{2\pi} S_{t_2-t_1}\big(x_{t_1}(\theta)\big)\Pi(x_{t_1})\, d\theta\, dx_{t_1} \\
=& 1 - \int_{x_{t_1}=0}^{w+u(t_2-t_1)} \int_{\theta=0}^{2\pi} \frac{1}{\pi} \Bigg[\exp\Big\{ -\int_{t=t_1}^{t_2} c\Big(\sqrt{x_{t_1}^2 + (u(t-t_1))^2 + 2x_{t_1}u(t-t_1)\cos\theta}\Big)^{-d} dt \Big\} \\
& \qquad \frac{x_{t_1}}{\big(w + u(t_2 - t_1)\big)^2} \Bigg] d\theta\, dx_{t_1}.
\end{aligned}
\tag{5.16}
$$

To sum up $f(R, T)$ is defined by,

$$
\begin{aligned}
f(R,T) &= \frac{\widetilde{f}(R,T)}{P_{t_2-t_1}} \\
&= \frac{k(R) \displaystyle\int_{\theta=0}^{2\pi} \frac{1}{2\pi} \exp\Big\{ -\int_{t=t_1}^{T} k\big(x(t \mid R, T, u, \theta)\big)dt \Big\} \Pi\big(x_{t_1}(\theta)\big)\, d\theta}{1 - \displaystyle\int_{x_{t_1}=0}^{w+u(t_2-t_1)} \int_{\theta=0}^{2\pi} \frac{1}{2\pi} S_{t_2-t_1}\big(x_{t_1}(\theta)\big)\Pi\big(x_{t_1}\big)\, d\theta\, dx_{t_1}} \\
&= \frac{\dfrac{cR^{-d}}{\pi} \displaystyle\int_{\theta=0}^{2\pi} \Bigg[\exp\Big\{ -\int_{t=t_1}^{T} c\big(\sqrt{R^2 + (u(T-t))^2 + 2Ru(T-t)\cos\theta}\big)^{-d} dt \Big\} }{1 - \dfrac{1}{\pi} \displaystyle\int_{x_{t_1}=0}^{w+u(t_2-t_1)} \int_{\theta=0}^{2\pi} \Bigg[\exp\Big\{ -\int_{t=t_1}^{t_2} c\Big(\sqrt{x_{t_1}^2 + (u(t-t_1))^2 + 2x_{t_1}u(t-t_1)\cos\theta}\Big)^{-d} dt \Big\}} \\
& \qquad \frac{\dfrac{\sqrt{R^2 + (u(T-t_1))^2 + 2Ru(T-t_1)\cos\theta}}{\big(w + u(t_2 - t_1)\big)^2} \Bigg] d\theta}{\dfrac{x_{t_1}}{\big(w + u(t_2 - t_1)\big)^2} \Bigg] d\theta\, dx_{t_1}}.
\end{aligned}
\tag{5.17}
$$

The likelihood function then is the product of the likelihood associated with each detected animal, assuming each animal i ($i = 1, \ldots, n$) moves independently and is detected independently.

$$L(\Theta; r, t) = \prod_{i=1}^{n} \Big(f(R_i, T_i) \Big), \tag{5.18}$$

$$\ell(\Theta; r, t) = \log \prod_{i=1}^{n} \Big(f(R_i, T_i) \Big) = \sum_{i=1}^{n} \log \big(f(R_i, T_i) \big). \tag{5.19}$$

We maximize it for estimating the detection function parameters $\Theta = (c, d)$.

5.2.2 Abundance estimation

Conditioning on number of detected animals n, and then using an Horvitz-Thompson-like (HTL) estimator, a possible estimator of abundance is given by

$$\hat{N} = \frac{\sum_{i=1}^{n} \frac{1}{\widehat{P}_{t_2-t_1}(R_i, T_i)}}{a_{t_2-t_1}} A = \sum_{i=1}^{n} \left(\frac{1}{\widehat{P}_{t_2-t_1}(R_i, T_i)} \right) \frac{A}{a_{t_2-t_1}}, \tag{5.20}$$

where $\widehat{P}_{t_2-t_1}(R_i, T_i)$ is the estimated probability of detection of the ith animal, i.e., the probability of detecting during the survey period $[t_1, t_2]$ an animal that is known to be at location R_i at time $T_i \in [t_1, t_2]$ defined by equation 5.21, A is the study region and $a_{t_2-t_1} = k\pi(w + u(t_2 - t_1))^2$ is the covered area including animal movement.

$$\begin{aligned} P_{t_2-t_1}(R, T) =& 1 - \text{ pr}\{\text{an animal is not detected during } [t_1, t_2] \text{ given that the animal is} \\ & \text{known to be at distance } R \text{ at time } T\} \\ =& 1 - \int_{\theta=0}^{2\pi} \frac{1}{2\pi} S_{t_2-t_1}\big(x_t(\theta)\big) \Pi\big(x_{t_1}(\theta \mid R, T, u)\big)\, d\theta \\ =& 1 - \int_{\theta=0}^{2\pi} \frac{1}{2\pi} \exp\left\{ - \int_{t=t_1}^{t_2} k\big(x(t \mid R, T, u, \theta)\big) dt \right\} \Pi\big(x_{t_1}(\theta \mid R, T, u)\big)\, d\theta, \end{aligned} \tag{5.21}$$

where $\Pi\big(x_{t_1}(\theta \mid R, T, u)\big)$ is defined by equation 5.11 therefore,

$$\begin{aligned} P_{t_2-t_1}(R, T) =& 1 - \int_{\theta=0}^{2\pi} \frac{1}{\pi} \exp\left\{ - \int_{t=t_1}^{t_2} c\Big(\sqrt{R^2 + (u(T-t))^2 + 2Ru(T-t)\cos\theta} \Big)^{-d} dt \right\} \\ & \frac{\sqrt{R^2 + (u(T-t_1))^2 + 2Ru(T-t_1)\cos\theta}}{\big(w + u(t_2 - t_1)\big)^2}\, d\theta. \end{aligned} \tag{5.22}$$

This leads to

$$N = \sum_{i=1}^{n} \left(\frac{1}{1 - \int_{\theta=0}^{2\pi} \frac{1}{2\pi} S_{t_2-t_1}\big(x_t(\theta)\big)\Pi\big(x_{t_1}(\theta \mid R_i, T_i, u)\big)\, d\theta} \right) \frac{A}{k\pi(w + u(t_2 - t_1))^2}, \tag{5.23}$$

This estimator suffers from a well-known problem with HTL estimators for estimating animal abundance (Borchers *et al.*, 2002): in practice it is not useful since some very low values of $\widehat{P}_{t_2-t_1}(R_i, T_i)$ can cause large bias. Therefore, instead of using the estimated detection probability of each detected animal, $\widehat{P}_{t_2-t_1}(R_i, T_i)$, it may be a better option to use the detection probability for an average animal during the survey interval $t_2 - t_1$ within the circle radius $w + u(t_2 - t_1)$ (as is done in the analogous situation in CDS, Buckland *et al.*, 2001).

Define $n_{t_2-t_1}$ as the number of animals detected during the survey period $[t_1, t_2]$ and $\upsilon_{t_2-t_1}$ as the effective area of detection, which is the product of the covered area and the averaged detection probability (equation 5.24). The concept is analogous to the effective area of detection in CDS (or in LTS the effective strip width), i.e., if all animals were detected within this area, and none beyond, then the expected number of animals detected would be the same as for the actual survey (Buckland *et al.*, 2001, pp. 53-54).

$$\hat{N} = \frac{n_{t_2-t_1}}{\hat{\upsilon}_{t_2-t_1}} A = \frac{n_{t_2-t_1}}{\widehat{P}_{t_2-t_1}\, a_{t_2-t_1}} A, \tag{5.24}$$

To define $\upsilon_{t_2-t_1}$ the approach is based on considering a truncation distance $w < \infty$; for example, Buckland et al. (2001) recommend selecting a truncation distance such that detection probability at that distance is approximately 0.1 (in our case that would be detection probability over the survey period assuming no movement). Therefore, $P_{t_2-t_1}$ is defined as equation 5.16, where animals may be detected in the covered area, even if they started outside. This results in integrating over all possible initial distances from which animals might reach the covered area and hence be detected or not. In other words, any animal starting at $w + u(t_2 - t_1)$ could move through the circular plot during the survey period $[t_1, t_2]$, becoming at risk of being detected. Hence the area $a_{t_2-t_1}$ we are covering related to this probability of an animal being seen is $k\pi(w + u(t_2 - t_1))^2$. Therefore,

$$N = \frac{n_{t_2-t_1}}{\left(1 - \int_{x_{t_1}=0}^{w+u(t_2-t_1)} \int_{\theta=0}^{2\pi} \frac{1}{2\pi} S_{t_2-t_1}\big(x_{t_1}(\theta)\big)\Pi(x_{t_1}) d\theta dx_{t_1}\right) k\pi(w + u(t_2 - t_1))^2} A. \tag{5.25}$$

5.3 Discussion and future work

Performance of the estimators derived in the previous section can be examined via a simulation study. Unfortunately, a successful implementation of such a study was not achieved in the time available. Here, therefore, we discuss approaches such a study that can form the basis for future work. The simulation study can be undertaken in discrete or continuous time. The discrete time formulation of $f(R,T)$ is, in practice, more intuitive to interpret, but requires an a priori specification of the discretization interval (the step length). Animal movement takes place in continuous time, so a continuous time simulation is more realistic. We suggest building upon the approch proposed by Bender *et al.* (2005), to generate survival times (in this case detection times). This involves simulating from the cumulative distribution function of the detection times, where the hazard is integrated over the simulated path of individuals.

The general relation between hazard and survival time can be used to develop the required distribution of detection times. The survival function $S : \mathbb{R}^+ \longrightarrow [0,1]$ is related to the hazard via:

$$S(\varphi) = \exp\Big\{ -\int_{t=t_1}^{\varphi} k(x)dt \Big\} = \exp\big\{ -H(\varphi)\big\}, \tag{5.26}$$

where H is called the cumulative hazard function. In the case when animals do not move, then the hazard would be constant in time, as the hazard is only dependent on distance, and distance is constant. However, when animals move, then the hazard is integrated over the animal path resulting in

$$S(\varphi) = \exp\Big\{ -\int_{t=t_1}^{\varphi} k\big(x(t|x_{t_1}, y_{t_1}, u, \theta)\big)dt \Big\}. \tag{5.27}$$

From the above we can get the cumulative hazard function. We use the hazard $k(x) = cx^{-d}c, d \in \mathbb{R}^+$ given by Hayes and Buckland (1983), where $x(t|x_{t_1}, y_{t_1}, u, \theta)$ denotes the distance of the animal to the circular point at time $t \in [t_1, \varphi]$ conditional on the animal starting at the position (x_{t_1}, y_{t_1}) and moving with constant speed u and fixed direction $\theta \in [0, 2\pi)$. Assuming that the circular observation point is centred in the position (x_p, y_p),

$$\begin{aligned} x(t|x_{t_1}, y_{t_1}, u, \theta) &= \sqrt{\Big(x_p - (x_{t_1} + ut\cos(\theta))\Big)^2 + \Big(y_p - (y_{t_1} + ut\sin(\theta))\Big)^2} \\ &= \sqrt{(x_{t_1} - x_p)^2 + (y_{t_1} - y_p)^2 + (ut)^2 + 2ut\big((x_{t_1} - x_p)\cos(\theta) + (y_{t_1} - y_p)\sin(\theta)\big)}. \end{aligned} \tag{5.28}$$

Some examples are given for different animal initial positions (Figure5.3).

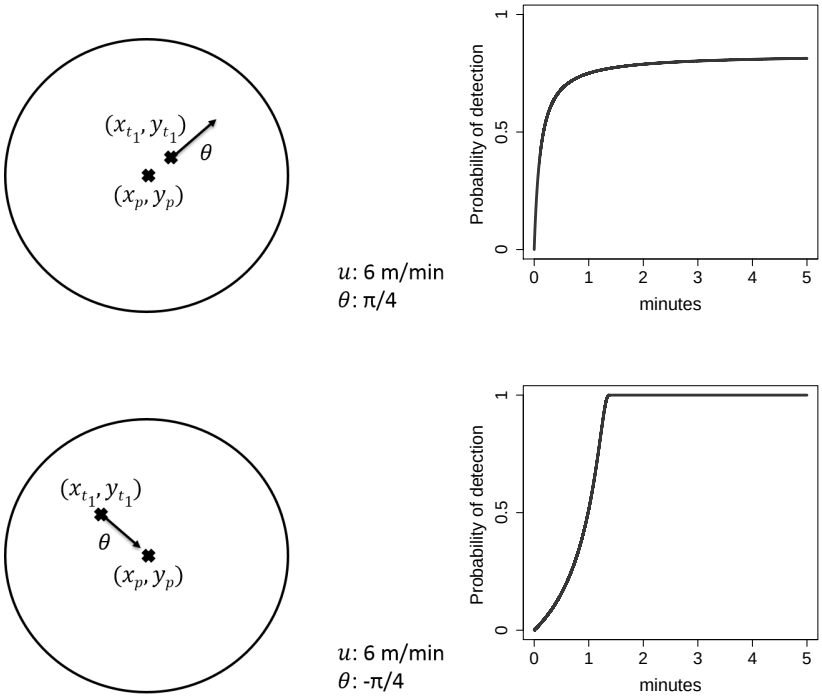

Figure 5.3: Probability of an animal being detected over time (on the right), given the animal initial position, speed and travel direction (on the left).

6

Discussion

6.1 Introduction

Incorporating animal movement into point-based surveys of wildlife abundance was the main goal of this thesis. While targeting this goal, we found, unexpectedly, some bias in point transect sampling (PTS) estimators when animals were still, under conditions where the true model was unknown and standard model selection techniques were employed. Therefore, we started by fully understanding the estimation process when assumptions were met (i.e., before any assumption was violated), on both PTS and line transect sampling (LTS). We found that although distance sampling (DS) estimators are asymptotically unbiased, for the recommended sample sizes the bias depended on the form of the true detection function. This provided a vital benchmark for interpreting the levels of bias seen in conventional DS estimators in scenarios where animals do move. We examined this in Chapter 3, as well as considering the simpler case of circular plot sampling (CPS). We found that for mobile animals the violation of the animal movement assumption leads to unrealistic abundance estimations in both methods.

We then derive estimators accounting for animal movement, for CPS (Chapter 4) and PTS (Chapter 5). In CPS, bias was tackled for three modes of movement. We consider linear movement, simple random walks and biased random walks, assuming that animals move independently at constant and known speed. We developed a formulation for PTS under linear animal movement. Although a simulation study showed the estimator appears still to be biased, the method performs better than estimators that ignore the animal movement. Examination of the reasons for this remaining bias is future work.

In the next two Sections we point towards future developments of the method and new research directions.

6.2 Further generalization of methods and future work

In this study we assume that all animals move in the same way, which in practice is unrealistic. A first extension would be to create a mode of movement described as mixtures of different behavioural states – e.g., directed travel (travelling) and tortuous travel (e.g., foraging). This would result in allowing for animals to have some individualism regarding their movements.

We just focus on movements at the time scale of a survey at an individual point, typically just a few minutes. Given this short time scale, it would be rare that animals switch behavioural mode while within range of the sensor/observer. Therefore we only consider single modes of movement. However, in some cases, the survey period can be at a larger scale (e.g., Harris, 2012), weeks or even years and over a medium-term and long-term time scales, realistic descriptions of animal movement should account for the fact that animals switch between different behavioural (and so movement) modes. Therefore, there is a different related issue due to movement that reflects wider scale movements at the survey level. There is strong interest in animal movement for reasons other than wildlife abundance estimation, and new, more realistic models are constantly being developed, as well as techniques for fitting them to data. It may well be that there is, in the future, some cross-fertilization from discoveries in the movement ecology literature through into density estimation.

In particular, estimation of cetaceans abundance and density from acoustic survey data, which is becoming increasingly common (Marques *et al.*, 2013), and with the ongoing technological advancement in devices capable of collecting such data, their use is becoming both cheaper and more widespread. Cetacean movement is very relevant for long-term fixed acoustic point surveys where individuals call relatively frequently so it is feasible to track them individually several times. We here only consider the time of first detection, and the information on successive detections are not used. Note that actually multiple detections of the same animal might not contain much information about detectability, which it really depends on whether successive sightings are independent or not, but it contains strong information about movement, at least at the scale over which detections occur. Therefore this movement related information could be used to estimate some parameters or even distributions of the animal movement process and incorporate this information in the method.

We also assume that animals move at constant and known speed. This approach could readily be generalized to uncertain movement parameters (unknown animal speed), by in each simulation sampling from a distribution of such parameters. Another generalization would be the use of non-constant speeds where the speed at each time step is sampled from a fixed or estimated distribution. When the simulation-based approach is used, another option to deal with the variable speed issue, as well as the unknown movement path issue is to superimpose samples of animal paths taken from, e.g., tag data. It is worth noting that this may not be straightforward – for example movement behaviour will almost certainly change in space so tag data needs to come from same season and location; also naive use might be problematic in some cases, e.g., deep diving whales where if you move the track then they can end up diving through the ocean floor.

In the thesis we dealt only with random movement of animals. It seems likely that, in the presence of responsive movement, the bias in density estimates will be even more extreme than those presented here. Therefore the possibility of responsive movement should certainly be considered when estimating abundance (Turnock and Quinn, 1991; Palka and Hammond, 2001).

In CDS methodology, the movement by some species towards or away from the observer is primarily a problem when it is undetected, and happens before the initial location has been recorded. In particular, for bird surveys, flushing can aid detection as long as the point from which the bird has emerged can be pinpointed. Alternatively, in a non-forested habitat, or in a marine situation, a second observer and double-platform methodology could be used (Borchers *et al.*, 1998). Unfortunately, with a species that is frequently very strongly attracted to the observation point or the observer, it can be impossible to detect the animal with certainty before it has reacted to the observer. For example, some cetaceans like white-beaked dolphins have been reported to be attracted to the ship (Palka and Hammond, 2001). Therefore, it would be wise to be conservative and avoid using CDS methods —or work in a correction for animal movement as Palka and Hammond (2001) did— on the species known to exhibit strong reactive behaviour before detection.

The first step, before even thinking about correcting for animal movement, is to be able to recognize it. Problematic responsive movement has been recognised in a number of studies and can sometimes be attributable to field design. For example, the use of a ladder as a survey platform in a study on Australian honeyeaters (Pyke, 1983) or wearing brightly coloured clothing with some North American bird species (Gutzwiller and Marcum, 1997)

might cause a reaction in the animal behaviour. This points to the importance of checking and verifying before and during the same field work that the method's assumptions are met. If undetected movement was not apparent during the survey itself, movement away from the observer prior to detection can sometimes be recognised at the analysis stage from the inspection of histograms of the distance data (Buckland *et al.*, 2001). Once a field technique that causes behavioural disruption has been identified it can often be avoided or corrected (e.g., Conant *et al.*, 1981; Southwell, 1994). It is thereby critical to tailor field methods and survey design to help ensure the assumptions are met, so far as possible. A pilot survey provides an important opportunity for discovering and dealing with such problems.

Once one realizes the presence of animal movement, if it is independent of the observer, the use of the proposed methodology leads to a reduction in bias on abundance estimators. A generalization of the proposed method in Chapter 5 is to incorporate a more general type of movement defined as a diffusion process as we did for CPS.

Entering in the computational aspects of the formulation for PTS under animal movement, the simulation was undertaken in discrete time, with a time step of $\tau = 1$ second. Because of the approximation used in deriving the 1-second hazard rate detection function, we were restricted to use low speeds relative to the fixed unit of time.

6.3 Concluding remarks

This thesis has described novel methods of estimating animal abundance when animal movement is present during the survey period. Prior to this work, in order to estimate animal density, DS practitioners were forced to assume that all individuals remain static during the time of the survey or if they moved they would be detected at its first position. For some species of animals this assumption quite clearly almost never hold, while ignoring it is discouraged as it leads to an overestimation of abundance based on the work presented in Chapter 3.

Although we developed unbiased estimators for CPS surveys, unfortunately, a successful implementation of the methodology for PTS was not achieved in the time available. We hope that future work will address this, and add alternative movement models. The rapid advancement of remote survey technology, particularly passive acoustics (Marques *et al.*, 2013), means that long-term point surveys will become increasingly common in the

future. Methods such as those described here, and mentioned as future developments, will therefore become increasingly important in the estimation of animal population size.

A

Distance sampling under model selection detection functions

A.1 Overview

This appendix contains supplemental results and details regarding some fitting issues we faced when running the simulation study. The following tables and figures are provided:

- The parameters used to generate the data for both detection function models, the hazard-rate (HR) and the exponential power series distribution (EPS) (Table A.1).
- The observed mean and median bias in P_a for each simulation scenario. (Tables A.2-A.5).
- In the main text we presented only smooth lines for median bias in N. Here we include the observed median (Figs. A.1-A.4) and mean (Figs. A.5-A.8) percentage bias for each simulation scenario.
- We also include the smooth lines for observed median bias in P_a (Fig. A.9).
- The proportion of time each candidate model is selected (Fig. A.10); the proportion of time k parameters ($k \in \{0, 1, \ldots, 5\}$) is selected (Fig. A.11).
- The percentage error conditional on the model selected when using model selection (Figs. A.12-A.15) and also when fitting the true model (Figs. A.16-A.19).
- A subset of individual fitted detection functions with model selection and the true model, for the particular case of the EPS distribution in a point transect sampling scenario for 120 observations (Figs. A.20-A.21).

- The percentage median bias when the monotonicity constraint is removed (scenario 2.1) represented by smooth lines (Fig. A.22), when fixing the number of parameters to be two or three in addition to removing the monotonicity constraint (scenarios 2.2-2.3) (Figs. A.23-A.24), and also when the number of parameters is constrained with the monotonicity constraint (scenarios 2.4-2.5) (Figs. A.25-A.26).

- The median and maximum values of the %Monte Carlo Error (MCE) on $\hat{N}$ across the different set of parameters for each simulation scenario over the sample sizes (Fig. A.27).

- The percentage root mean square error (Fig. A.28).

- The coverage probability, the proportion of 95% confidence intervals estimates that contained the true value (Fig. A.29).

- An example is given to examine the effect that truncating the data at the analysis stage has on bias. The raw median bias when data is truncated at distance 20 instead of 30 for a sample size of 240, when using conventional model selection with the monotonicity constraint and fitting the true model (Fig. A.30).

A.2 Code

The simulation code is available here:
https://github.com/Ro-PG/Distance-sampling-model-selection.

A.3 Fitting issues

Running the simulation some practical fitting issues were found. Conventional distance sampling (CDS) and multiple-covariate distance sampling (MCDS) analyses were also available within the package `mrds` in R (Laake *et al.*, 2014). However we used the CDS engine in Distance (Thomas *et al.*, 2010) instead, as it is more commonly used and it was found more reliable in preliminary studies. Since the EPS detection function is not available in Distance software, when fitting the true model under the EPS scenarios we implemented our own likelihood function, and maximized it via R function `optim`. The CDS engine was in general more robust than the optim function. Less than 2% of the

times Distance software returned an error in one of the models fitted. By contrast, despite fixing a threshold to ensure that $\hat{P}$ was realistic, sometimes `optim` appeared to converge but led to inconsistent low point estimates for detection probability (< 0.08). Therefore, when fitting the true model for EPS scenarios, the root-mean-square error (RMSE) was higher than for other scenarios, being dominated by the contribution of this small number of inconsistent estimates, especially for low sample sizes.

A.4 Supplemental materials

Table A.1: Parametrizations of the hazard-rate and exponential power series functions used in the simulation and their average probability of detection P_a.

Data generated from		Probability of detection	
		Line transect	Point transect
HR (σ, b)	$\text{HR}_1\,(6.9, 1.5)$	0.40	0.24
	$\text{HR}_2\,(8.5, 1.7)$	0.44	0.27
	$\text{HR}_3\,(10, 2)$	0.48	0.30
	$\text{HR}_4\,(11.5, 2.3)$	0.52	0.33
	$\text{HR}_5\,(13, 2.6)$	0.56	0.36
	$\text{HR}_6\,(14.5, 3)$	0.60	0.40
	$\text{HR}_7\,(16, 3.4)$	0.64	0.45
	$\text{HR}_8\,(17.4, 3.9)$	0.68	0.49
EPS (λ, ν)	$\text{EPS}_1\,(13.8, 1.12)$	0.41	0.26
	$\text{EPS}_2\,(16, 1.35)$	0.46	0.30
	$\text{EPS}_3\,(18.1, 1.65)$	0.52	0.35
	$\text{EPS}_4\,(19.7, 2)$	0.56	0.39
	$\text{EPS}_5\,(21.2, 2.5)$	0.61	0.43
	$\text{EPS}_6\,(22.5, 3.2)$	0.66	0.49
	$\text{EPS}_7\,(23.8, 3.9)$	0.71	0.54
	$\text{EPS}_8\,(25, 4.9)$	0.76	0.60

Table A.2: Percentage mean bias in P_a, for line and point transect sampling using detection function model selection (ms) and true model (tm) as model for inference for 8 sets of parameters of the hazard-rate (HR) distribution, over a range of sample sizes, $n \in \{60, 90, 120, 240, 500, 5000\}$.

			P_a percentage mean bias							
			HR_1	HR_2	HR_3	HR_4	HR_5	HR_6	HR_7	HR_8
LT	ms	Sample size 60	3.06	1.09	-1.18	-2.88	-4.43	-5.76	-6.98	-8.02
		Sample size 90	0.73	-0.52	-1.99	-3.55	-4.59	-5.60	-6.25	-6.58
		Sample size 120	-0.36	-1.20	-2.46	-3.46	-4.74	-5.55	-5.98	-5.98
		Sample size 240	-1.28	-2.34	-2.90	-3.51	-4.16	-5.13	-4.61	-4.02
		Sample size 500	-1.21	-2.07	-2.45	-2.67	-2.86	-3.67	-3.10	-2.20
		Sample size 5000	-0.46	-1.09	-0.70	-0.69	-0.46	-0.83	-0.86	-0.88
	tm	Sample size 60	1.40	0.25	-0.71	-1.12	-1.45	-1.64	-1.80	-1.82
		Sample size 90	0.11	-0.30	-0.66	-1.14	-1.22	-1.35	-1.30	-1.29
		Sample size 120	-0.26	-0.38	-0.51	-0.64	-1.20	-1.25	-1.25	-1.36
		Sample size 240	-0.88	-1.12	-0.79	-0.53	-0.72	-1.15	-1.03	-0.91
		Sample size 500	-0.63	-0.85	-0.23	-0.23	-0.41	-1.14	-1.04	-0.69
		Sample size 5000	-0.12	-1.49	-0.04	-0.08	-0.01	-1.16	-1.10	-0.90
PT	ms	Sample size 60	16.13	9.46	1.15	-2.64	-6.63	-9.57	-12.03	-12.69
		Sample size 90	10.17	2.95	-1.45	-4.87	-7.24	-10.36	-11.49	12.76
		Sample size 120	6.49	1.87	-2.65	-4.43	-7.26	-9.57	-11.18	-10.82
		Sample size 240	2.56	-0.76	-3.38	-4.45	-5.35	-7.78	-9.41	-7.47
		Sample size 500	-0.38	-2.28	-3.88	-5.00	-5.32	-6.67	-8.08	-5.65
		Sample size 5000	-1.08	-1.72	-1.87	-1.63	-1.32	-1.25	-2.03	-1.20
	tm	Sample size 60	8.55	5.04	1.08	-0.27	-1.74	-1.94	-2.61	-2.92
		Sample size 90	4.75	1.00	-0.63	-1.38	-1.56	-2.25	-2.35	-2.35
		Sample size 120	2.53	0.92	-0.27	-0.15	-0.81	-1.73	-2.26	-2.24
		Sample size 240	1.59	0.61	0.62	1.27	0.35	-1.04	-2.02	-1.74
		Sample size 500	-0.22	-0.25	-0.07	-0.06	-0.37	-1.80	-3.79	-2.74
		Sample size 5000	-0.61	-1.26	0.06	-0.36	0.05	-0.36	-4.94	-2.11

Table A.3: Percentage mean bias in P_a, for line transect sampling using detection function model selection (ms) and true model (tm) as model for inference for 8 sets of parameters of the exponential power series (EPS) distribution, over a range of sample sizes, $n \in \{60, 90, 120, 240, 500, 5000\}$.

				P_a percentage mean bias							
				EPS_1	EPS_2	EPS_3	EPS_4	EPS_5	EPS_6	EPS_7	EPS_8
LT	ms	Sample size	60	18.48	12.04	6.83	2.40	-1.50	-4.49	-6.04	-6.67
			90	15.75	10.51	6.04	2.22	-1.13	-3.37	-4.90	-5.44
			120	14.61	9.89	5.59	1.76	-1.10	-2.93	-4.17	-4.92
			240	12.06	8.38	4.54	1.14	-1.15	-2.17	-3.23	-3.46
			500	10.84	7.24	4.18	0.77	-1.20	-1.36	-2.43	-2.74
			5000	7.88	4.54	1.69	0.20	-0.25	-0.54	-0.49	-0.66
	tm	Sample size	60	0.15	-0.92	-1.50	-1.78	-2.02	-2.30	-2.71	-3.11
			90	-0.47	-0.95	-0.85	-1.00	-1.06	-1.22	-1.26	-1.69
			120	-0.22	-0.39	-0.72	-1.01	-0.72	-0.69	-1.00	-1.31
			240	-0.69	-0.51	-0.59	-0.61	-0.56	-0.51	-0.45	-0.45
			500	-0.22	-0.12	-0.18	-0.21	-0.20	-0.11	-0.07	-0.18
			5000	0.04	-0.01	-0.01	-0.05	0.06	0.01	-0.01	-0.02
PT	ms	Sample size	60	36.77	23.87	12.43	4.91	-1.23	-5.93	-8.29	-9.89
			90	33.43	20.13	11.45	4.41	-1.42	-4.29	-6.73	-8.28
			120	30.99	20.47	10.88	3.98	-1.39	-4.03	-5.58	-7.31
			240	26.72	17.09	8.66	2.47	-2.34	-3.49	-4.46	-6.05
			500	22.42	15.12	7.69	0.99	-2.73	-3.45	-4.55	-5.51
			5000	14.31	7.94	3.24	0.41	-0.53	-1.60	-1.26	-1.33
	tm	Sample size	60	3.92	2.09	0.27	-0.95	-1.20	-1.36	-1.84	-2.72
			90	4.02	0.99	0.23	-0.20	-0.77	-0.92	-1.11	-1.51
			120	2.56	1.36	0.30	0.37	-0.18	-0.54	-0.59	-0.73
			240	0.80	0.18	-0.26	0.04	-0.14	0.04	-0.30	-0.49
			500	0.10	-0.01	0.12	-0.02	-0.38	-0.27	-0.23	-0.28
			5000	0.17	0.11	-0.02	-0.04	-0.06	-0.03	-0.04	-0.06

Table A.4: Percentage median bias in P_a, for line and point transect sampling using detection function model selection (ms) and true model (tm) as model for inference for 8 sets of parameters of the hazard-rate (HR) distribution, over a range of sample sizes, $n \in \{60, 90, 120, 240, 500, 5000\}$.

			P_a percentage median bias							
			HR_1	HR_2	HR_3	HR_4	HR_5	HR_6	HR_7	HR_8
LT	ms	Sample size 60	1.31	-0.15	-0.63	-2.94	-4.03	-5.36	-7.12	-7.71
		Sample size 90	-0.76	-0.99	-2.40	-3.53	-4.47	-6.13	-6.47	-5.92
		Sample size 120	-1.08	-1.35	-2.69	-3.33	-4.57	-6.26	-6.32	-4.87
		Sample size 240	-1.58	-2.29	-3.23	-3.42	-3.74	-5.77	-4.18	-2.75
		Sample size 500	-1.15	-2.39	-2.64	-2.47	-2.54	-3.53	-2.33	-1.46
		Sample size 5000	-0.32	-0.87	-0.49	-0.45	-0.26	-0.68	-0.73	-0.74
	tm	Sample size 60	0.01	-0.73	-0.95	-1.18	-1.81	-1.93	-1.41	-1.10
		Sample size 90	-0.81	-0.60	-0.57	-1.16	-1.31	-1.76	-1.26	-0.54
		Sample size 120	-0.97	-0.30	-0.18	-0.39	-1.33	-1.36	-1.21	-0.88
		Sample size 240	-1.17	-1.54	-0.74	-0.36	-0.68	-1.23	-1.34	-0.69
		Sample size 500	-0.63	-1.29	-0.25	-0.20	-0.41	-1.58	-1.44	-0.54
		Sample size 5000	-0.06	-1.53	-0.03	-0.06	0.01	-1.32	-1.32	-0.98
PT	ms	Sample size 60	8.81	4.47	-0.89	-2.44	-6.09	-10.37	-14.34	-13.86
		Sample size 90	4.52	-1.46	-3.60	-5.89	-5.80	-10.40	-14.43	-13.62
		Sample size 120	2.12	-0.32	-4.57	-5.44	-5.85	-9.96	-14.21	-12.14
		Sample size 240	2.28	-0.39	-4.14	-5.65	-3.83	-8.04	-12.17	-5.22
		Sample size 500	-0.80	-2.78	-4.02	-5.79	-3.99	-6.77	-7.58	-3.49
		Sample size 5000	-1.18	-1.55	-1.18	-1.13	-0.70	-0.74	-1.38	-0.48
	tm	Sample size 60	1.97	0.89	-1.19	-1.49	-2.44	-2.74	-3.07	-3.50
		Sample size 90	-0.39	-2.03	-1.33	-1.87	-1.71	-2.49	-2.89	-2.70
		Sample size 120	-1.27	-0.33	-0.57	-0.95	-0.93	-2.04	-2.80	-2.54
		Sample size 240	1.16	0.25	0.23	0.98	0.62	-1.28	-2.47	-1.75
		Sample size 500	-1.04	-0.63	-0.41	-0.21	-0.33	-1.81	-4.37	-2.67
		Sample size 5000	-0.86	-1.01	0.13	-0.24	0.00	-0.38	-4.95	-0.36

Table A.5: Percentage median bias in P_a, for line transect sampling using detection function model selection (ms) and true model (tm) as model for inference for 8 sets of parameters of the exponential power series (EPS) distribution, over a range of sample sizes, $n \in \{60, 90, 120, 240, 500, 5000\}$.

				P_a percentage median bias							
				EPS_1	EPS_2	EPS_3	EPS_4	EPS_5	EPS_6	EPS_7	EPS_8
LT	ms	Sample size	60	20.89	13.88	8.58	3.39	-0.68	-4.38	-7.34	-8.19
			90	16.66	12.18	7.16	2.16	-0.50	-2.88	-5.66	-6.28
			120	14.80	11.45	6.50	1.43	-0.92	-2.03	-5.05	-5.82
			240	12.54	9.02	5.75	0.51	-2.38	-1.01	-4.08	-3.63
			500	11.59	6.99	5.24	0.44	-2.11	-0.40	-3.75	-1.75
			5000	7.64	4.80	1.67	0.16	-0.39	-0.36	-0.13	-0.34
	tm	Sample size	60	0.59	-0.67	-0.39	0.24	-0.37	-0.36	-0.63	-0.63
			90	-0.02	-0.19	0.05	-0.11	0.02	-0.04	0.07	-0.13
			120	0.58	0.49	0.14	-0.22	0.20	0.12	-0.21	0.05
			240	-0.43	0.05	-0.16	-0.30	-0.25	-0.08	-0.19	-0.09
			500	-0.03	0.03	-0.19	-0.19	0.03	-0.01	0.08	-0.09
			5000	0.14	0.03	0.01	-0.01	0.09	0.01	-0.01	-0.02
PT	ms	Sample size	60	42.85	28.23	13.75	3.73	-1.62	-4.25	-8.80	-12.50
			90	39.86	24.92	11.99	2.43	-4.39	-2.23	-6.96	-11.11
			120	36.82	25.47	11.82	1.55	-5.51	-0.80	-5.76	-10.27
			240	26.26	22.34	10.74	0.89	-6.35	-0.23	-4.66	-9.75
			500	22.63	15.07	10.34	0.33	-4.83	-3.17	-4.52	-8.53
			5000	15.01	8.00	2.53	0.15	-1.02	-1.64	-0.60	-0.52
	tm	Sample size	60	-0.20	1.38	0.50	0.06	-0.07	-0.50	-0.52	-0.82
			90	1.35	0.59	0.46	0.44	-0.42	-0.15	0.28	0.09
			120	1.03	1.04	0.47	1.06	0.05	-0.35	0.02	0.49
			240	1.05	0.76	-0.35	-0.07	-0.03	0.17	-0.12	-0.13
			500	0.20	-0.20	0.07	0.25	-0.24	-0.21	-0.17	-0.04
			5000	0.15	0.06	0.08	-0.09	-0.05	0.02	-0.03	-0.07

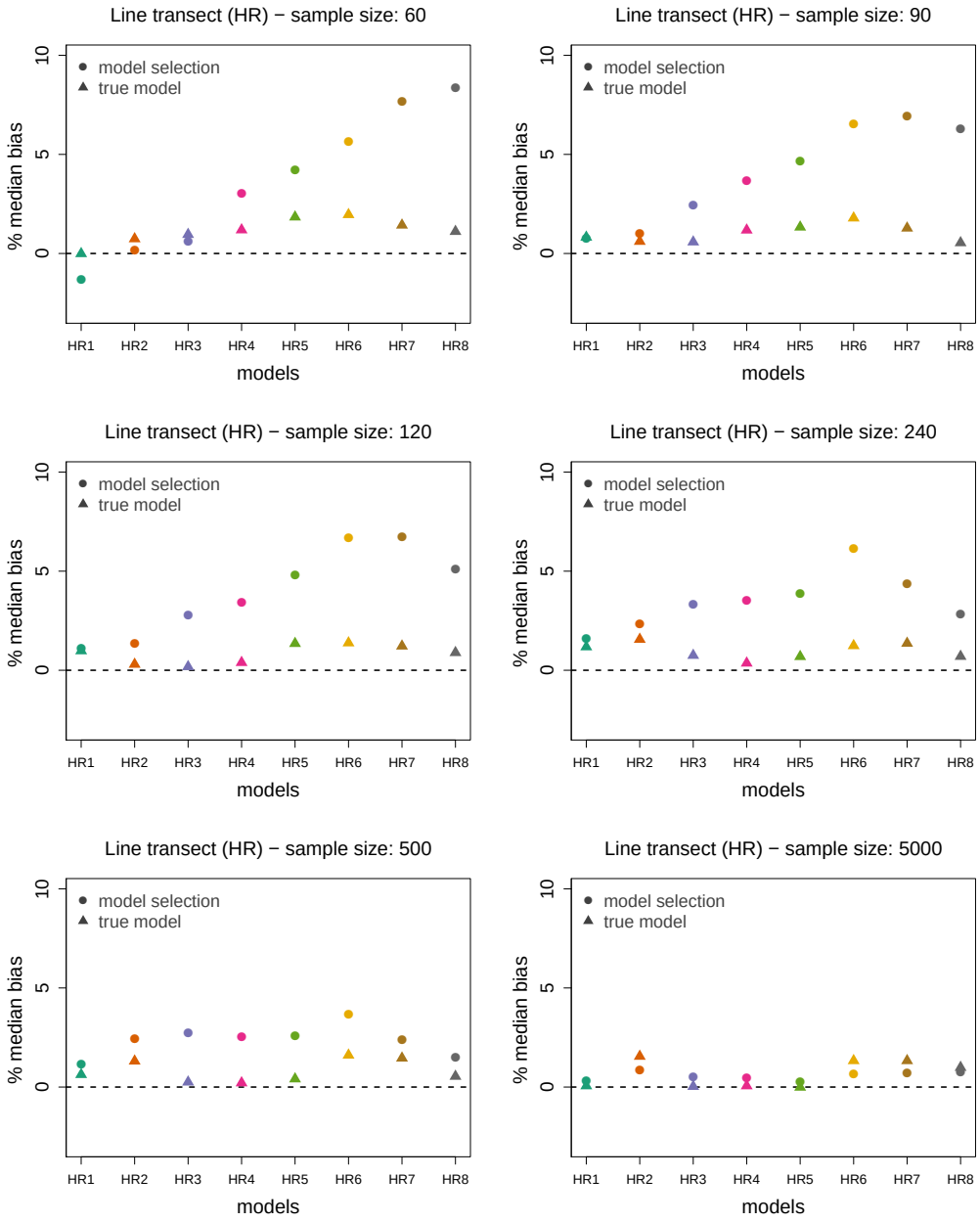

Figure A.1: Percentage median bias in N for line transect sampling using detection function model selection ($\circ$) and true model ($\triangle$) as model for inference for 8 sets of parameters of the hazard-rate (HR) distribution, over a range of sample sizes, $n \in \{60, 90, 120, 240, 500, 5000\}$.

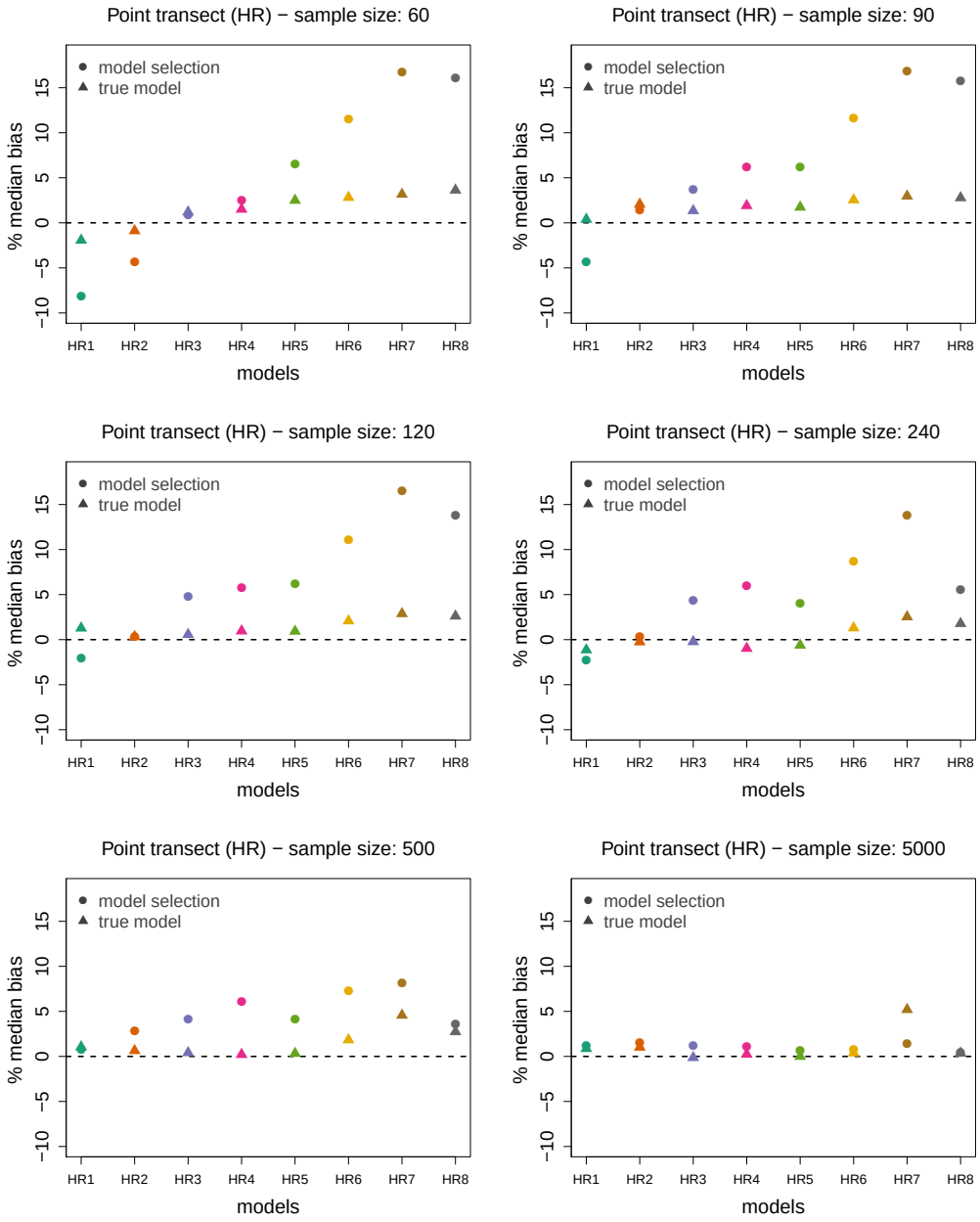

Figure A.2: Percentage median bias in N for point transect sampling using detection function model selection ($\circ$) and true model ($\triangle$) as model for inference for 8 sets of parameters of the hazard-rate (HR) distribution, over a range of sample sizes, $n \in \{60, 90, 120, 240, 500, 5000\}$.

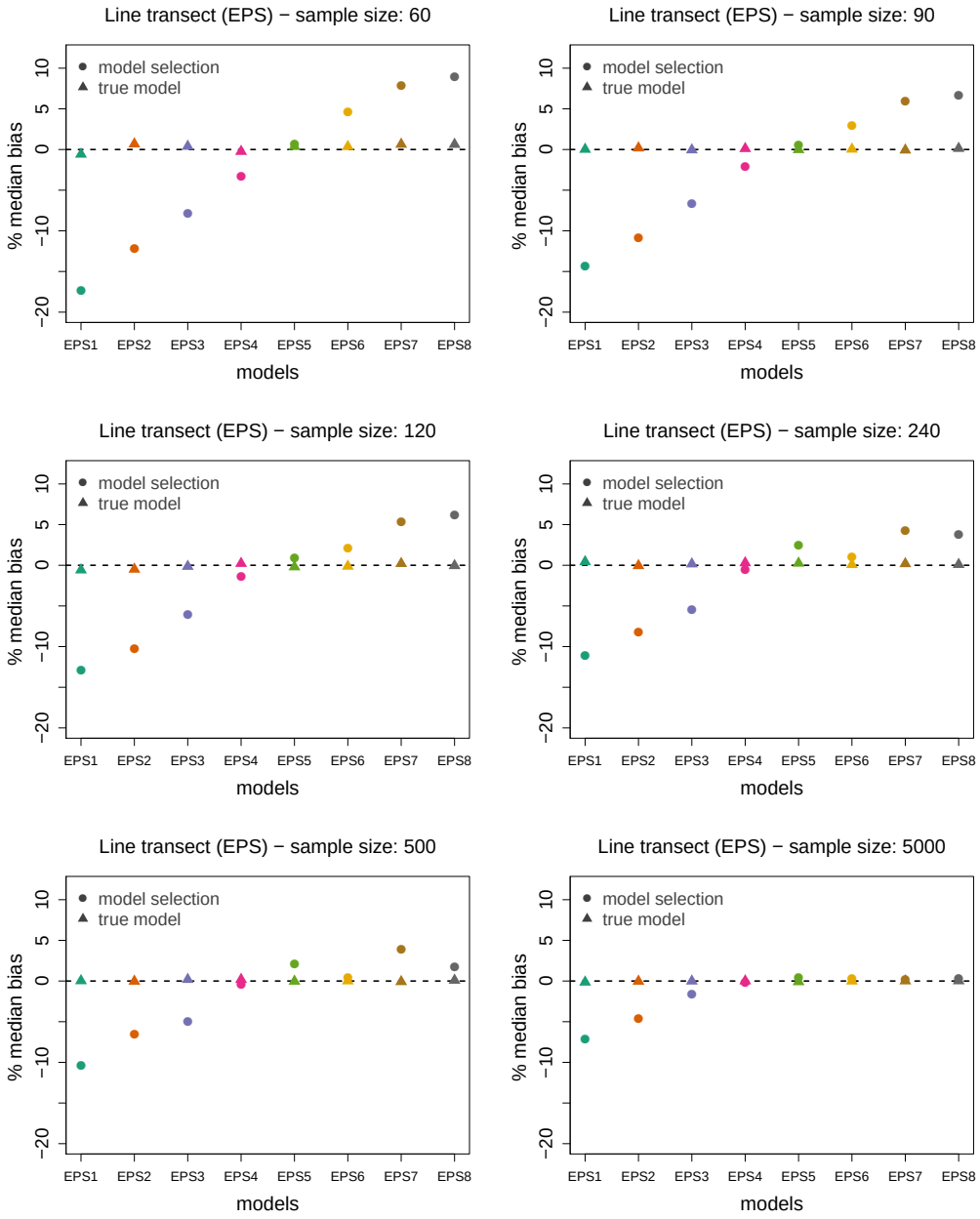

Figure A.3: Percentage median bias in N for line transect sampling using detection function model selection ($\circ$) and true model ($\triangle$) as model for inference for 8 sets of parameters of the exponential power series (EPS) distribution, over a range of sample sizes, $n \in \{60, 90, 120, 240, 500, 5000\}$.

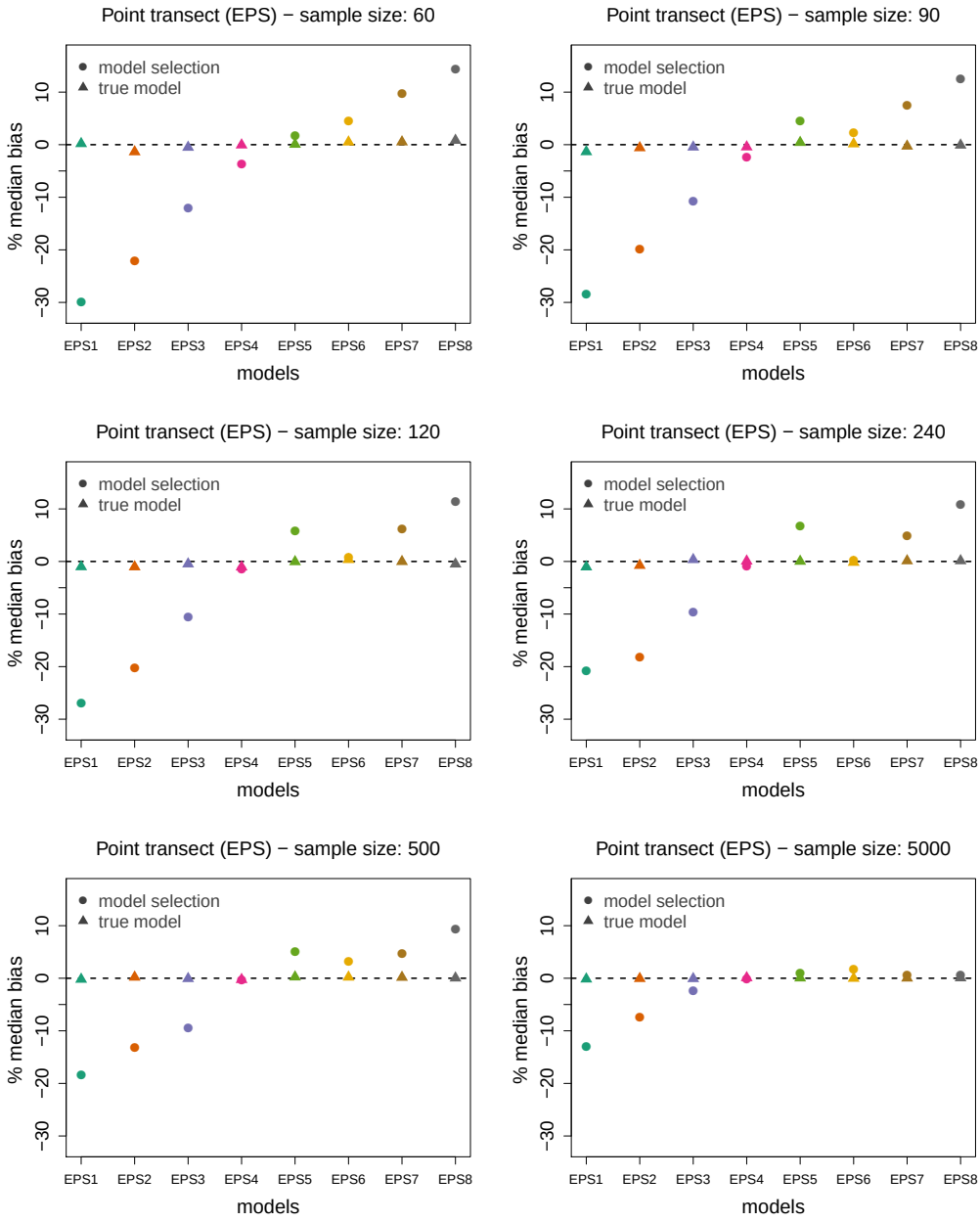

Figure A.4: Percentage median bias in N for point transect sampling using detection function model selection ($\circ$) and true model ($\triangle$) as model for inference for 8 sets of parameters of the exponential power series (EPS) distribution, over a range of sample sizes, $n \in \{60, 90, 120, 240, 500, 5000\}$.

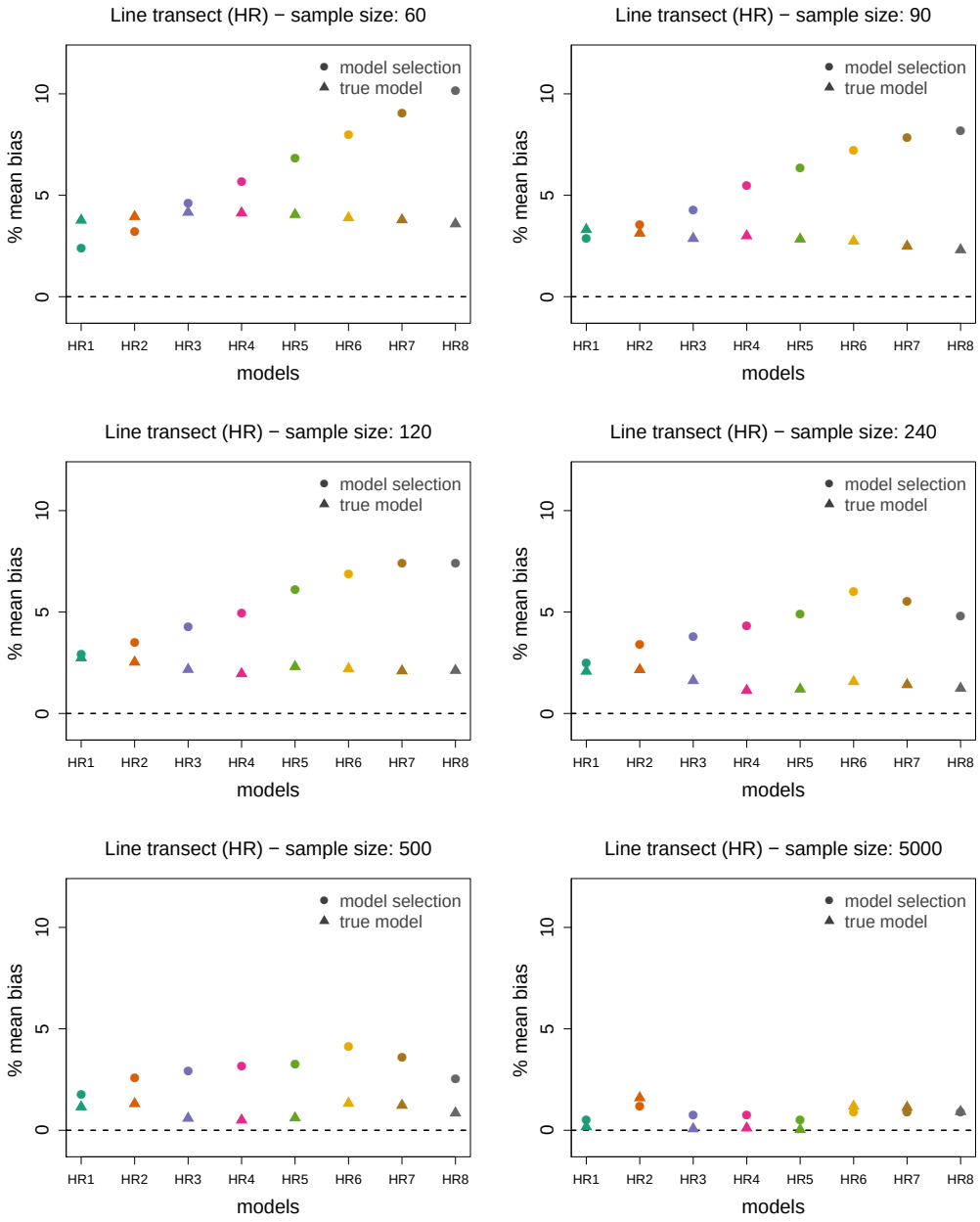

Figure A.5: Percentage mean bias in N for line transect sampling using detection function model selection ($\circ$) and true model ($\triangle$) as model for inference for 8 sets of parameters of the hazard-rate (HR) distribution, over a range of sample sizes, $n \in \{60, 90, 120, 240, 500, 5000\}$.

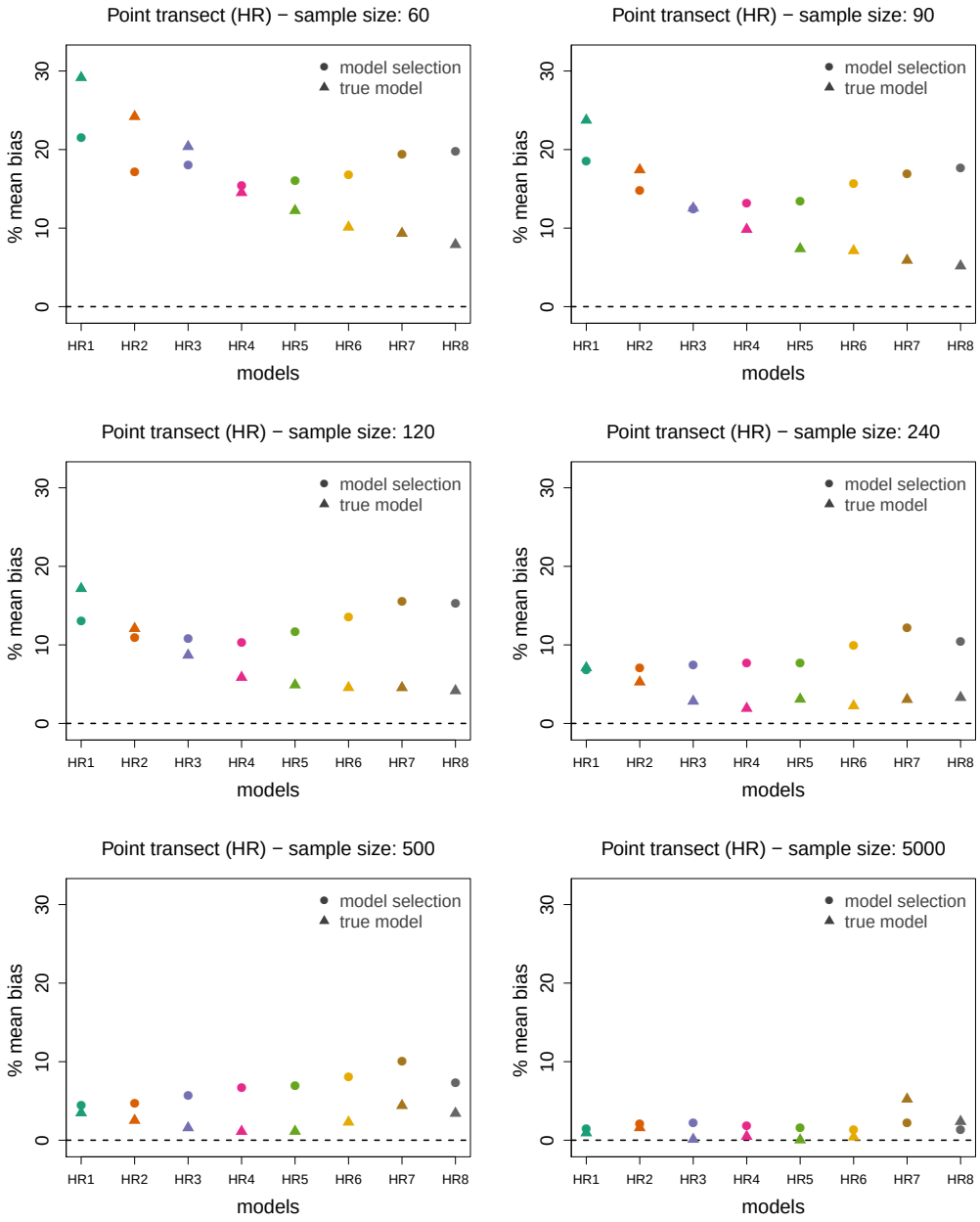

Figure A.6: Percentage mean bias in N for point transect sampling using detection function model selection ($\circ$) and true model ($\triangle$) as model for inference for 8 sets of parameters of the hazard-rate (HR) distribution, over a range of sample sizes, $n \in \{60, 90, 120, 240, 500, 5000\}$.

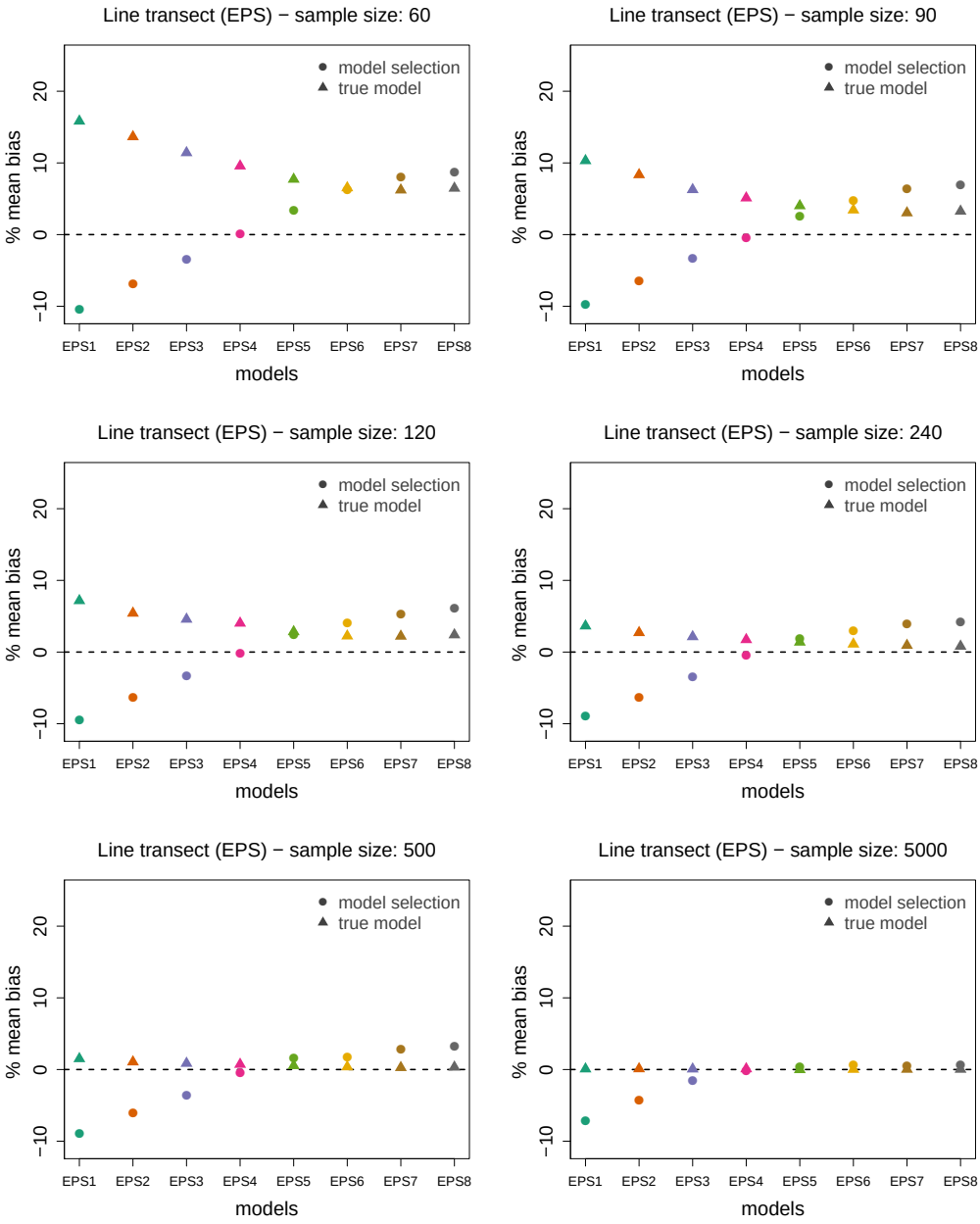

Figure A.7: Percentage mean bias in N for line transect sampling using detection function model selection ($\circ$) and true model ($\triangle$) as model for inference for 8 sets of parameters of the exponential power series (EPS) distribution, over a range of sample sizes, $n \in \{60, 90, 120, 240, 500, 5000\}$.

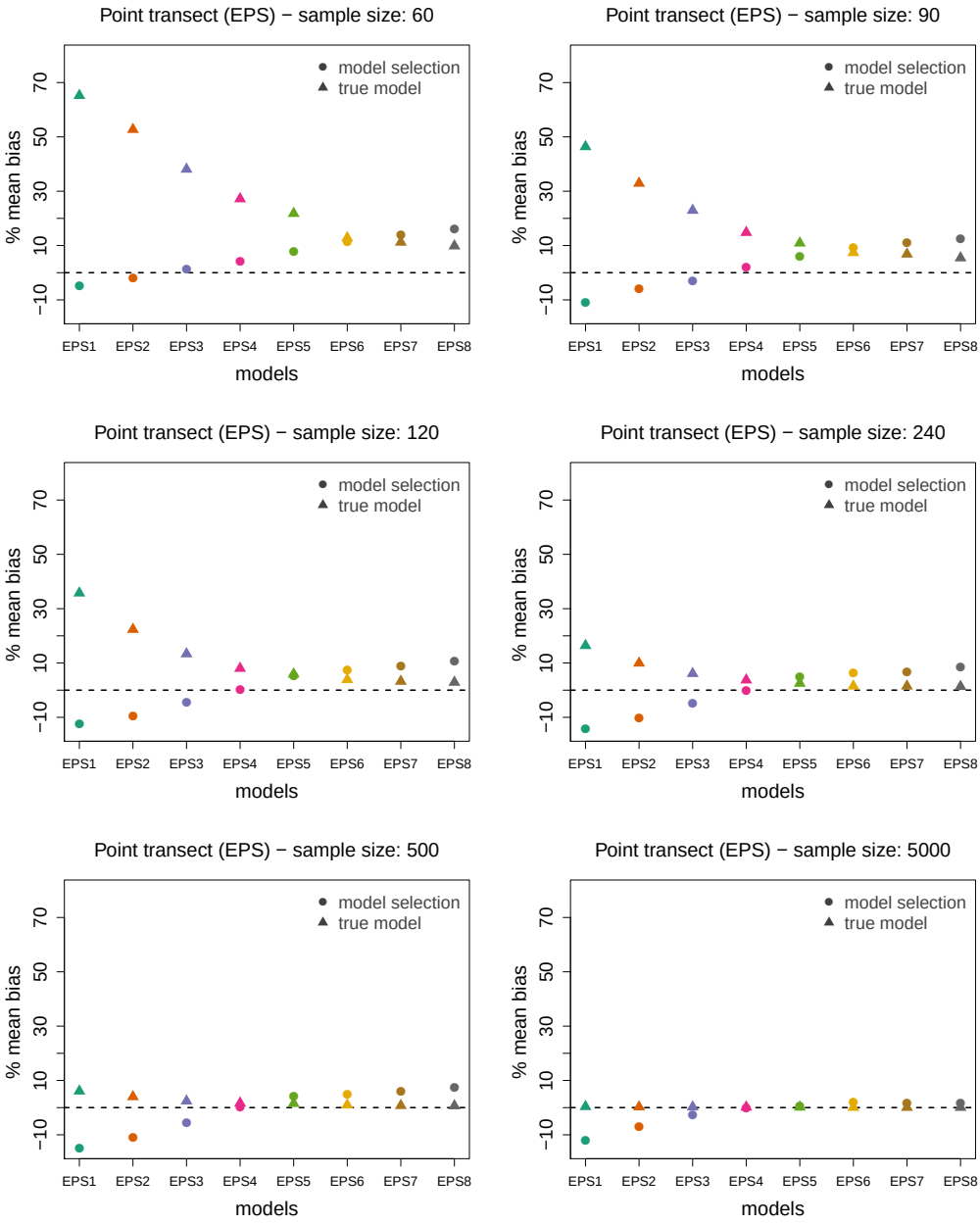

Figure A.8: Percentage mean bias in N for point transect sampling using detection function model selection ($\circ$) and true model ($\triangle$) as model for inference for 8 sets of parameters of the exponential power series (EPS) distribution, over a range of sample sizes, $n \in \{60, 90, 120, 240, 500, 5000\}$.

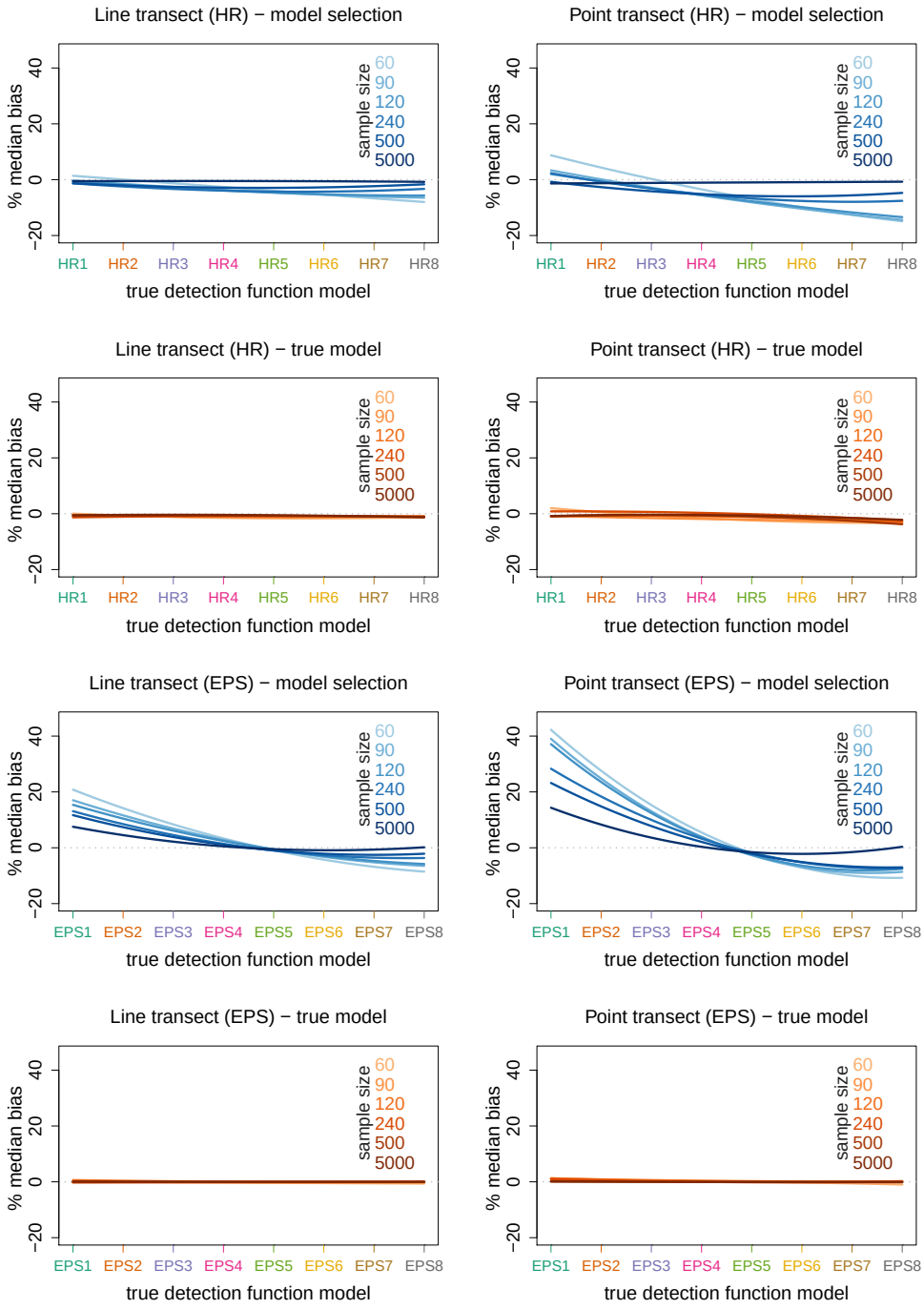

Figure A.9: Percentage median bias in P_a using detection function model selection (blue lines) and true model (orange lines) as model for inference for 8 sets of parameters of the hazard-rate (HR) and exponential power series (EPS) distributions, over a range of sample sizes, $n \in \{60, 90, 120, 240, 500, 5000\}$. Shown are smoothed lines of raw results.

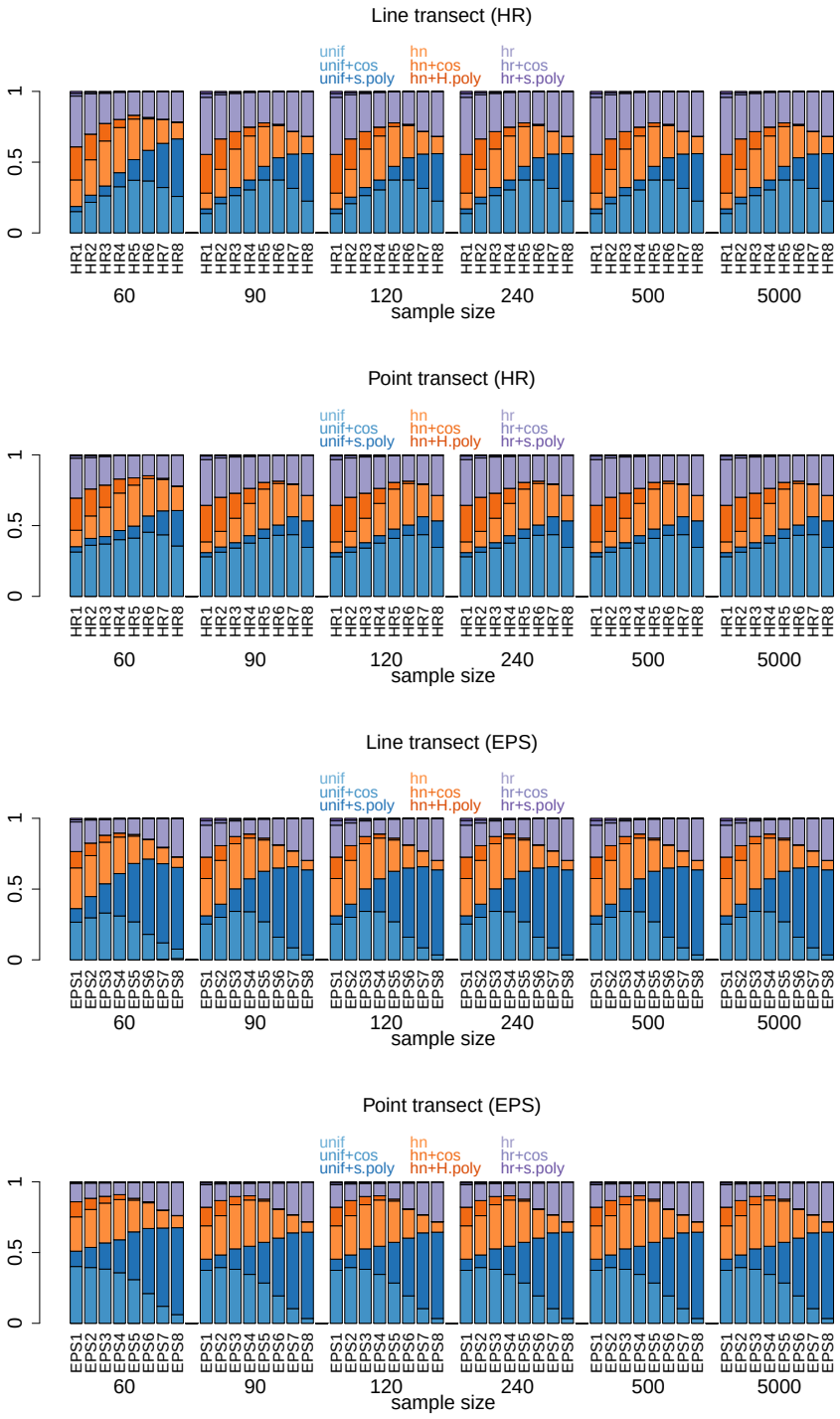

Figure A.10: Proportion of time each candidate model class is selected in line and point transect scenarios for the 8 sets of parameters of the hazard-rate (HR) and exponential power series (EPS) distributions, over a range of sample sizes, $n \in \{60, 90, 120, 240, 500, 5000\}$.

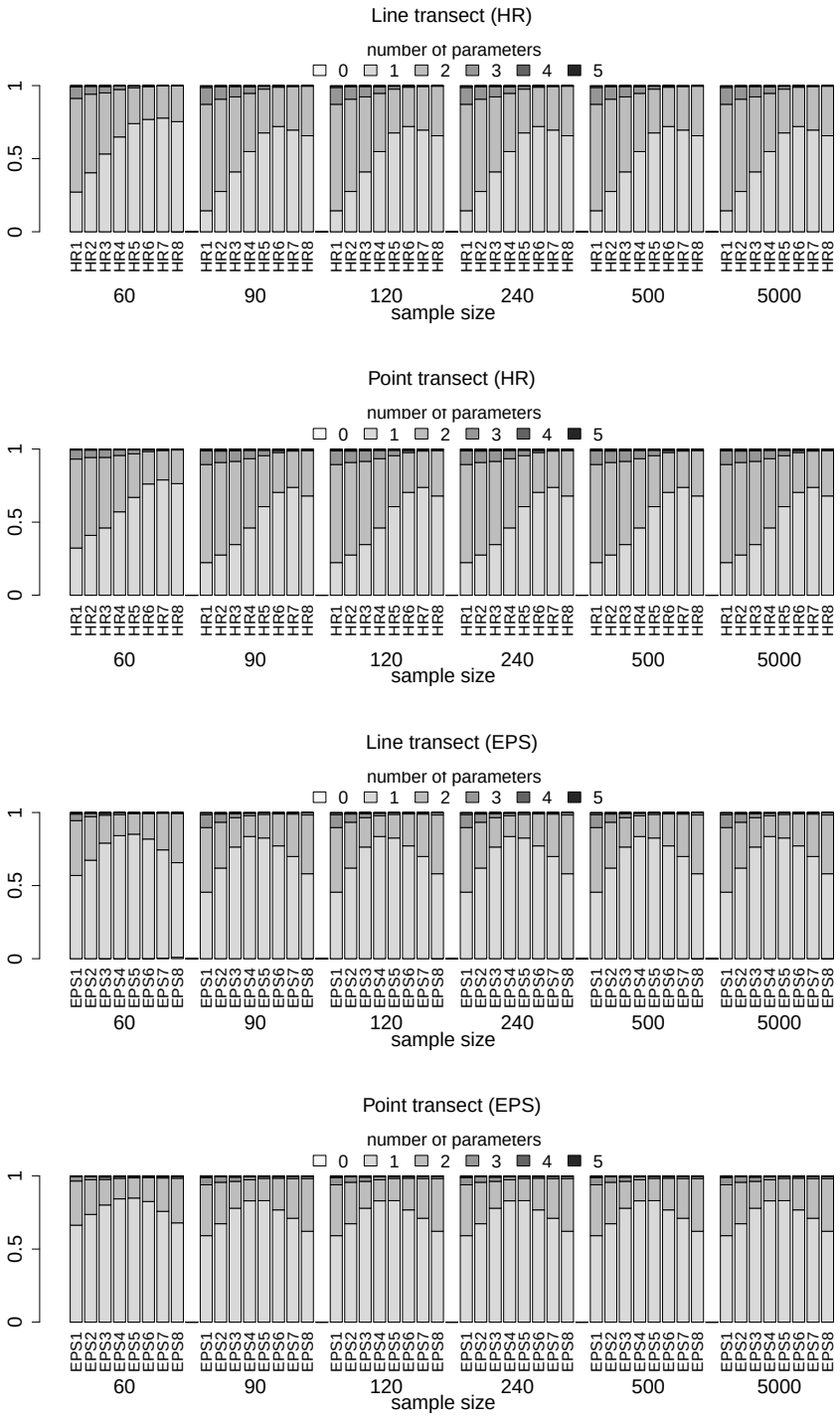

Figure A.11: Proportion of time models with k parameters ($k \in \{0, 1, \ldots, 5\}$) is selected in line and point transect scenarios for the 8 sets of parameters of the hazard-rate (HR) and exponential power series (EPS) distributions, over a range of sample sizes, $n \in \{60, 90, 120, 240, 500, 5000\}$.

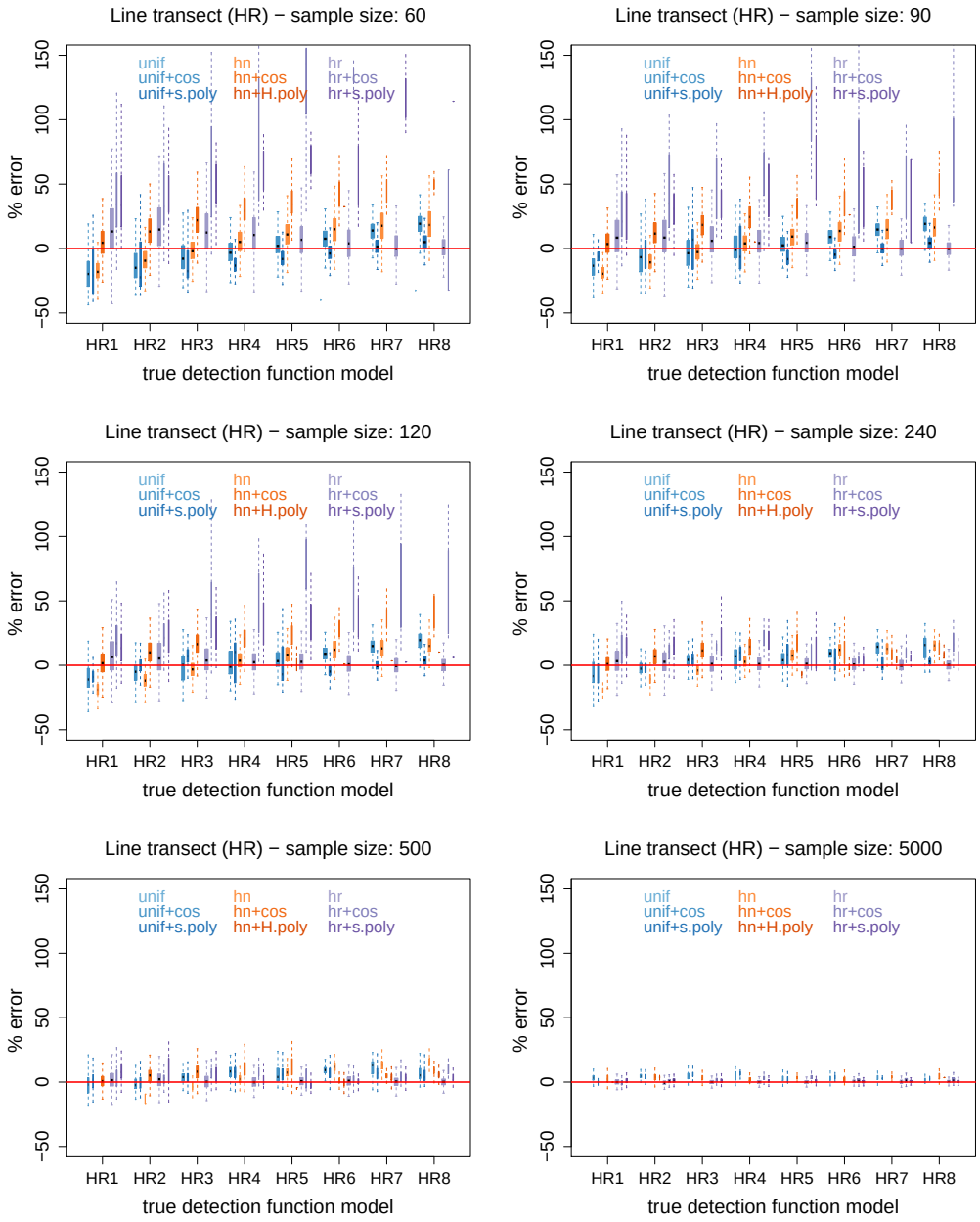

Figure A.12: Percentage error in N introduced by each model of the candidate set of model selection detection function, for the 8 sets of parameters of the hazard rate (HR) distribution under line transect sampling, over a range of sample sizes, $n \in \{60, 90, 120, 240, 500, 5000\}$. Box plots width is proportional to the number of times each model is selected.

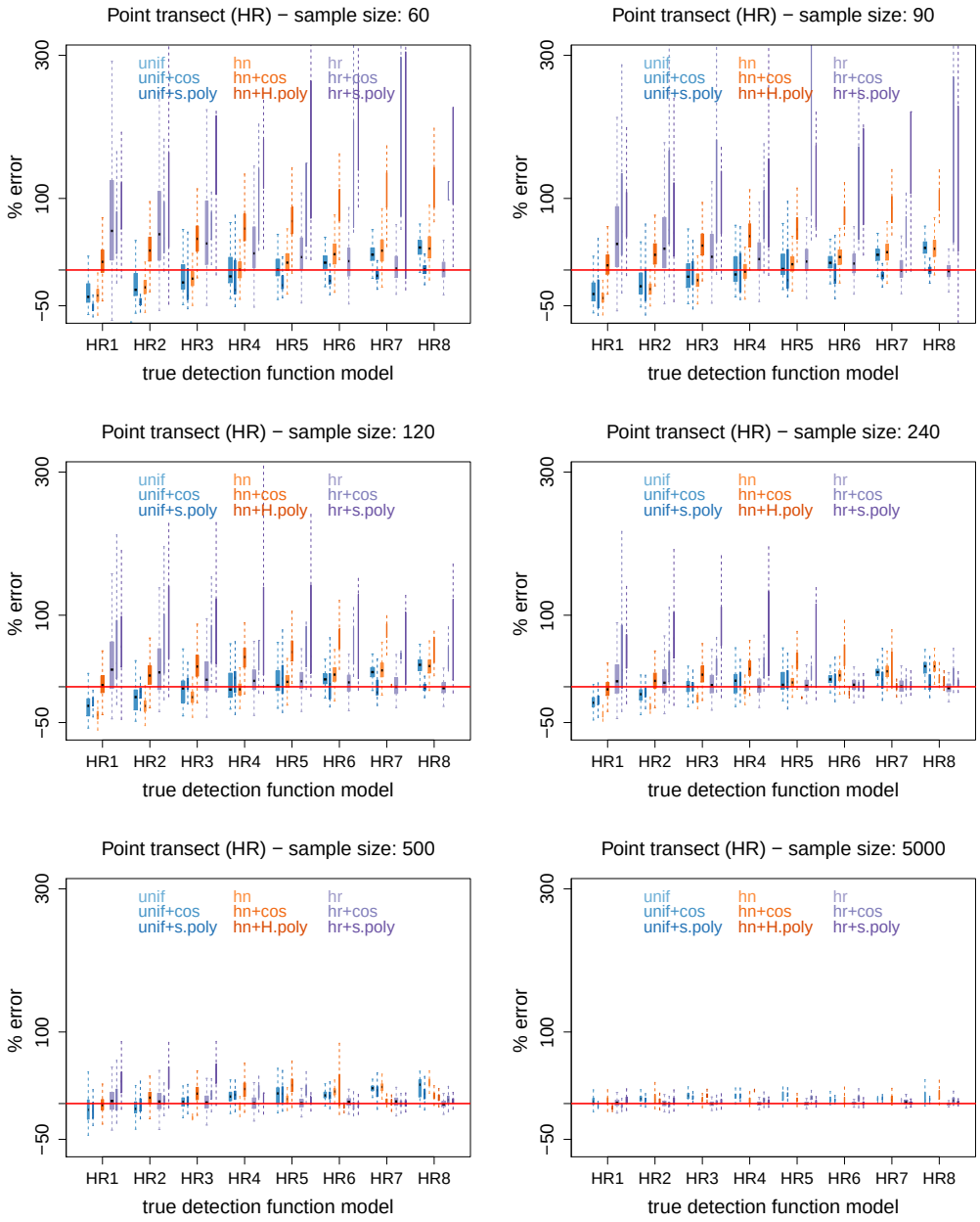

Figure A.13: Percentage error in N introduced by each model of the candidate set of model selection detection function, for the 8 sets of parameters of the hazard rate (HR) distribution under point transect sampling, over a range of sample sizes, $n \in \{60, 90, 120, 240, 500, 5000\}$. Box plots width is proportional to the number of times each model is selected.

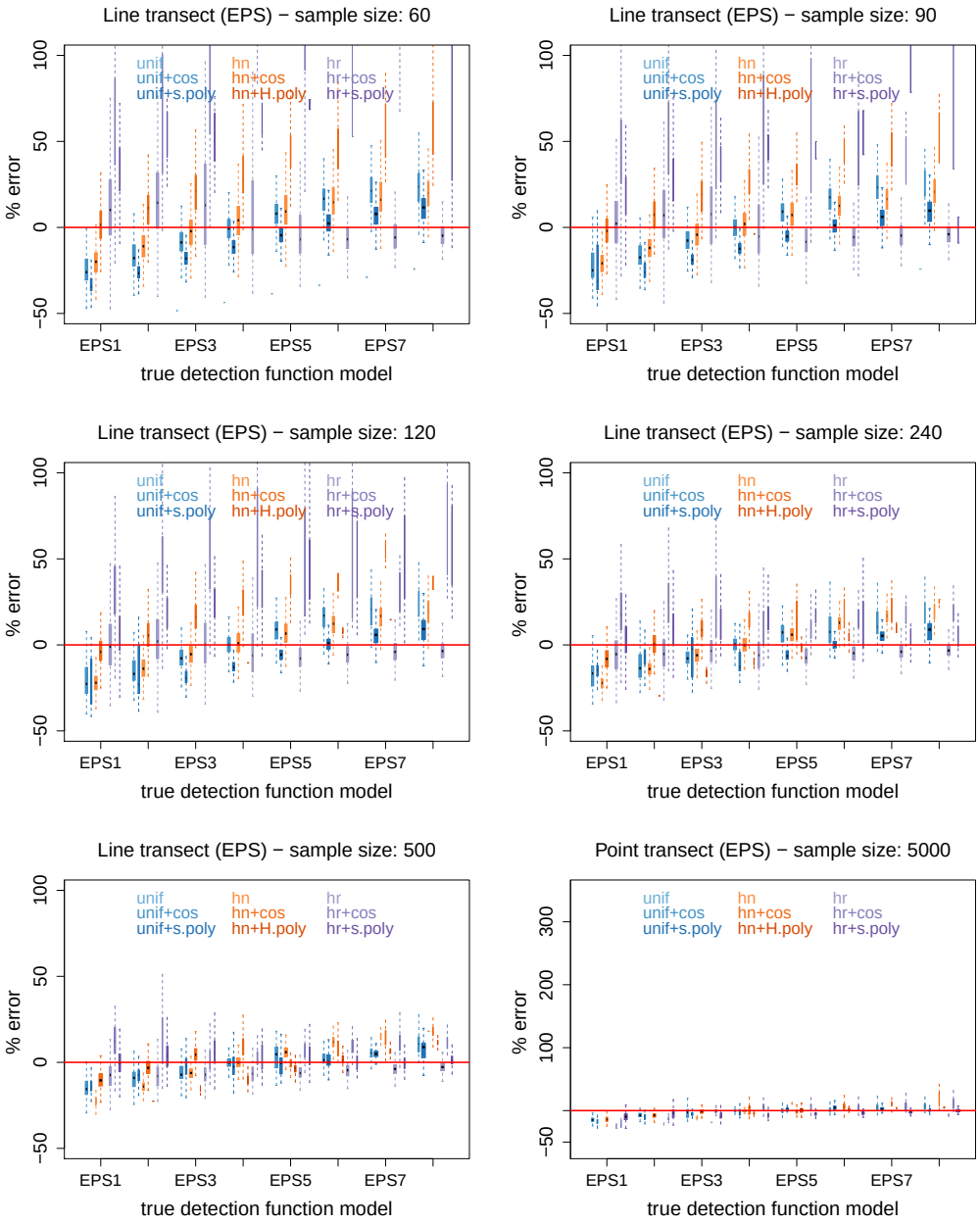

Figure A.14: Percentage error in N introduced by each model of the candidate set of model selection detection function, for the 8 sets of parameters of the exponential power series (EPS) distribution under line transect sampling, over a range of sample sizes, $n \in \{60, 90, 120, 240, 500, 5000\}$. Box plots width is proportional to the number of times each model is selected.

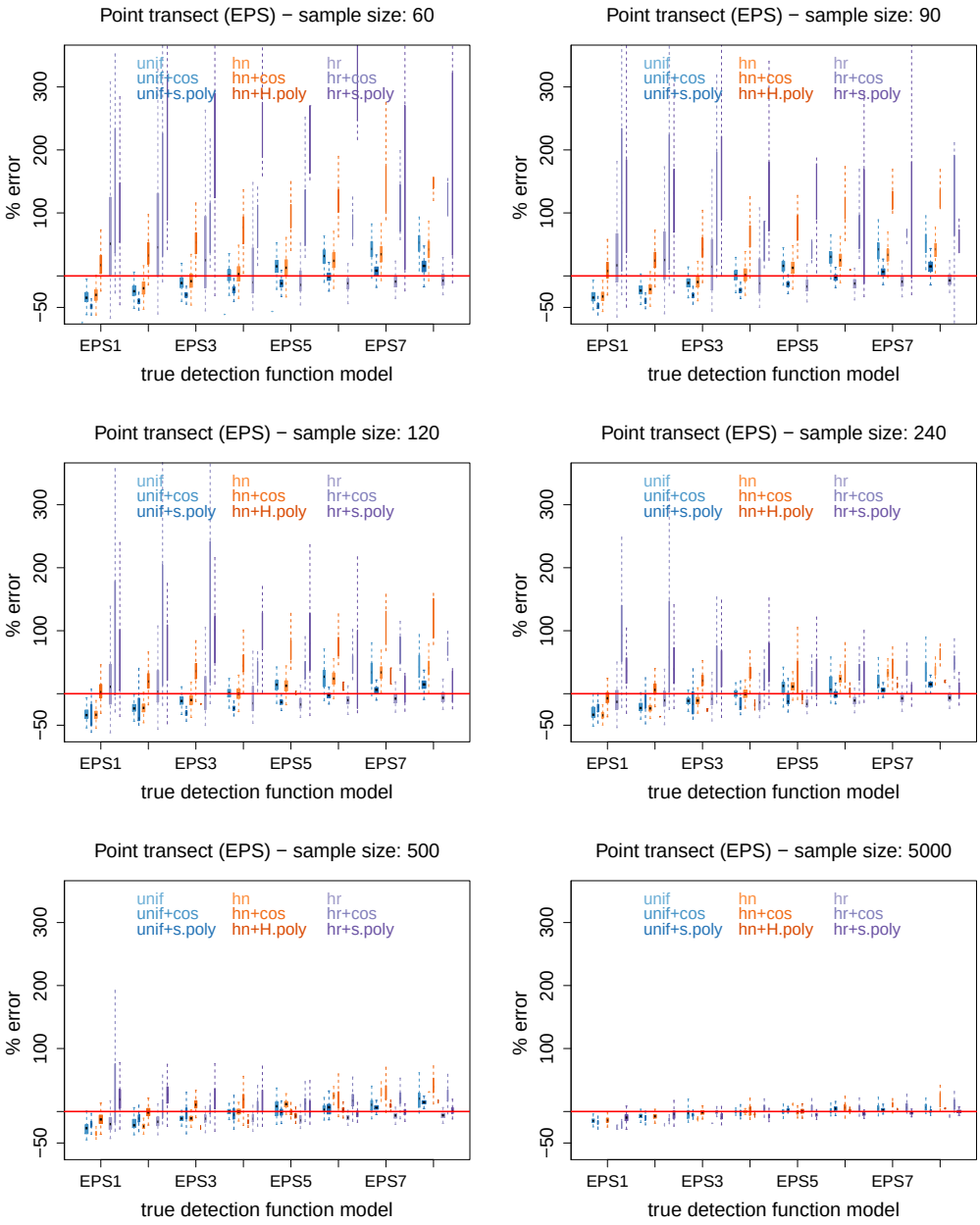

Figure A.15: Percentage error in N introduced by each model of the candidate set of model selection detection function, for the 8 sets of parameters of the exponential power series (EPS) distribution under point transect sampling, over a range of sample sizes, $n \in \{60, 90, 120, 240, 500, 5000\}$. Box plots width is proportional to the number of times each model is selected.

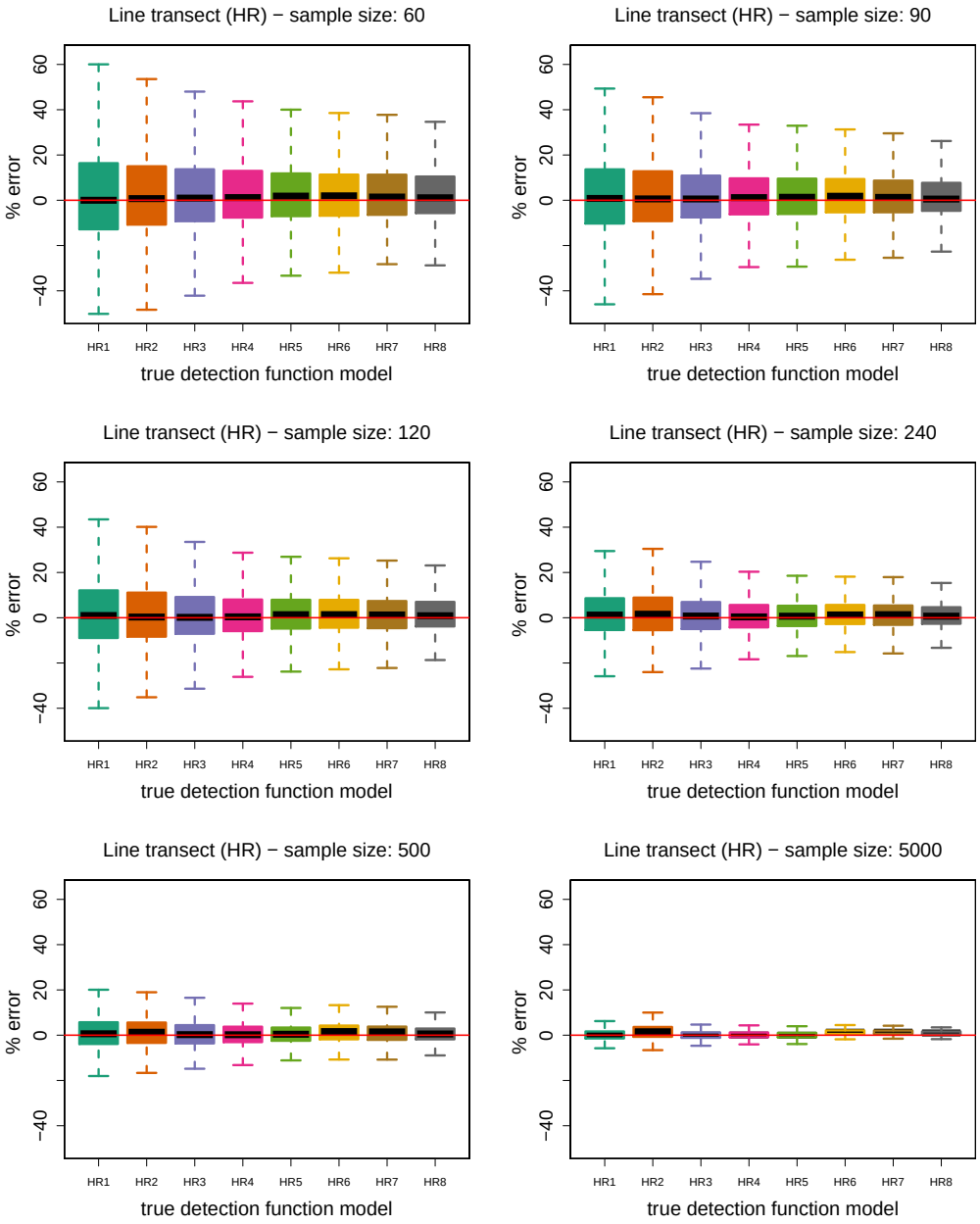

Figure A.16: Distribution of the percentage error in N when only the true model is in the candidate set, for the 8 sets of parameters of the hazard rate (HR) distribution under line transect sampling, over a range of sample sizes, $n \in \{60, 90, 120, 240, 500, 5000\}$.

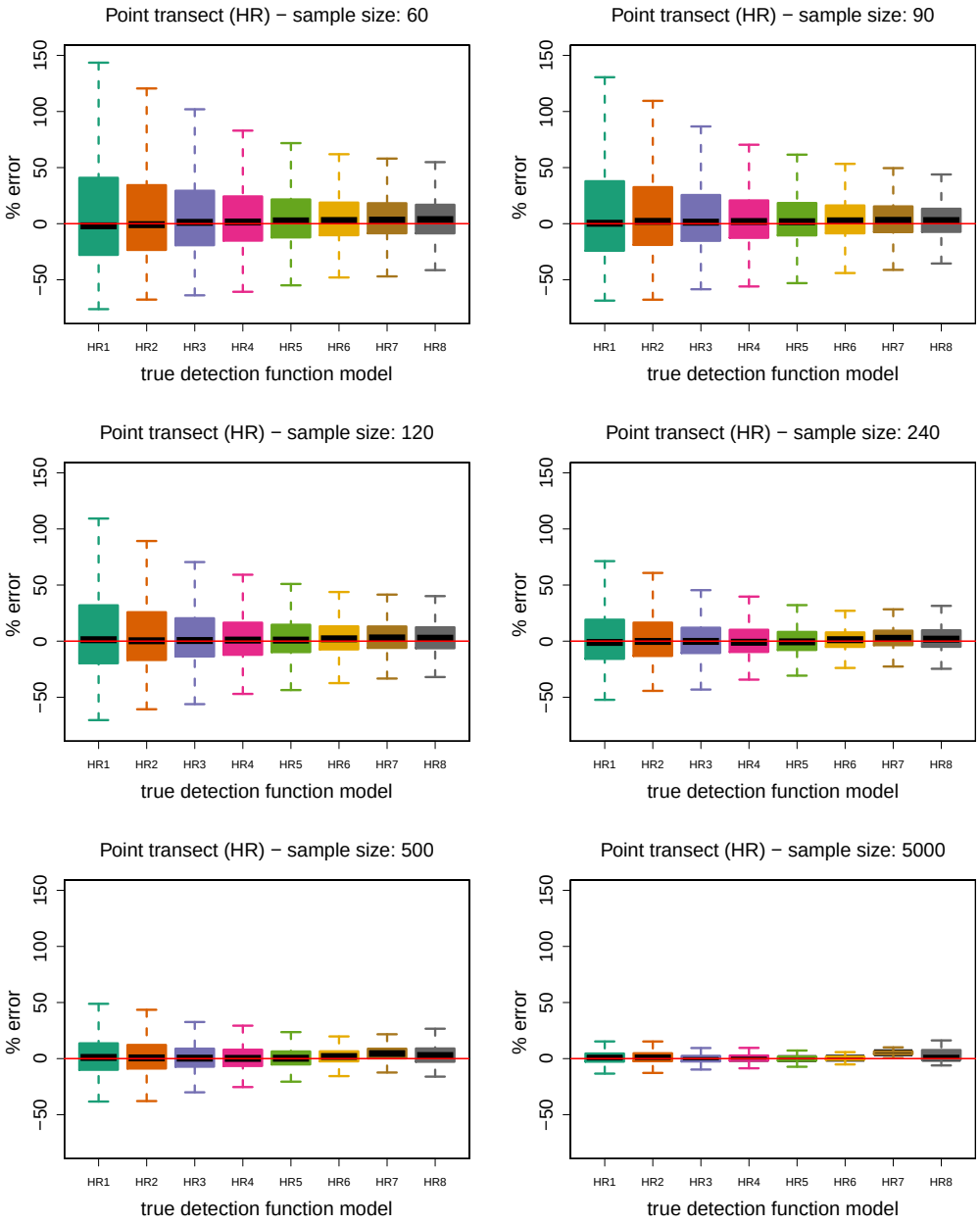

Figure A.17: Distribution of the percentage error in N when only the true model is in the candidate set, for the 8 sets of parameters of the hazard rate (HR) distribution under point transect sampling, over a range of sample sizes, $n \in \{60, 90, 120, 240, 500, 5000\}$.

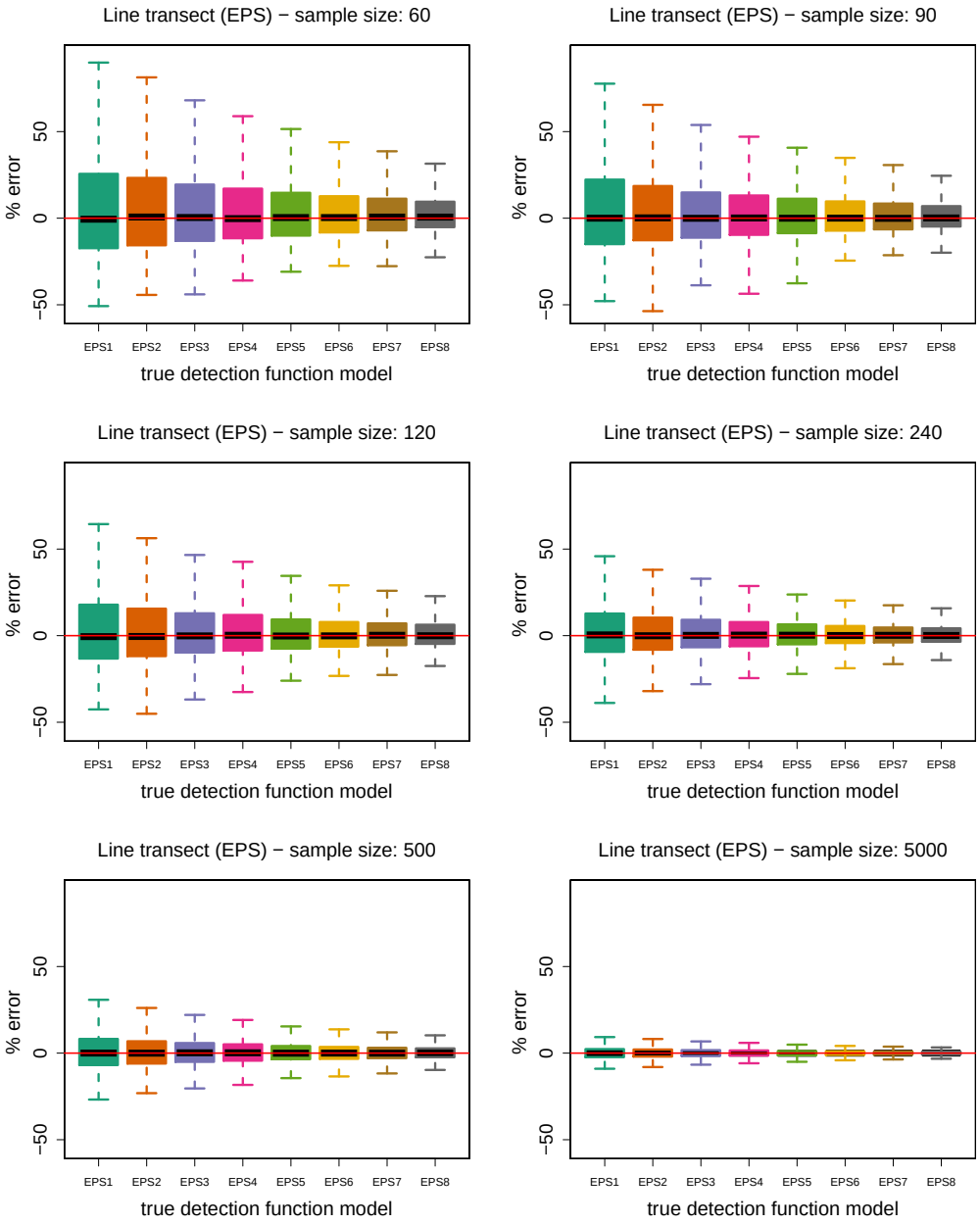

Figure A.18: Distribution of the percentage error in N when only the true model is in the candidate set, for the 8 sets of parameters of the exponential power series (EPS) distribution under line transect sampling, over a range of sample sizes, $n \in \{60, 90, 120, 240, 500, 5000\}$.

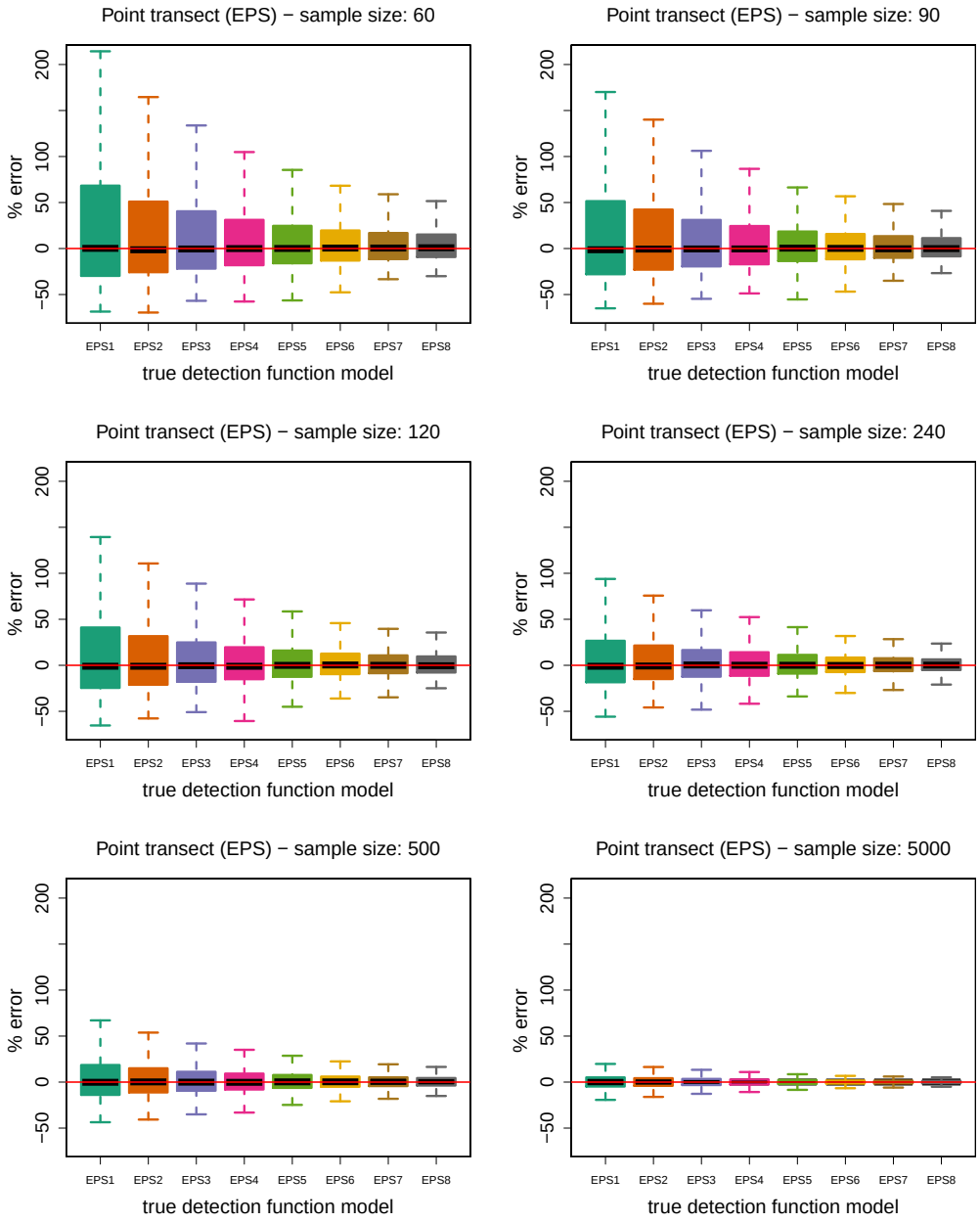

Figure A.19: Distribution of the percentage error in N when only the true model is in the candidate set, for the 8 sets of parameters of the exponential power series (EPS) distribution under point transect sampling, over a range of sample sizes, $n \in \{60, 90, 120, 240, 500, 5000\}$.

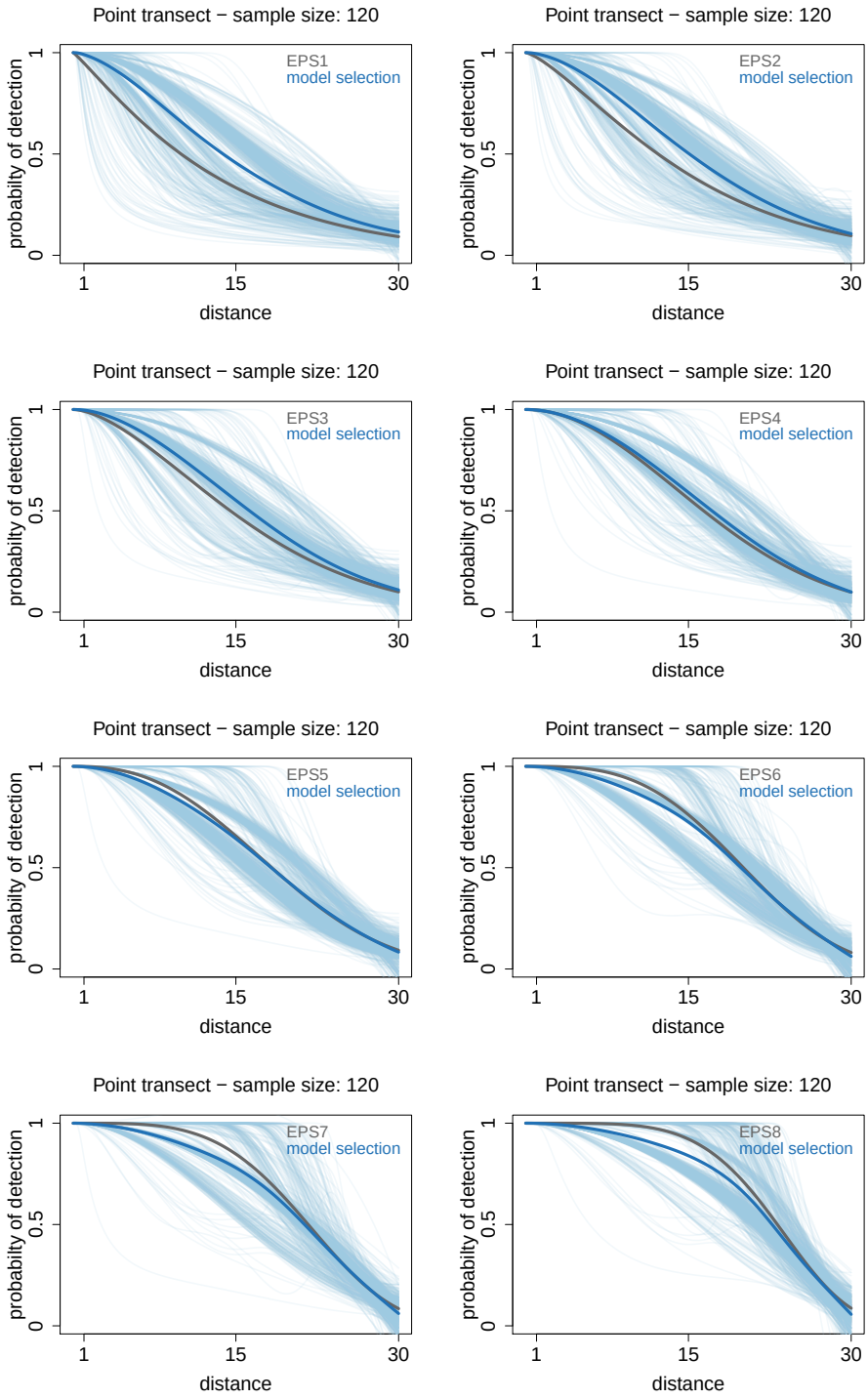

Figure A.20: Set of detection functions fitted using detection function model selection (thin blue lines) with the average detection function represented by the thick blue line, when the data are generated by each of the 8 sets of parameters of the exponential power series (EPS) distribution (grey line) in a point transect sampling with 120 observations scenario.

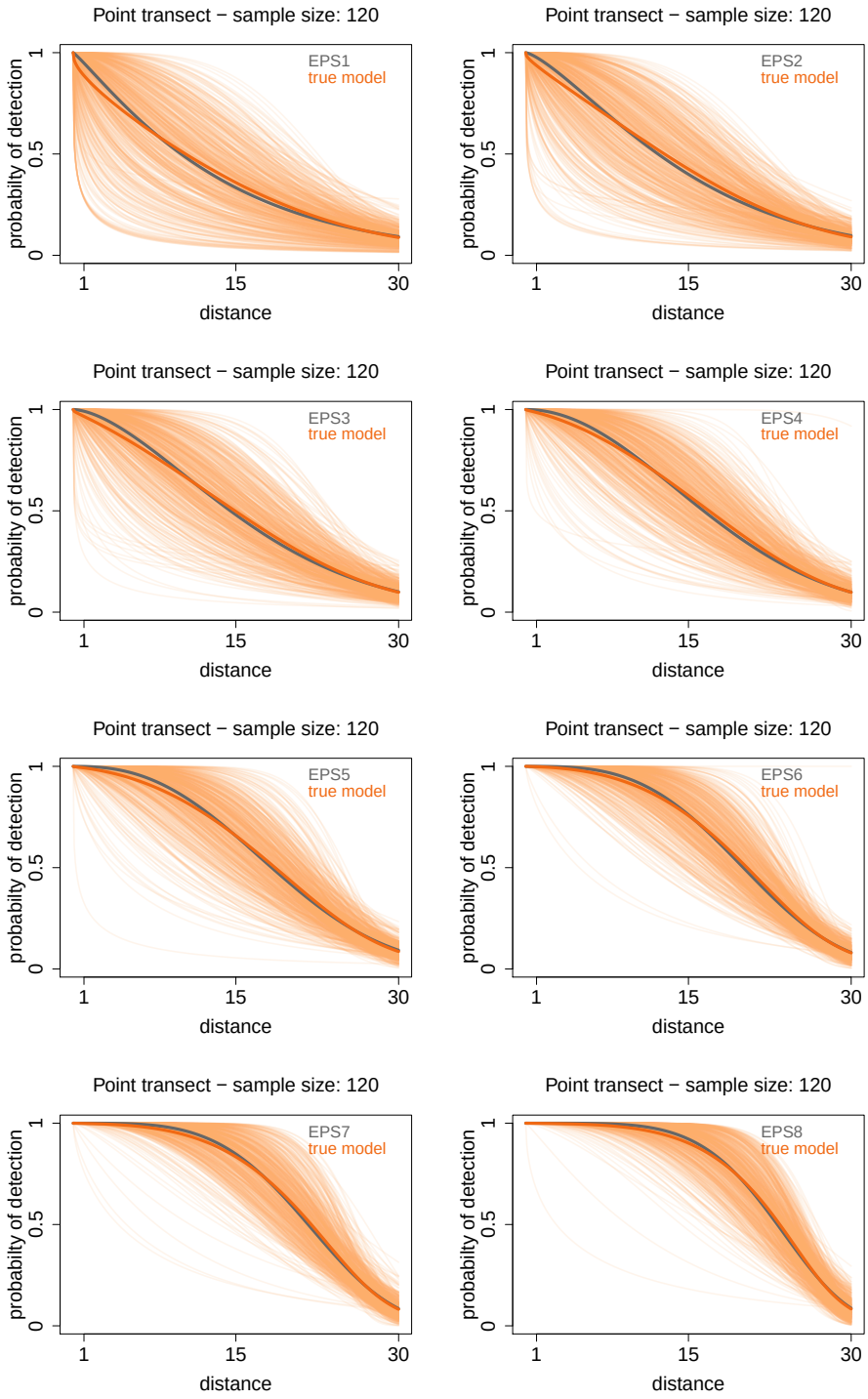

Figure A.21: Set of detection function fitted using the true model (thin orange lines) with the average detection function represented by the thick orange line, when the data are generated by each of the 8 sets of parameters of the exponential power series (EPS) distribution (grey line) in a point transect sampling with 120 observations scenario.

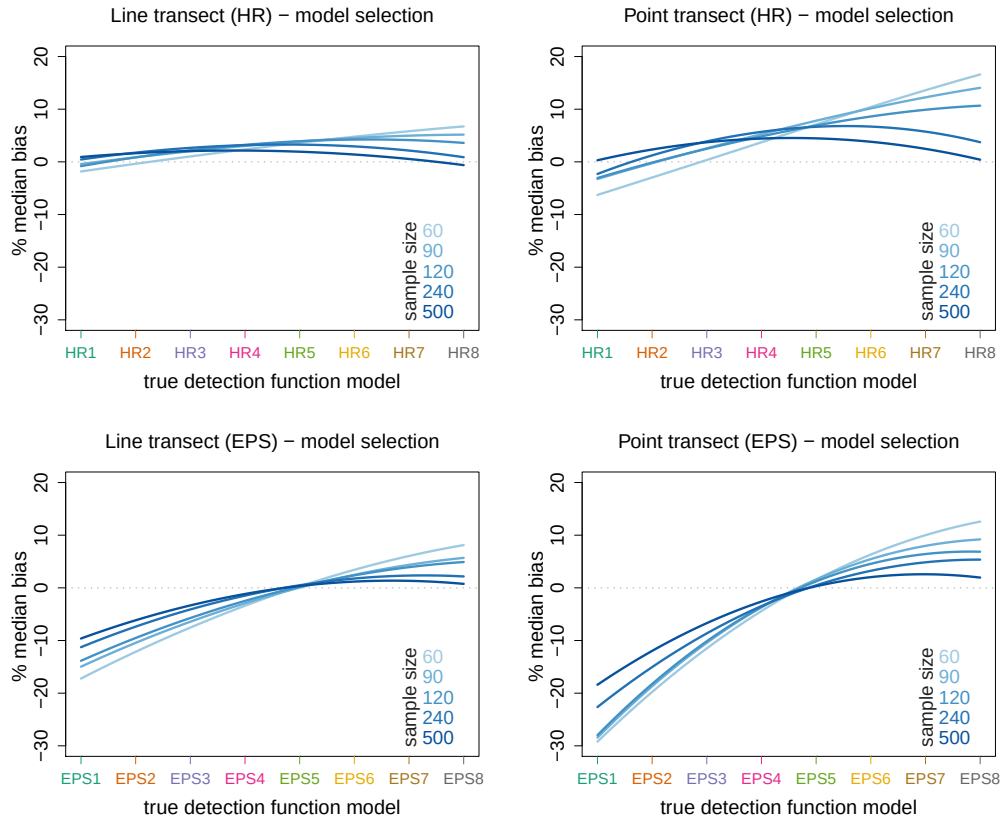

Figure A.22: Percentage median bias in N using detection function model selection removing the monotonicity constraint and for 8 sets of parameters of the hazard-rate (HR) and exponential power series (EPS) distributions, over a range of sample sizes, $n \in \{60, 90, 120, 240, 500\}$. Shown are smoothed lines of raw results.

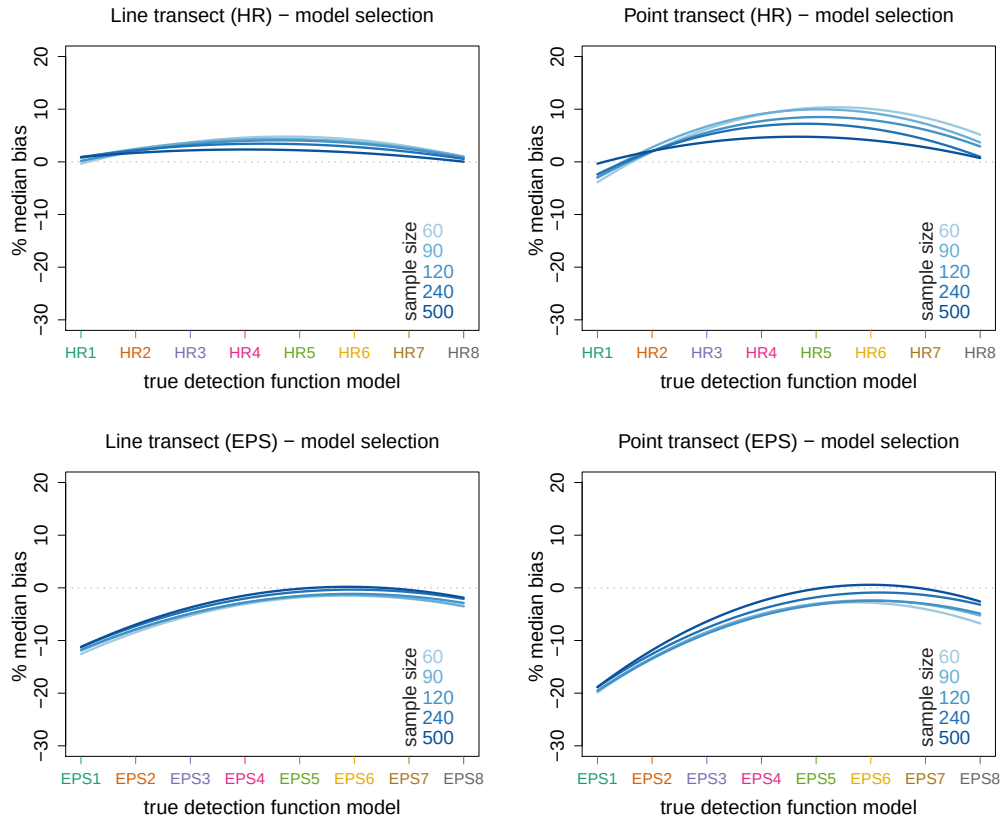

Figure A.23: Percentage median bias in N using detection function model selection removing the monotonicity constraint and considering only 2-parameters models for 8 sets of parameters of the hazard-rate (HR) and exponential power series (EPS) distributions, over a range of sample sizes, $n \in \{60, 90, 120, 240, 500\}$. Shown are smoothed lines of raw results.

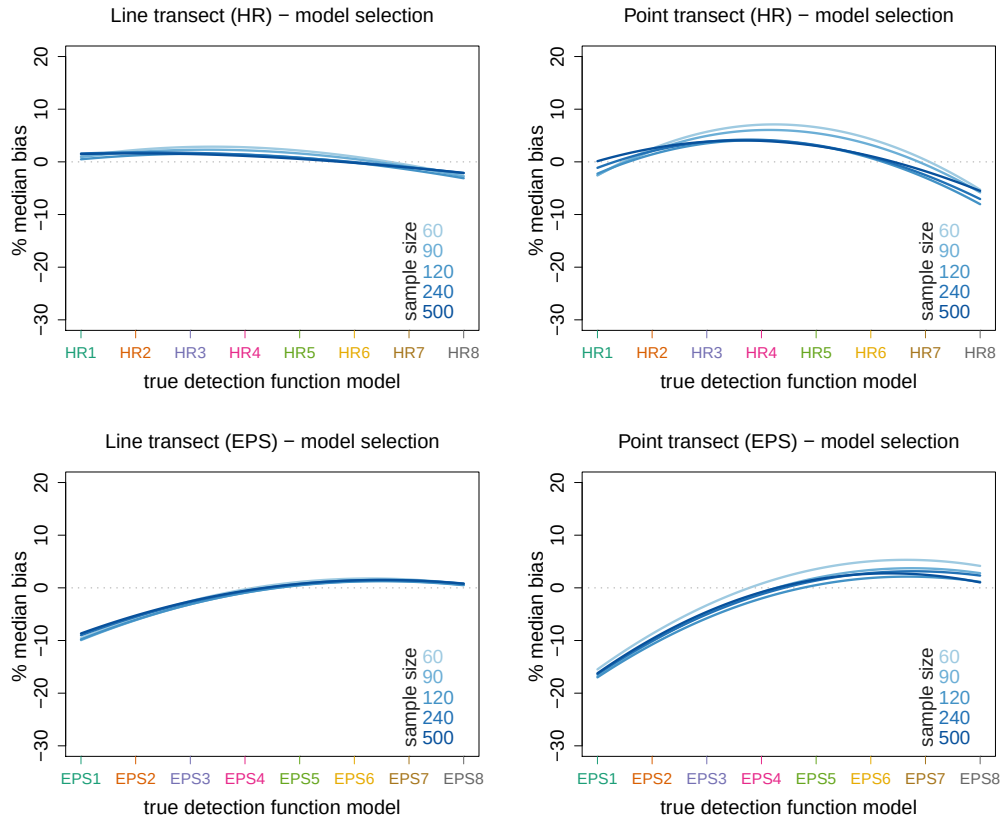

Figure A.24: Percentage median bias in N using detection function model selection removing the monotonicity constraint and considering only 3-parameters models for 8 sets of parameters of the hazard-rate (HR) and exponential power series (EPS) distributions, over a range of sample sizes, $n \in \{60, 90, 120, 240, 500\}$. Shown are smoothed lines of raw results.

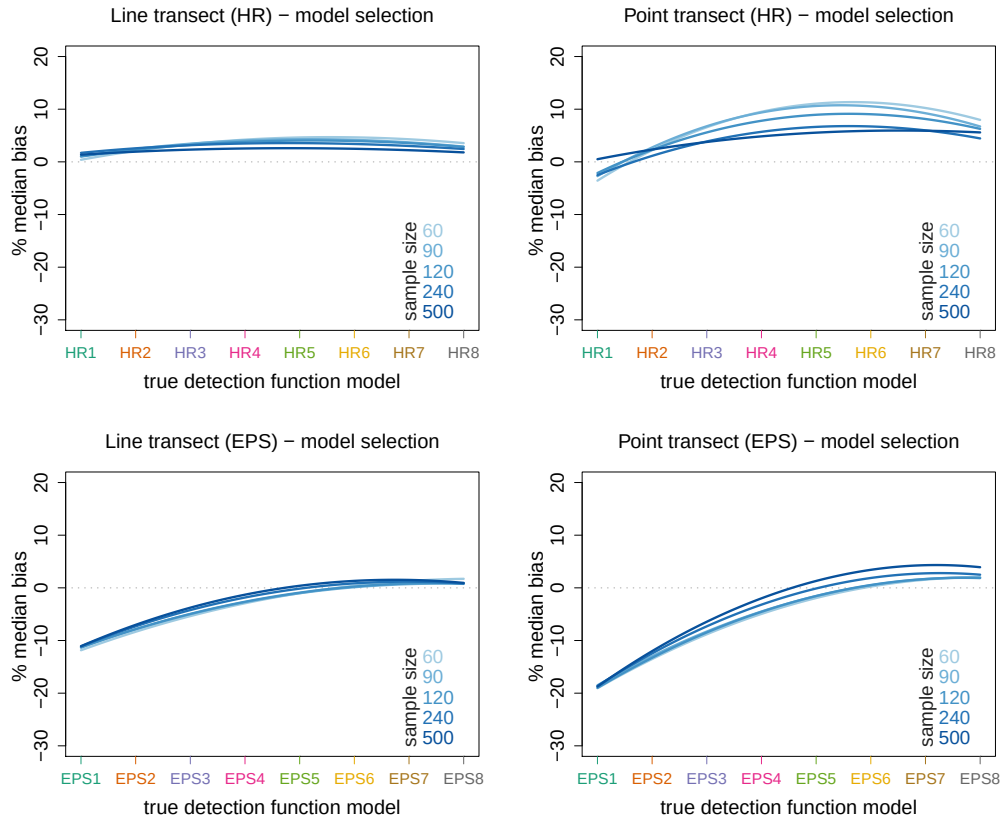

Figure A.25: Percentage median bias in N using detection function model selection with the monotonicity constraint and considering only 2-parameters models for 8 sets of parameters of the hazard-rate (HR) and exponential power series (EPS) distributions, over a range of sample sizes, $n \in \{60, 90, 120, 240, 500\}$. Shown are smoothed lines of raw results.

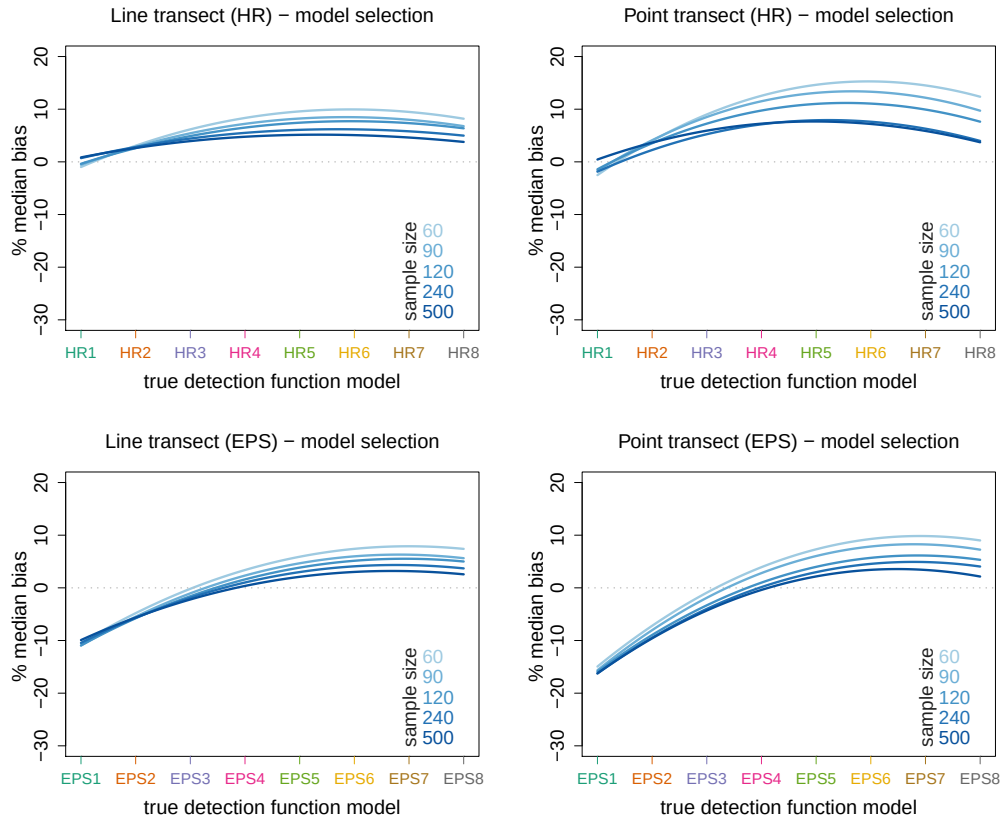

Figure A.26: Percentage median bias in N using detection function model selection with the monotonicity constraint and considering only 3-parameters models for 8 sets of parameters of the hazard-rate (HR) and exponential power series (EPS) distributions, over a range of sample sizes, $n \in \{60, 90, 120, 240, 500\}$. Shown are smoothed lines of raw results.

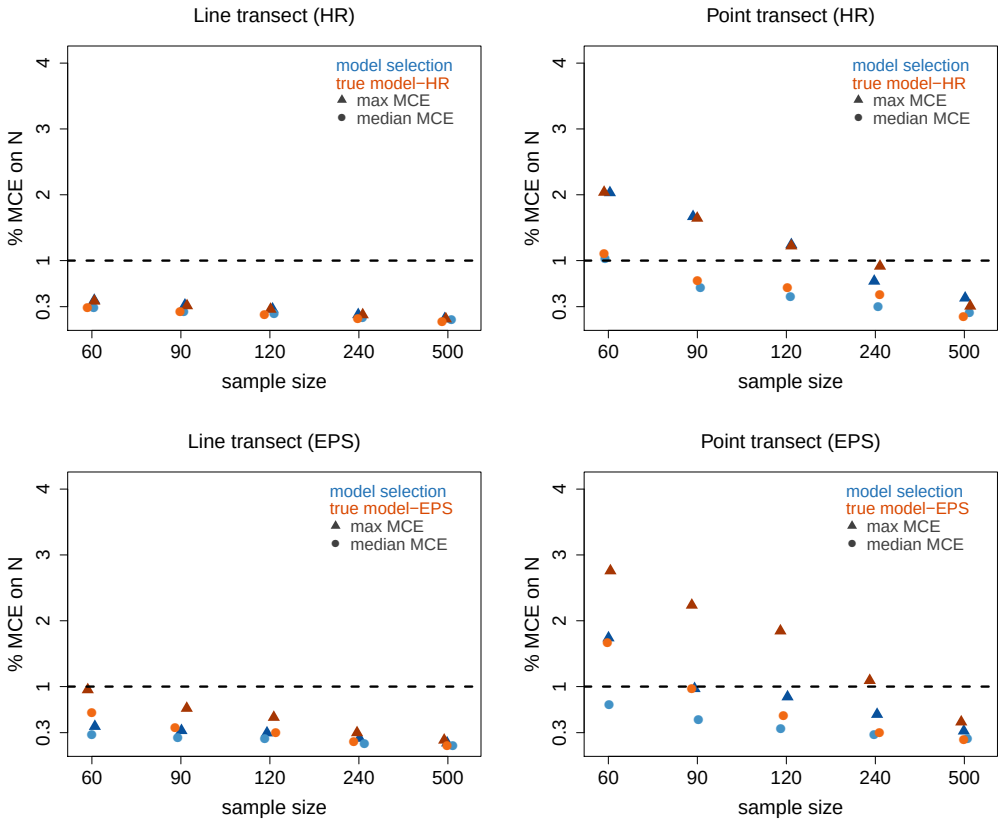

Figure A.27: Maximum (△) and median (○) percentage Monte Carlo error (MCE) on $\hat{P}_a$ along the 8 sets of parameters of the hazard-rate (HR) and exponential power series (EPS) distributions, for detection function model selection and the true model, over a range of sample sizes, $n \in \{60, 90, 120, 240, 500\}$.

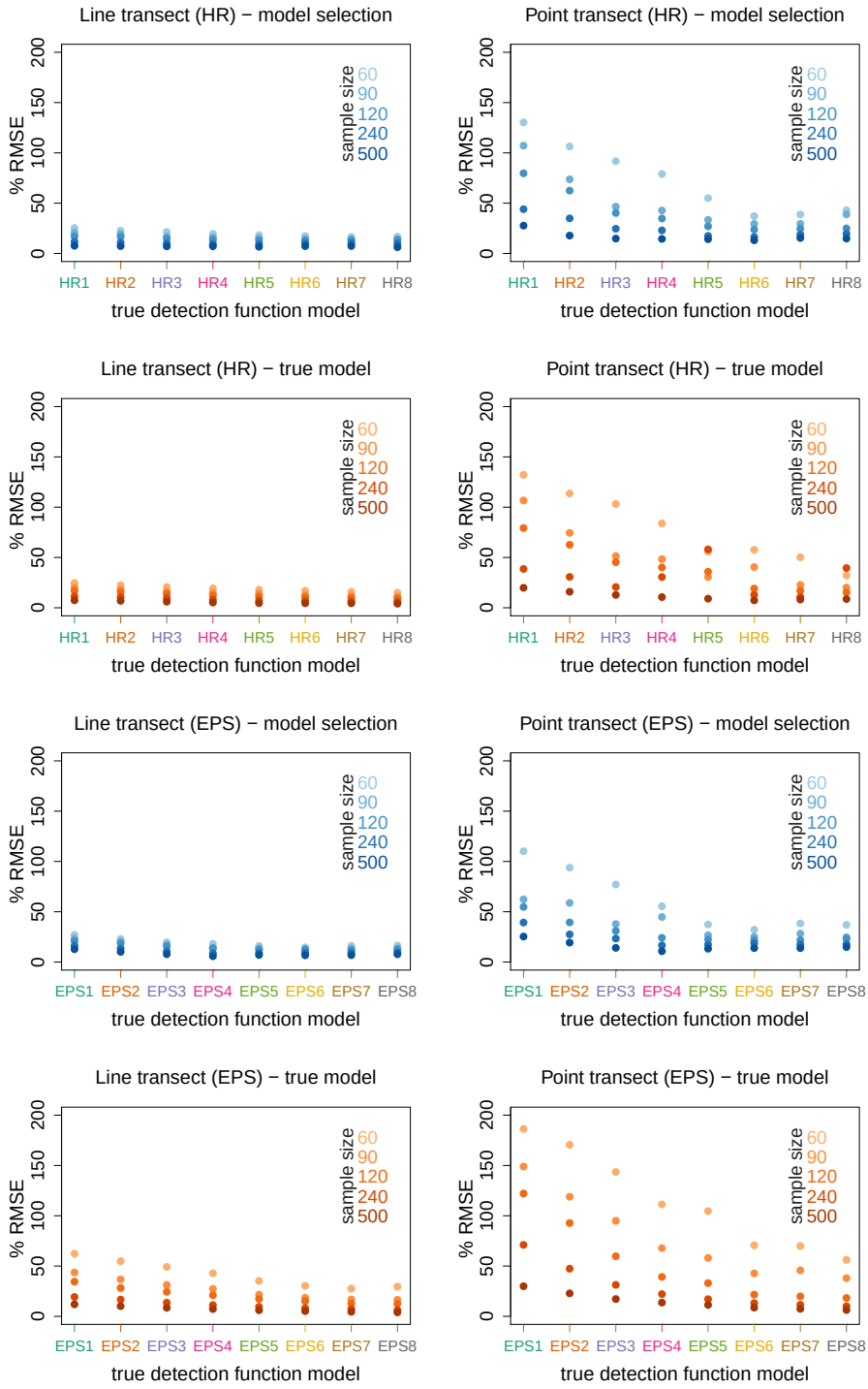

Figure A.28: Percentage root-mean-square error (RRMSE) in N using detection function model selection (left column) and true model (right column) as model for inference for 8 sets of parameters of the hazard-rate (HR) and exponential power series (EPS) distributions, over a range of sample sizes, $n \in \{60, 90, 120, 240, 500\}$.

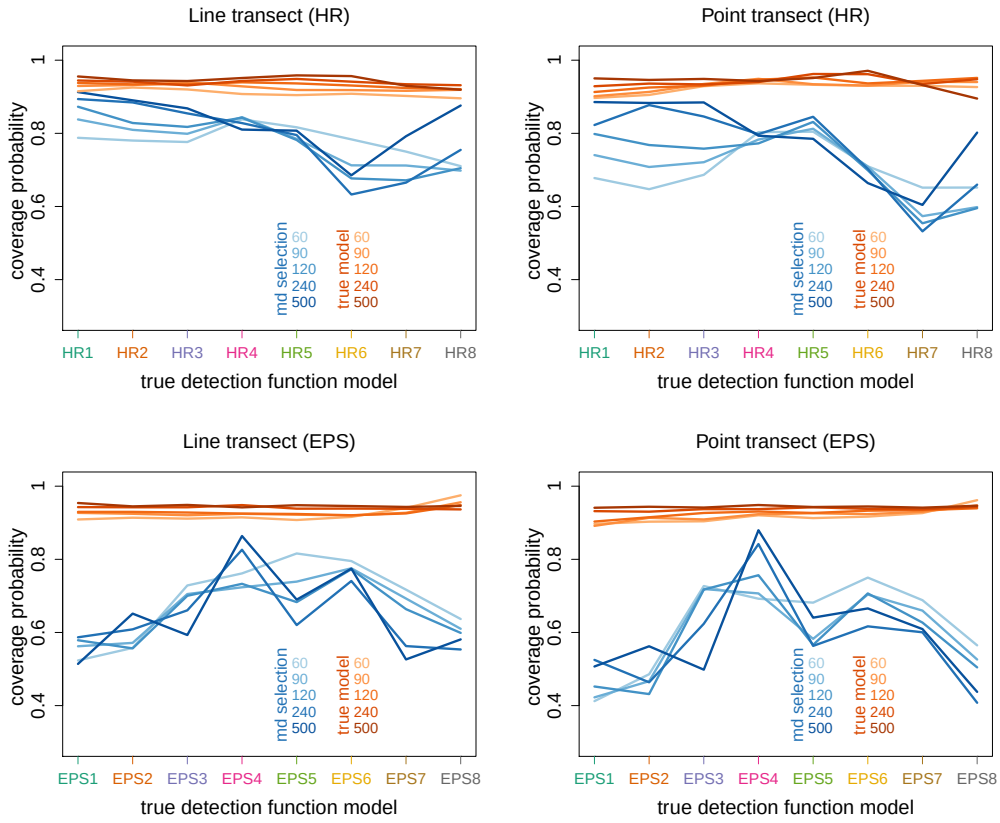

Figure A.29: Coverage probability (proportion of 95% confidence interval estimates that contains the true N value) for detection function model selection and the true model along the 8 sets of parameters of the hazard-rate (HR) and exponential power series (EPS) distributions, over a range of sample sizes, $n \in \{60, 90, 120, 240, 500\}$.

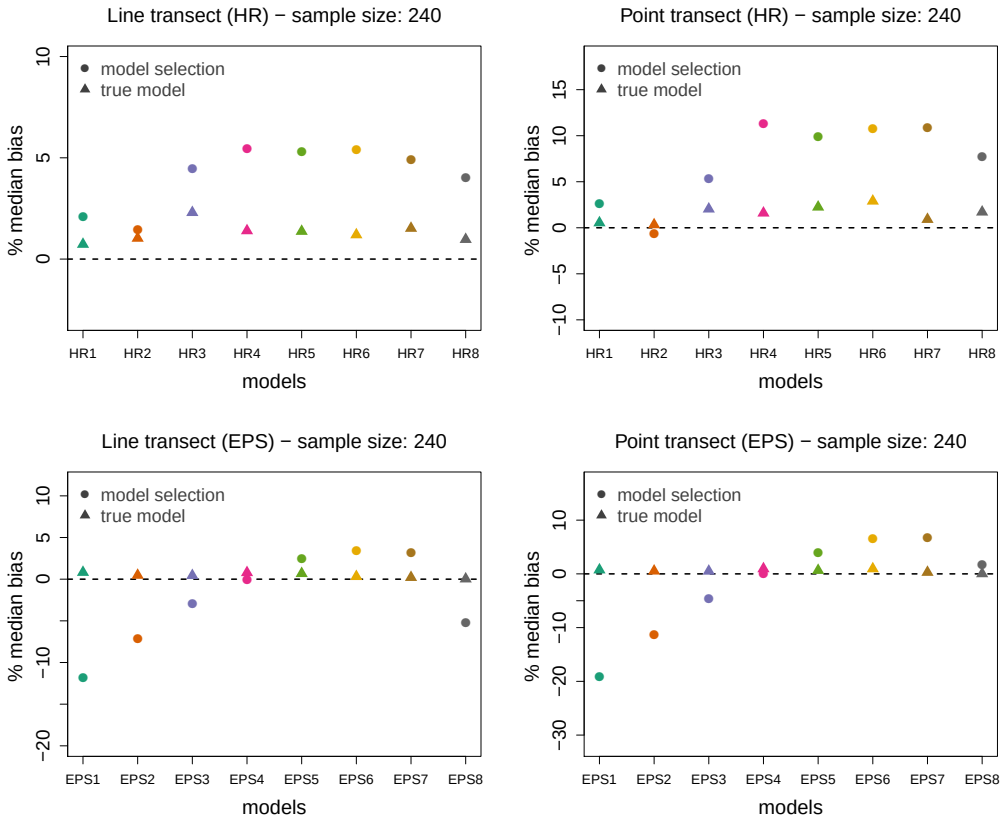

Figure A.30: Percentage median bias in N for line and point transect sampling when $w = 20$, using detection function model selection ($\circ$) and true model ($\triangle$) as model for inference for 8 sets of parameters of the hazard-rate (HR) and exponential power series (EPS) distribution, for 240 observations.

Bibliography

Aho, K., Derryberry, D., and Peterson, T. (2014). Model selection for ecologists: the worldviews of AIC and BIC. *Ecology*, **95**, 631–636.

Akaike, H. (1974). A new look at the statistical model identification. *Automatic Control, IEEE Transactions*, **19**, 716–723.

Anderson, D. R., Burnham, K. P., Lubow, B. C., Thomas, L., Corn, P. S., Medica, P. A., and Marlow., R. W. (2001). Field testing line transect estimation of desert tortoise abundance. *Journal of Wildlife Management*, **65**, 583–597.

Barabesi, L. and Fattorini, L. (2013). Random versus stratified location of transects or points in distance sampling: theoretical results and practical considerations. *Environmental and Ecological Statistics*, **20**, 215–236.

Bender, R., Augustin, T., and Blettner, M. (2005). Generating survival times to simulate Cox proportional hazards models. *Statistics in Medicine*, **24**, 1713–1723.

Benhamou, S. (2006). Detecting an orientation component in animal paths when the preferref direction is individual-dependent. *Ecology*, **87**, 518–528.

Bénichou, O., Coppey, M., Moreau, M., Suet, P. H., and Voituriez, R. (2005). Optimal search strategies for hidden targets. *Physical Review Letters*, **94**, 198101.

Berg, H. C. (1993). *Random Walks in Biology*. Princeton University Press.

Bibby, C. J. (2000). *Bird Census Techniques*. Elsevier.

Bibby, C. J. and Buckland, S. T. (1987). Bias of bird census results due to detectability varying with habitat. *Acta Oecologica, Oecologia Generalis.*, **8**, 103–112.

Blackwell, P. G. (1997). Random diffusion models for animal movement. *Ecological Modelling*, **100**, 87–102.

Blihovde, W. B. (2006). Terrestrial movements and upland habitat use of Gopher frogs in central Florida. *Southeastern Naturalist*, **5**, 265–276.

Block, B. A., Costa, D. P., Boehlert, G. W., and Kochevar, R. E. (2002). Revealing pelagic habitat use: the tagging of Pacific pelagics program. *Oceanologica Acta*, **25**, 255–266.

Bollinger, E. K., Gavin, T. A., and McIntyre, D. C. (1988). Comparison of transects and circular-plots for estimating densities. *The Journal of Wildlife Management*, **52**, 777–786.

Borchers, D. L. (1996). *Line transect abundance estimation with uncertain detection on the trackline*. Ph.D. thesis, University of Cape Town.

Borchers, D. L., Buckland, S. T., Goedhart, P. W., Clarke, E. D., and Hedley, S. L. (1998). Horvitz-Thompson estimators for double-platform line transect surveys. *Biometrics*, **54**, 1221–1237.

Borchers, D. L., Buckland, S. T., and Zucchini, W. (2002). *Estimating Animal Abundance: Closed Populations*. London: Springer.

Borchers, D. L., Laake, J. L., Southwell, C., and Paxton, C. G. M. (2006). Accommodating unmodeled heterogeneity in double-observer distance sampling surveys. *Biometrics*, **62**, 372–378.

Borchers, D. L., Pike, D. G., Gunnlaugsson, T., and Víkingsson, G. A. (2009). Minke whale abundance estimation from the nass 1987 and 2001 aerial cue–counting surveys taking appropriate account of distance estimation errors. *NAMMCO Scientific Publications*, **7**, 95–110.

Borchers, D. L., Marques, T. A., Gunnlaugsson, T., and Jupp, P. E. (2010). Estimating distance sampling detection functions when distances are measured with errors. *Journal of Agricultural, Biological, and Environmental Statistics*, **15**, 346–361.

Bovet, P. and Benhamou, S. (1988). Spatial analysis of animals' movements using a correlated random walk model. *Journal of Theoretical Biology*, **131**, 419–433.

Breed, G. A., Golson, E. A., and Tinker, M. T. (2017). Predicting animal home-range structure and transitions using a multistate Ornstein-Uhlenbeck biased random walk. *Ecology*, **98**, 32–47.

Brewer, M. J., Butler, A., and Cooksley, S. L. (2016). The relative performance of AIC, AICc and BIC in the presence of unobserved heterogeneity. *Methods in Ecology and Evolution*, **7**, 679–692.

Brown, R. (1828). A brief account of microscopical observations made in the months of june, july and august 1827, on the particles contained in the pollen of plants; and on the general existence of active molecules in organic and inorganic bodies. *Philosophical Magazine Series 2*, **4**, 161–173.

Buckland, S. T. (2006). Point-transect surveys for songbirds: robust methodologies. *Auk*, **123**, 345–357.

Buckland, S. T., Anderson, D. R., Burnham, K. P., and Laake, J. L. (1993). Distance Sampling: Estimating Abundance of Biological Populations. *Chapman and Hall London*.

Buckland, S. T., Burnham, K. P., and Augustin, N. H. (1997). Model selection: An integral part of inference. *Biometrics*, **53**, 603–618.

Buckland, S. T., Anderson, D. R., Burnham, K. P., Laake, J. L., Borchers, D. L., and Thomas, L. (2001). *Introduction to Distance Sampling*. Oxford: Oxford University Press.

Buckland, S. T., Anderson, D. R., Burnham, K. P., Laake, J. L., Borchers, D. L., and Thomas, L. (2004). *Advanced Distance Sampling*. Oxford: Oxford University Press.

Buckland, S. T., Summers, R. W., Borchers, D. L., and Thomas, L. (2006). Point transect sampling with traps or lures. *Journal of Applied Ecology*, **43**, 377–384.

Buckland, S. T., Borchers, D. L., Johnston, A., Henrys, P. A., and Marques, T. A. (2007). Line transect methods for plant surveys. *Biometrics*, **63**, 989–998.

Buckland, S. T., Laake, J. L., and Borchers, D. L. (2010). Double-observer line transect methods: Levels of independence. *Biometrics*, **66**, 169–177.

Buckland, S. T., Rexstad, E. A., Marques, T. A., and Oedekoven, C. (2015). *Distance Sampling: Methods and Applications*. Springer.

Burnham, K. P. and Anderson, D. R. (2002). *Model Selection and Multimodel Inference: a Practical Information Theoretic Approach*. Springer Science & Business Media.

Burnham, K. P., Anderson, D. R., and Laake, J. L. (1980). Estimation of density from line transect sampling of biological populations. *Wildlife Monographs*, **72**, 3–202.

Burnham, K. P., Anderson, D. R., and Huyvaert, K. P. (2011). AIC model selection and multimodel inference in behavioral ecology: some background, observations, and comparisons. *Behavioral Ecology and Sociobiology*, **65**, 23–35.

Byers, J. A. (2001). Correlated random walk equations of animal dispersal resolved by simulation. *Ecology*, **82**, 1680–1690.

Cassey, P. and Mcardle, B. H. (1999). An assessment of distance sampling techniques for estimating animal abundance. *Environmetrics*, **10**, 261–278.

Charif, R. A., Clapham, P. J., and Clark, C. W. (2001). Acoustic detections of singing humpback whales in deep waters off the British Isles. *Marine Mammal Science*, **17**, 751–768.

Cheung, A., Zhang, S., Stricker, C., and Srinivasan, M. V. (2008). Animal navigation: general properties of directed walks. *Biological Cybernetics*, **99**, 197–217.

Codling, E. A. and Hill, N. A. (2005). Sampling rate effects on measurements of correlated and biased random walks. *Journal of Theoretical Biology*, **233**, 573–588.

Codling, E. A., Plank, M. J., and Benhamou, S. (2008). Random walk models in biology. *Journal of the Royal Society Interface*, **5**, 813–834.

Codling, E. A., Bearon, R. N., and Thorn, G. J. (2010). Diffusion about the mean drift location in a biased random walk. *Ecology*, **91**, 3106–3113.

Conant, S., Collins, M. S., and Ralph, C. J. (1981). Effects of observers using different methods upon the total population estimates of two resident island birds. *Studies in Avian Biology*, **6**, 377–381.

Du Fresne, S., Fletcher, D., and Sawson, S. (2006). The effect of line-transect placement in a coastal distance sampling survey. *Journal of Cetacean Research and Management*, **8**, 79–85.

Durant, S. M., Craft, M. E., Hilborn, R., Bashir, S., Hando, J., and Thomas, L. (2011). Long-term trends in carnivore abundance using distance sampling in Serengeti National Park, Tanzania. *Journal of Applied Ecology*, **48**, 1490–1500.

Durban, J. W. and Pitman, R. L. (2012). Antarctic killer whales make rapid, round-trip movements to subtropical waters: evidence for physiological maintenance migrations? *Biology Letters*, **8**, 274–277.

Durbin, J. and Williams, D. (1992). The first-passage density of the Brownian motion process to a curved boundary. *Journal of Applied Probability*, **29**, 291–304.

Ekblom, R. (2010). Evaluation of the analysis of distance sampling data: a simulation study. *Ornis Svecica*, **20**, 45–53.

Ellingson, A. R. and Lukacs, P. M. (2003). Improving methods for regional landbird monitoring: a reply to Hutto and Young. *Wildlife Society Bulletin*, **31**, 896–902.

Fancy, S. G., Pank, L. F., Whitten, K. R., and Regelin, W. L. (1989). Seasonal movements of caribou in Arctic Alaska as determined by satellite. *Canadian Journal of Zoology*, **67**, 644–650.

Fauchald, P. and Tveraa, T. (2003). Using first-passage time in the analysis of area-restricted search and habitat selection. *Ecology*, **84**, 282–288.

Fewster, R. M. and Buckland, S. T. (2004). Assessment of distance sampling estimators. *Advanced Distance Sampling. Oxford University Press, Oxford, UK*, pages 281–306.

Fewster, R. M., Buckland, S. T., Burnham, K. P., Borchers, D. L., P. E. Jupp, J. L. L., and Thomas, L. (2009). Estimating the encounter rate variance in distance sampling. *Biometrics*, **65**, 225 – 236.

Gillespie, D., Berggren, P., Brown, S., Kuklik, I., Lacey, C., Lewis, T., Matthews, J., McLanaghan, R., Moscrop, A., and Tregenza, N. (2005). Relative abundance of harbour porpoises (*Phocoena phocoena*) from acoustic and visual surveys of the Baltic Sea and adjacent waters during 2001 and 2002. *Journal of Cetacean Research and Management*, **7**, 51–57.

Glennie, R., Buckland, S. T., and Thomas, L. (2015). The effect of animal movement on line transect estimates of abundance. *PLoS One*, **10**, e0121333.

Gurarie, E. and Ovaskainen, O. (2013). Towards a general formalization of encounter rates in ecology. *Theoretical Ecology*, **6**, 189–202.

Gutzwiller, K. J. and Marcum, H. A. (1997). Bird reactions to observer clothing color: implications for distance-sampling techniques. *The Journal of wildlife management*, **61**, 935–947.

Harris, D., Matias, L., Thomas, L., Harwood, J., and Geissler, W. H. (2013). Applying distance sampling to fin whale calls recorded by single seismic instruments in the northeast Atlantic. *The Journal of the Acoustical Society of America*, **134**, 3522–3535.

Harris, D. V. (2012). *Estimating whale abundance using sparse hydrophone arrays*. Ph.D. thesis, University of St Andrews.

Harris, M. P. and Murray, S. (1981). Monitoring of puffin numbers at Scottish colonies. *Bird Study*, **28**, 15–20.

Hayes, R. J. and Buckland, S. T. (1983). Radial-distance models for the line-transect method. *Biometrics*, **39**, 29–42.

Heupel, M. R., Simpfendorfer, C. A., and Fitzpatrick, R. (2010). Large–scale movement and reef fidelity of grey reef sharks. *PloS One*, **5**, e9650.

Holmes, E. E., Lewis, M. A., Banks, J., and Veit, R. (1994). Partial differential equations in ecology: spatial interactions and population dynamics. *Ecology*, **75**(1), 17–29.

Hooten, M. B., Hanks, E. M., Johnson, D. S., and Alldredge, M. W. (2014). Temporal variation and scale in movement-based resource selection functions. *Statistical Methodology*, **17**, 82–98.

Horvitz, D. G. and Thompson, D. J. (1952). A generalization of sampling without replacement from a finite universe. *Journal of the American Statistical Association*, **47**, 663–685.

Howe, E. J., Buckland, S. T., Després-Einspenner, M.-L., and Kühl, H. S. (2017). Distance sampling with camera traps. *Methods in Ecology and Evolution*, **8**, 1558–1565.

Hurvich, C. M. and Tsai, C.-L. (1989). Regression and time series model selection in small samples. *Biometrika*, **76**, 297–307.

Hutchinson, J. and Waser, P. M. (2007). Use, misuse and extensions of "ideal gas" models of animal encounter. *Biological Reviews*, **82**, 335–359.

Jacoby, D. M., Brooks, E. J., Croft, D. P., and Sims, D. W. (2012). Developing a deeper understanding of animal movements and spatial dynamics through novel application of network analyses. *Methods in Ecology and Evolution*, **3**, 574–583.

Johnson, A. R., Wiens, J. A., Milne, B. T., and Crist, T. O. (1992a). Animal movements and population dynamics in heterogeneous landscapes. *Landscape Ecology*, **7**, 63–75.

Johnson, A. R., Milne, B. T., and Wiens, J. A. (1992b). Diffusion in fractcal landscapes: simulations and experimental studies of tenebrionid beetle movements. *Ecology*, **73**, 1968–1983.

Kareiva, P. M. and Shigesada, N. (1983). Analyzing insect movement as a correlated random walk. *Oecologia*, **56**, 234–238.

Koblitz, J. C., Amundin, M., Carlström, J., Thomas, L., Carlén, I., Teilmann, J., Tregenza, N., Wennerberg, D., Kyhn, L., Svegaard, S., *et al.* (2014). Large-scale static acoustic survey of a low-density population—estimating the abundance of the Baltic sea harbor porpoise. *The Journal of the Acoustical Society of America*, **136**, 2248–2248.

Koehler, E., Brown, E., and Haneuse, S. J.-P. A. (2009). On the assessment of Monte Carlo error in simulation-based statistical analyses. *The American Statistician*, **63**, 155–162.

Kou, S. and Zhong, H. (2016). First-passage times of two-dimensional brownian motion. *Advances in Applied Probability*, **48**, 1045–1060.

Kyhn, L. A., Tougaard, J., Thomas, L., Duve, L. R., Stenback, J., Amundin, M., Desportes, G., and Teilmann, J. (2012). From echolocation clicks to animal density—acoustic sampling of harbor porpoises with static dataloggers. *The Journal of the Acoustical Society of America*, **131**, 550–560.

Laake, J., Borchers, D., Thomas, L., Miller, D., and Bishop, J. (2014). *mrds: Mark-Recapture Distance Sampling (mrds)*. R package version 2.1.10.

Langrock, R., Hopcraft, J. G. C., Blackwell, P. G., Goodall, V., King, R., Niu, M., Patterson, T. A., Pedersen, M. W., Skarin, A., and Schick, R. S. (2014). Modelling group dynamic animal movement. *Methods in Ecology and Evolution*, **5**, 190–199.

Lewis, M. A. and Murray, J. D. (1993). Modelling territoriality and wolf-deer interactions. *Nature*, **366**, 738–740.

Liedvogel, M., Åkesson, S., and Bensch, S. (2011). The genetics of migration on the move. *Trends in Ecology & Evolution*, **26**, 561–569.

Marques, T. A. (2004). Predicting and correcting bias caused by measurement error in line transect sampling using multiplicative error models. *Biometrics*, **60**, 757–763.

Marques, T. A., Munger, L., Thomas, L., Wiggins, S., and Hildebrand, J. A. (2011). Estimating North Pacific right whale *Eubalaena Japonica* density using passive acoustic cue counting. *Endangered Species Research*, **13**, 163–172.

Marques, T. A., Thomas, L., Martin, S. W., Mellinger, D. K., Ward, J. A., Moretti, D. J., Harris, D., and Tyack, P. L. (2013). Estimating animal population density using passive acoustics. *Biological Reviews*, **88**, 287–309.

Marra, P. P., Francis, C. M., Mulvihill, R. S., and Moore, F. R. (2005). The influence of climate on the timing and rate of spring bird migration. *Oecologia*, **142**, 307–315.

Marsden, S. J. (1999). Estimation of parrot and hornbill densities using a point count distance sampling method. *Ibis*, **141**, 327–390.

Matias, L. and Harris, D. (2015). A single-station method for the detection, classification and location of fin whale calls using ocean-bottom seismic stations. *The Journal of the Acoustical Society of America*, **138**, 504–520.

McClintock, B. T., King, R., Thomas, L., Matthiopoulos, J., McConnell, B. J., and Morales, J. M. (2012). A general discrete-time modeling framework for animal movement using multistate random walks. *Ecological Monographs*, **82**, 335–349.

McClintock, B. T., Johnson, D. S., Hooten, M. B., Ver Hoef, J. M., and Morales, J. M. (2014). When to be discrete: the importance of time formulation in understanding animal movement. *Movement Ecology*, **2**, 1–14.

McCulloch, C. E. and Cain, M. L. (1989). Analyzing discrete movement data as a correlated random walk. *Ecology*, **70**, 383–388.

McDonald, M. A. (2006). An acoustic survey of baleen whales off Great Barrier Island, New Zealand. *New Zealand Journal of Marine and Freshwater Research*, **40**, 519–529.

McDonald, M. A. and Fox, C. G. (1999). Passive acoustic methods applied to fin whale population density estimation. *The Journal of the Acoustical Society of America*, **105**, 2643–2651.

McKenzie, H. W., Lewis, M. A., and Merrill, E. H. (2009). First passage time analysis of animal movement and insights into the functional response. *Bulletin of Mathematical Biology*, **71**, 107–129.

Mellinger, D. K., Stafford, K. M., Moore, S., Dziak, R. P., and Matsumoto, H. (2007). Fixed passive acoustic observation methods for cetaceans. *Oceanography*, **20**, 36.

Miller, D. L. and Thomas, L. (2015). Mixture models for distance sampling detection functions. *PLoS One*, **10**, e0118726.

Moorcroft, P. R. and Lewis, M. A. (2013). *Mechanistic Home Range Analysis. (MPB-43)*. Princeton University Press.

Ovaskainen, O. (2008). Analytical and numerical tools for diffusion-based movement models. *Theoretical Population Biology*, **73**, 198–211.

Palka, D. L. and Hammond, P. S. (2001). Accounting for responsive movement in line transect estimates of abundance. *Canadian Journal of Fisheries and Aquatic Sciences*, **58**, 777–787.

Parsons, K. M., Balcomb, K. C., Ford, J. K. B., and Durban, J. W. (2009). The social dynamics of southern resident killer whales and conservation implications for this endangered population. *Animal Behaviour*, **77**, 963–971.

Patterson, T. A., Thomas, L., Wilcox, C., Ovaskainen, O., and Matthiopoulos, J. (2008). State–space models of individual animal movement. *Trends in Ecology & Evolution*, **23**, 87–94.

Pearson, K. (1905). The problem of the random walk. *Nature*, **72**, 294.

Pollock, K. H. (1978). A family of density estimators for line-transect sampling. *Biometrics*, **34**, 475–478.

Potts, J. M., Buckland, S. T., Thomas, L., and Savage, A. (2012). Estimating abundance of cryptic but trappable animals using trapping point transects: a case study for key largo woodrats. *Methods in Ecology and Evolution*, **3**, 695–703.

Prieto Gonzalez, R., Thomas, L., and Marques, T. A. (2017). Estimation bias under model selection for distance sampling detection functions. *Environmental and Ecological Statistics*, **24**, 399–414.

Pyke, G. H. (1983). Seasonal pattern of abundance of honeyeaters and their resources in heathland areas near Sydney. *Austral Ecology*, **8**, 217–233.

R Core Team (2014). *R: A Language and Environment for Statistical Computing*. R Foundation for Statistical Computing, Vienna, Austria.

R Core Team (2016). *R: A Language and Environment for Statistical Computing*. R Foundation for Statistical Computing, Vienna, Austria.

Redner, S. (2001). *A Guide to First-Passage Processes*. Cambridge University Press.

Riotte-Lambert, L., Benhamou, S., and Chamaillé-Jammes, S. (2015). How memory-based movement leads to nonterritorial spatial segregation. *The American Naturalist*, **185**, 103–116.

Roeder, K., Dennis, B., and Garton, E. O. (1987). Estimating density from variable circular plot censuses. *The Journal of Wildlife Management*, **51**, 224–230.

Rutz, C. and Hays, G. C. (2009). New frontiers in biologging science. *Biology Letters*, **5**, 289–292.

Schwarz, G. *et al.* (1978). Estimating the dimension of a model. *The Annals of Statistics*, **6**, 461–464.

Shibata, R. (1981). An optimal selection of regression variables. *Biometrika*, **68**, 45–54.

Shmueli, G. (2010). To explain or to predict? *Statistical Science*, **25**, 289–310.

Siniff, D. B. and Jessen, C. (1969). A simulation model of animal movement patterns. *Advances in Ecological Research*, **6**, 185–219.

Skellam, J. G. (1973). The formulation and interpretation of mathematical models of diffusionary processes in population biology. *The Mathematical Theory of the Dynamics of Biological Populations*, **63**.

Sober, E. (2002). Instrumentalism, parsimony, and the Akaike framework. *Philosophy of Science*, **69**, 112–123.

Southwell, C. (1994). Evaluation of walked line transect counts for estimating macropod density. *The Journal of Wildlife Management*, **58**, 348–356.

Spitzer, F. (2013). *Principles of Random Walk*. Springer Science & Business Media.

Steinberg, E. K. and Kareiva, P. (1997). Challenges and opportunities for empirical evaluation of spatial theory. *Spatial Ecology: The Role of Space in Population Dynamics and Interspecific Interactions*, **30**, 318–332.

Stober, J. M., Prieto Gonzalez, R., Smith, L., Marques, T. A., and Thomas, L. (2017). Techniques for estimating the size of low density gopher tortoise populations. *Journal of Fish and Wildlife Management*, **8**, 377–386.

Sumner, M. D., Wotherspoon, S. J., and Hindell, M. A. (2009). Bayesian estimation of animal movement from archival and satellite tags. *PLoS One*, **4**, e7324.

Taper, M. L. and Lele, S. R. (2010). *The Nature of Scientific Evidence: Statistical, Philosophical, and Empirical Considerations*. University of Chicago Press.

Thomas, L., Buckland, S. T., Burnham, K. P., Anderson, D. R., Laake, J. L., Borchers, D. L., and Strindberg., S. (2002). Distance sampling. *Encyclopedia of Environmetrics*, **1**, 544–552.

Thomas, L., Buckland, S. T., Rexstad, E. A., Laake, J. L., Strindberg, S., Hedley, S. L., Bishop, J. R., Marques, T. A., and Burnham, K. P. (2010). Distance software: design and analysis of distance sampling surveys for estimating population size. *Journal of Applied Ecology*, **47**, 5–14.

Turchin, P. (1991). Translating foraging movements in heterogeneous environments into the spatial distribution of foragers. *Ecology*, **72**, 1253–1266.

Turchin, P. (1998). *Quantitative Analysis of Movement: Measuring and Modeling Population Redistribution in Animals and Plants*. Sinauer Associates Sunderland.

Turnock, B. J. and Quinn, T. J. (1991). The effect of responsive movement on abundance estimation using line transect sampling. *Biometrics*, **47**, 701–715.

Tyack, P. L., Johnson, M., Soto, N. A., Sturlese, A., and Madsen, P. T. (2006). Extreme diving of beaked whales. *Journal of Experimental Biology*, **209**, 4238–4253.

Van Moorter, B., Visscher, D., Benhamou, S., Börger, L., Boyce, M. S., and Gaillard, J.-M. (2009). Memory keeps you at home: a mechanistic model for home range emergence. *Oikos*, **118**, 641–652.

Watwood, S. L., Miller, P. J., Johnson, M., Madsen, P. T., and Tyack, P. L. (2006). Deep-diving foraging behaviour of sperm whales (*Physeter macrocephalus*). *Journal of Animal Ecology*, **75**, 814–825.

Weng, K. C., Castilho, P. C., Morrissette, J. M., Landeira-Fernandez, A. M., Holts, D. B., Schallert, R. J., Goldman, K. J., and Block, B. A. (2005). Satellite tagging and cardiac physiology reveal niche expansion in salmon sharks. *Science*, **310**, 104–106.

Wildman, V. J. and Ramsey, F. L. (1985). Estimated effective area surveyed with the cumulative distribution function. Technical Report 106, Departament of Statistics, Oregon State University, Corvallis, OR, USA.

Williams, B. K., Nichols, J. D., and Conroy, M. J. (2002). *Analysis and Management of Animal Populations*. Academic Press.

Williams, R. and Thomas, L. (2007). Distribution and abundance of marine mammals in the coastal waters of British Columbia, Canada. *Journal of Cetacean Research and Management*, **9**, 15–28.

With, K. A. (1994). Using fractal analysis to assess how species perceive landscape structure. *Landscape Ecology*, **9**, 25–36.

With, K. A., Cadaret, S. J., and Davis, C. (1999). Movement responses to patch structure in experimental fractal landscapes. *Ecology*, **80**, 1340–1353.

Wood, S. (2012). *Package mgcv*. R package version 1.8.19.

Wu, H.-i., Li, B.-L., Springer, T. A., and Neill, W. H. (2000). Modelling animal movement as a persistent random walk in two dimensions: expected magnitude of net displacement. *Ecological Modelling*, **132**, 115–124.

Glossary

Here we list the common acronyms and notation used within this thesis.

Acronyms

AIC	Akaike information criterion.
AIC_c	Akaike information criterion with a correction for finite sample sizes.
BIC	Bayesian information criterion.
BCRW	Biased correlated random walk.
BRW	Biased random walk.
CDS	Conventional distance sampling.
CI	Confidence interval.
CPS	Circular plot sampling.
CRW	Correlated random walk.
DS	Distance sampling.
EPS	Exponential power series.
HN	Half normal.
HR	Hazard-rate.
LRT	Likelihood-ratio test.
LTS	Line transect sampling.
MCDS	Multiple-covariate distance sampling.
MCE	Monte Carlo error.
MDD	Mean dispersal distance.
MR	Mark-recapture.
MRDS	Mark-recapture distance sampling.
MSD	Mean square displacement.
PAM	Passive acoustic monitoring.
pdf	Probability density function.
PS	Plot sampling.

PTS	Point transect sampling.
RMSE	Root mean square error.
RRMSE	Relative root mean square error.
RW	Random walk.
SECR	Spatially explicit capture-recapture.

Survey layaout

A	The study region.
a	The covered area.
$a_{t_2-t_1}$	The effective extended encounter region during the time interval $[t_1, t_2]$.
k	The number of transects, lines or points.
L	The total line transects length.
w	The truncation distance.
u	The speed of the animal.
τ	The simulation time step.
$[t_1, t_2]$	The total interval of time of the survey.
l	The animal step length.
θ	The direction of the animal.
δ	The distance between the animal location and the centre of attraction.
α	The constant of the scaled distance.
μ	The animal expected turning angle.
ρ	The strength of bias to the centre of attraction.
(p_x, p_y)	The animal centre of attraction.
r	The distance from the animal to the circular plot.
γ	The angle defined by animals entering in the circular plot.
ξ	The distance the animal moves during the time interval $[t_1, t_2]$.
η	The tangent of the animal initial position to the circular plot.
ϕ	The animal's turning angle.
ν	The total time steps an animal travels during the time interval $[t_1, t_2]$.

Observed data

n	The number of detected animals in the covered area, i.e., the sample size.
$n_{t_2-t_1}$	The number of detected animals in the covered area during the interval of time $[t_1, t_2]$.

R	The distance to the location where the animal is first detected.
T	The time of the animal first detection.

Parameters

D	The animal density.
N	The animal abundance.
P_a	The average probability of detecting an animal within the covered area.
P_t	The average probability of detection associated with the interval $[t_1, t]$.
P_c	The inclusion probability, i.e., the probability of an animal being included in the sample.
$E(R_{t_2-t_1})$	The mean dispersal distance (MDD), i.e., the expected absolute distance from the origin after $\nu = t_2 - t_1$ steps.
$E(R^2_{t_2-t_1})$	The mean square displacement (MSD), i.e., the expected value of the square of the absolute distance from the origin.
β	The intercept of the generalized additive model.

Functions

$f : \mathbb{R}^+ \to \mathbb{R}^+$	The pdf of observed distances.
$g : \mathbb{R}^+ \to [0, 1]$	The detection function, the probability of detecting an animal at a given distance from the observer. HR $\quad g(y; \sigma, b) = 1 - \exp\left(-\left(\frac{y}{\sigma}\right)^{-b}\right) \quad \sigma > 0; \;\; b > 0.$ EPS $\quad g(y; \lambda, \nu) = \exp\left(-\left(\frac{y}{\lambda}\right)^{\nu}\right) \quad \lambda > 0; \;\; \nu > 0.$
$\pi : \mathbb{R}^+ \to [0, 1]$	The true distribution of animals from the observer.
$E : \mathbb{R} \to \mathbb{R}$	The expectation of a random variable X, i.e., $E(X) = \int_{-\infty}^{\infty} x f_X(x) dx$.
$f_{WC} : [0, 2\pi] \to \mathbb{R}^+$	The pdf of animal turning angle when θ follows a wrapped Cauchy distribution.
$\vartheta_{t_2-t_1} : \mathbb{R} \times \mathbb{R} \to \mathbb{R}^+$	The pdf for the animal spatial distribution over the total interval of time $[t_1, t_2]$.
$\rho : \mathbb{R}^+ \to [0, 1]$	The strength of bias to the centre of attraction, i.e., $\rho(\delta; \alpha) = \tanh(\alpha\delta)$.
$f_\rho : \mathbb{R} \to \mathbb{R}^+$	The pdf of the strength of bias ρ.
$k : \mathbb{R}^+ \to [0, 1]$	The hazard function, i.e., the probability of detecting an animal at a given distance, i.e., $k(r) = cr^{-d}, c, d \in \mathbb{R}^+$.

$h : \mathbb{R}^+ \to [0, 1]$	The 1-second probability of detecting an animal at a given distance, equivalent to the HR over 1 second.
$q : \mathbb{R}^+ \longrightarrow [0, 1]$	The probability of animal presence in a circular plot given its distance r to the centre of the circle, in a particular instant of time t.
$q_{t_2-t_1} : \mathbb{R}^+ \times \mathbb{R}^+ \to [0, 1]$	The probability of animal presence in a circular plot, during an interval $[t_1, t_2]$, given its distance r_{t_1} to the centre of each circle at time t_1 and speed u.
$s : \mathbb{R}^+ \times \mathbb{R}^+ \to \mathbb{R}$	The smooth function of the generalized additive model.
$f : \mathbb{R}^+ \times [t_1, t_2] \to \mathbb{R}^+$	The pdf of detecting an animal for the first time at distance R to the centre of the circular plot and at time T, conditional on the survey time period $[t_1, t_2]$.
$\widetilde{f} : \mathbb{R}^+ \times [t_1, \infty) \longrightarrow \mathbb{R}^+$	The pdf of detecting for the first time an animal at distance R to the centre of the circular plot and at time $T \in [t_1, \infty)$.
$x : [t_1, T] \to \mathbb{R}^+$	The function returning the distance of the animal from the observer at time $t \in [t_1, T]$ conditional on the animal being detected at distance R at time T and that it was moving linearly with constant speed $u \geq 0$, and direction $\theta \in [0, 2\pi)$.
$\Pi : \mathbb{R}^+ \to \mathbb{R}^+$	The pdf of an animal being at distance x_t at time t conditional on the animal being detected at distance R at time T and that it was moving linearly with constant speed $u \geq 0$ and θ direction, $\theta \in [0, 2\pi)$.
$P_{t_2-t_1} : \mathbb{R}^+ \times \mathbb{R}^+ \longrightarrow [0, 1]$	The probability of detecting an animal moving linearly at constant speed u during the survey time period $[t_1, t_2]$.
$S_{t_2-t_1} : \mathbb{R}^+ \longrightarrow [0, 1]$	The "survival" function (i.e., probability of remaining undetected) of the animal starting at initial distance x_{t_1}, following the direction θ, during the sampled time interval $[t_1, t_2]$.